SCHOOL OF ENGINEERING AND SCIENCE

Nonlinear analysis of earthquake-induced vibrations

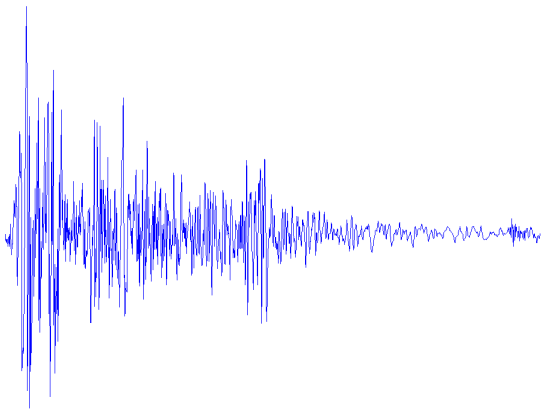

Master of Science Final Project

Vlad Inculeț

advised by
Lars V. Andersen, Associate Professor, PhD

January 29, 2016

School of Engineering and Science
Fibigerstraede 10
DK-9220 Aalborg East
Denmark
http://en.ses.aau.dk/

Abstract

The report is a support for the study of structural behavior under certain loads.

First, simply suported steel beams and simply supported reinforced concrete beams, under uniformly distributed loads, are analyzed, by both analytical and numerical methods. Second, embedded columns and multy-storey structures, made out first of steel and then reinforced concrete, are studied.

The analytical equations are derived according to the theory involved and then encoded in Matlab so they can be used in then future for other similar problems. For the numerical analysis, two Finite Element programs are used, i.e. Abaqus and a 2D code created in Matlab.

The report is a useful tool for the ones who want to study in detail reinforced concrete sections, plastic behavior, and also for the ones who want to learn how to model structures subjected to seismic loads in Abaqus, by means of accelerograms.

The report is supported by a DVD. Its content can also be requested by contacting the author at vincul12@student.aau.dk or vladinculetz@gmail.com.

In circulation: 3 copies
Number of pages: 79 total, 34.2 calculated with 2400 keystrokes per page, spaces included
Appendix: DVD
Closed: January 29, 2016

Contents

Nonlinear analysis of earthquake-induced vibrations

by Vlad Inculeț

January 29, 2016

1 Introduction

1.1 General description

This report deals with problems related to the loading of structures and structural elements by means of statically applied loads and dynamic applied loads. The courses of *Structural Mechanics* and *Structural Dynamics* constitute a prerequisite for a better understanding of the topics. Examples are used to illustrate the *results* pertinent to certain loading cases. Typically, *results* refer to stresses, strains and displacements at certain points within the elements as well as their variation in time. In the beginning, simple examples are used, then the difficulty progressively increases. The examples and their progression are chosen with respect to certain aspects i.e.

- *Material properties*

  Steel is used primordially, being easier to analyze than reinforced concrete due to its isotropic behavior, linear elasticity and homogeneity. After that, reinforced concrete is used under the assumptions of linear elasticity in the compressed fiber and zero tensile capacity. Finally, a reinforced concrete model with non-linear behavior is created and analyzed.

- *Structure's geometry*

  In the beginning, simply supported beams are analyzed. Then, the focus sets on embedded columns and multi-storey framed structures.

- *Loading case*

  Uniformly distributed loads are applied to the elements' surfaces in the first steps. After that, cyclic loads are implemented, and ultimately, earthquake loads by means of accelerograms.

New information is gathered step by step, the ultimate goal being analyzing a multi-storey reinforced concrete structure subjected to two different earthquakes, California's 1940 El Centro earthquake and Romania's 1977 Vrancea earthquake.

1.2 Calculation methods

The analysis is performed by means of three different methods:

- *Analytical*

  The analytical approach is used for specific beam theories, for elements of steel, and for elements of reinforced concrete under the assumptions of linear elasticity in the compressed fiber and zero tensile capacity. The hand calculations are only used for the static load case. For making it easier to access the results for a general input, the procedures are programmed using Matlab R2014a programming language.

- *MatLab 2D FEA*

  A 2D Finite Element code is created in Matlab. The code is valid for linear elastic, isotropic and homogeneous elements. Therefore, it is used as a validation for loading of steel elements, keeping in mind the yielding stress of the steel. This code is also used for the analysis of the earthquake loading

- *Abaqus 3D FEA*

  The analysis is performed in the commercial Finite Element code Abaqus is performed for all type of materials (steel and nonlinear reinforced concrete), geometries (simply supported beams, columns, frames and multi-storey frames)and loading scenarios (static loads, cyclic loading, earthquake loading).

1.3 Seismology introduction

1.3.1 General aspects

Earthquakes are geological phenomena produced by the sudden release of energy in seismic sources, located at different depths (tens of kilometers or hundreds of kilometers), and generate seismic waves. At the ground surface, earthquakes manifest by means of seismic motion, with a duration that can be expressed in terms of seconds (tens of seconds or hundreds of seconds). The mechanism of producing of an earthquake is briefly depicted in Figure 1.1.

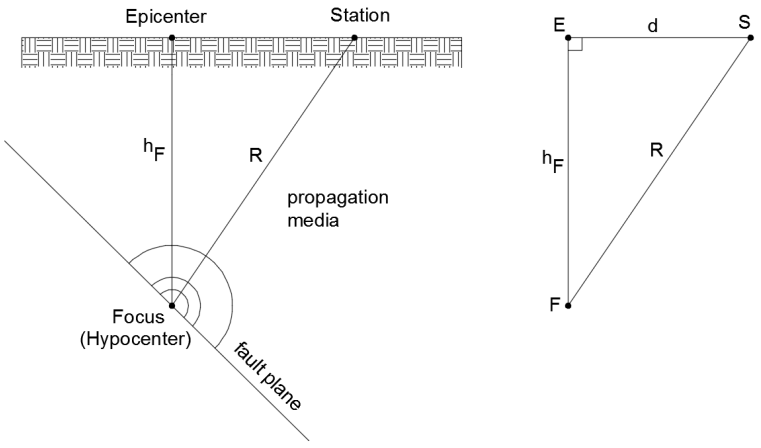

Figure 1.1: Scheme of an earthquake [Autocad]

F	Focus (hypocenter), theoretical point in which the process of rupture and release of seismic energy is initialized
E	Epicenter, point on ground surface that is connected with the Focus with a vertical line
S	Seismic station, where the accelerograms are recorded
h_F	Focal depth
R	Hypocentral distance
d	Epicentral distance

The seismic energy is released in the seismic source and it is transmitted throughout the propagation media by means of propagation waves. The seismic source can be:

- punctual
- linear (linear fault)
- surface like (fault plane)

An accelerogram is a graph that shows the variation of a ground acceleration in time during an earthquake. Accelerograms are recorded in seismic stations, by means of accelerometers, on three different directions:

- north-south (NS)
- east-west (EW)
- up-down (UD)

Figure 1.2 shows the accelerograms of the California's 1940 El Centro Earthquake, on the three directions mentioned above.

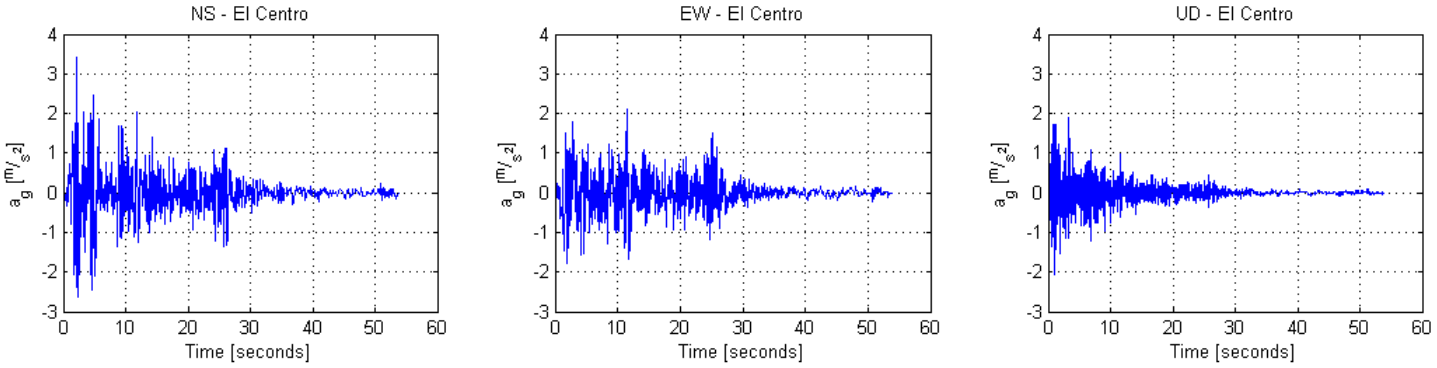

Figure 1.2: California's 1940 El Centro Earthquake accelerograms [Matlab]

The seismic stations record the ground motion with the help of some special tools, such as accelerometers and seismographs. The seismographs are very sensitive and describe very well weak seismic motion while strong motion signals are generally treated by means of accelerometers. An example of these two important tools are shown in Figure 1.3.

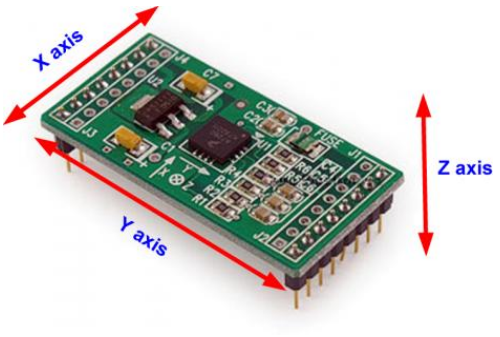

(a) MMA7260Q Accelerometer

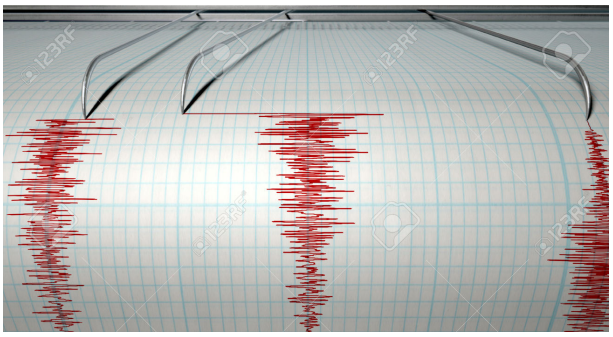

(b) Seismograph

Figure 1.3: Main tools for recording the ground motion [`http://myamicus.co.uk`, `http://star-telegram.com`]

Depending on the depth of the hypocenter (focal depth), earthquakes are classified in:

- surface earthquakes: $h_F < 60 \sim 70\ km$
- intermediate earthquakes: $70\ km < h_F < 250 \sim 300\ km$
- deep earthquakes: $300\ km < h_F < 700 \sim 800\ km$

1.3.2 Seismic waves

The seismic waves are waves that travel throughout a propagation media structure as consequence of an earthquake. They propagate in all the directions and there are of two main types:

- *Body waves*

  The Body waves propagate inside the Earth's structure. Their velocity depend on the material that they cross and on the distance to the hypocenter. The body waves are also of two types:

  P waves, also called primary waves, compression waves or longitudinal waves, propagate roughly in a straight line manner. They are the fastest type of seismic waves, the first ones to be recorded by the seismopraphs.

  S waves, also called secondary waves, shear waves or transversal waves, propagate perpendicular to the direction of the P waves.

- *Surface waves*

  The surface waves are the waves guided by the surface of the earth. They are less fast than body waves but their amplitude is usually higher. There are two main types of surface waves:

  Love waves, discovered by Augustus Edward Hough Love in 1911, are the fastest of the surface waves. They are horizontal shear waves and can be perceived as S waves without the horizontal component.

  Rayleigh waves, discovered by John William Strutt Rayleigh (Lord Rayleigh) in 1885, are the seismic surface waves that can be compared to the undulations at the surface of a lake, with both horizontal and vertical components.

The propagation of the seismic waves are illustrated in Figure 1.4.

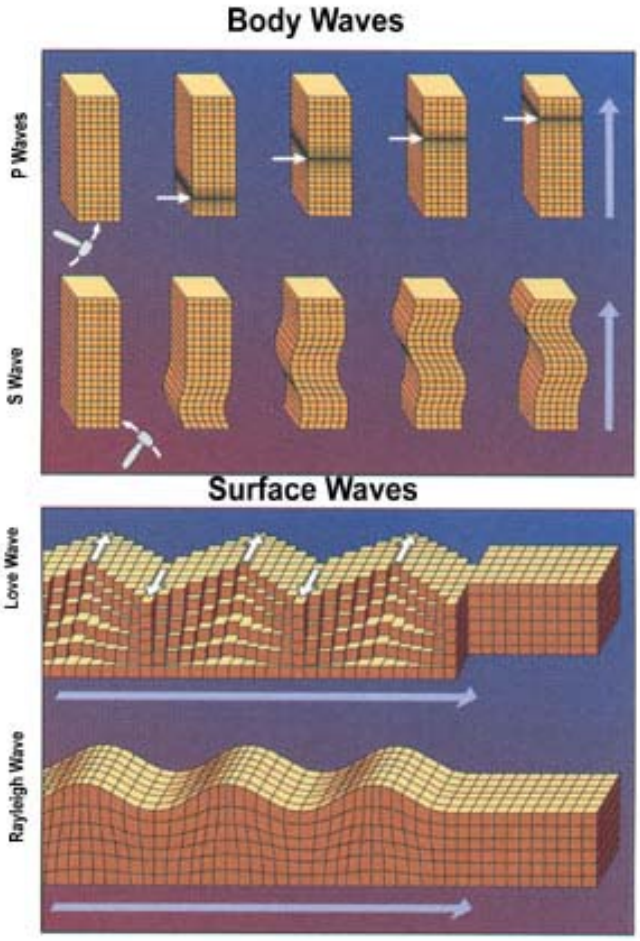

Figure 1.4: Propagation of the seismic waves [`https://en.wikipedia.org/wiki/seismic_wave`]

1.3.3 Seismic magnitude

The seismic magnitude is a parameter determined according to the recordings at the ground level, used for characterizing the severity of the seismic event. This parameter has an energetic signification.

- *Classical definition*

  The local magnitude is defined as logarithm in base 10 of the maximum amplitude of the displacement (measured in μm) measured with a standard seismograph at a distance of 100km from epicenter on a hard terrain.

$$M_L = \log \frac{A}{A^*} \tag{1.1}$$

The terms of Equation 1.1 are:

M_L	Local magnitude
A	maximum amplitude of the displacement of the terrain
A^*	correction

This logarithmic scale was developed by Charles Francis Richter in 1930 and it is also known as Richter scale.

- *Magnitude scales*

M_L	Local magnitude
M_S	Surface waves magnitude, used for surface earthquakes
M_b	Body waves magnitude, used for intermediate earthquakes
M_d	Duration magnitude, used for weak earthquakes
M_w	Moment magnitude, defined based on the seismic moment, used for all earthquakes

The seismic moment is defined as the product between the displacement of the fault and the force required to complete the displacement.

The earthquake with highest magnitude that has ever been recorded happened in Chile in 1960, with $M_w = 9.5$, $M_S = 8.3$ and focal depth $33km$.

1.3.4 Seismic intensity

The seismic intensity (not to be confused with the magnitude), is a scale with discrete values that depend on the the effects of the earthquake at the surface of the earth. The intensity scales used in general are the Mercalli modified scale (MM56), the Medvedev Sponheuer Karnik scale (MSK) and the European Macroseismic Scale (EMS-98).

All the stated scales are consistent and comprise a 12 steps system, where 1 defines the earthquakes that can hardly be felt and 12 defines earthquakes that cause major landscape changes and total damage.

1.3.5 Seismology vs Earthquake Engineering

Seismology is the science that studies seismic sources and the physical phenomena associated with occurrence of the earthquakes.

Earthquake engineering is the science that deals with the design and the reliability of the structures subjected or potentially subjected to earthquake action.

In earthquake engineering, the relevant parameters are the ones associated with the seismic motion of the terrain:

PGA	Peak ground velocity
PGV	Peak ground acceleration
PGD	Peak ground displacement

In the design process, seismic maps are used for the assessment of ground acceleration, which are given with specific MRI (main recurrence intervals) that are specified in the map legend. Figure 1.5 depicts the seismic map of Europe, where values of ground acceleration are given with a 475-year Return Period. This means that, on average, every 475 years there will be one earthquake with the peak ground acceleration stated on the zonation map. The values are obtained by statistical analysis, i.e. fitting curves, calculation of quantiles, evaluation of uncertainties, performed on a data set representing earthquakes that happened in the past.

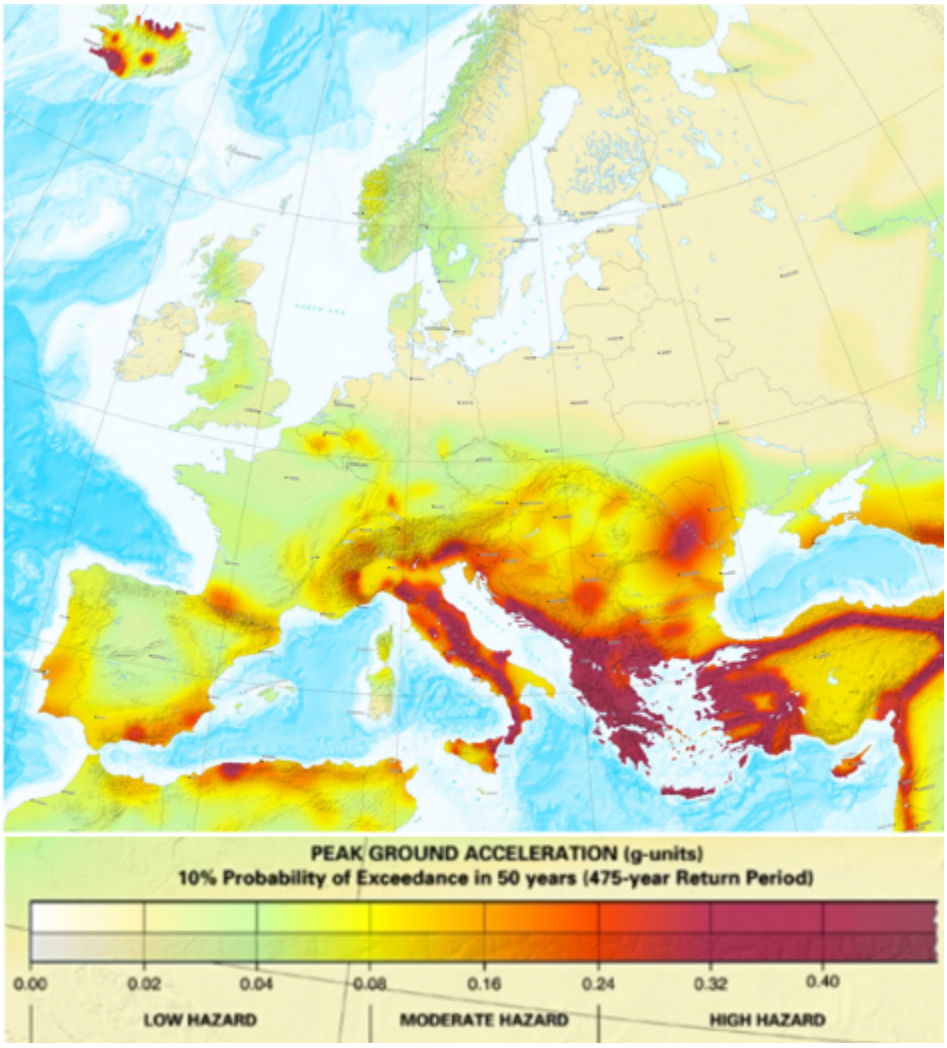

Figure 1.5: Seismic zonation of Europe [`http://preventionweb.net`]

2 Static loading

2.1 Rectangular cross-section steel beam

The first example consists of a simply supported steel beam of rectangular cross-section subjected to uniform static loading. The static scheme, bending moment diagram and shear force diagram, for a beam of length L and a distributed load of magnitude q, are shown in Figure 2.1.

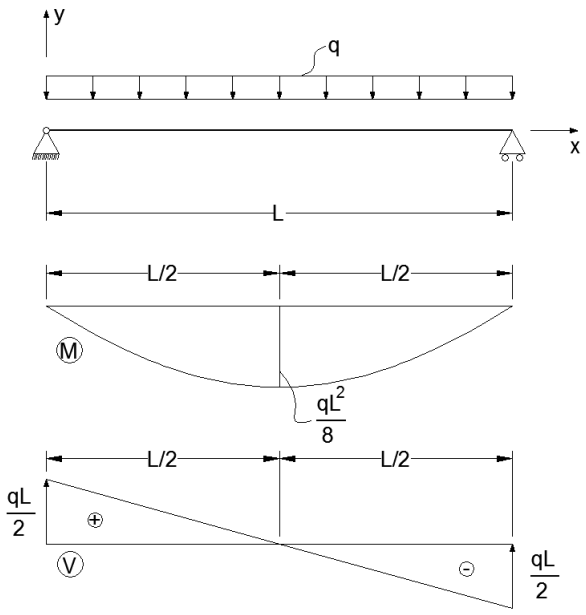

Figure 2.1: Static scheme, moment and shear force diagrams [Autocad]

As stated in the introduction, three things are of interest at this point, i.e. strains, stresses and displacements, and their variation along the cross-section and along beam's axis respectively.

The sign convention, which will remain as stated throughout the report, is the following:

Shear force	(+) if the force rotates the element clockwise, (-) otherwise
Bending moment	No signs are used because the moment diagram is always drawn on the stretched fiber
Strains and stresses	Tension is (+) and compression is (-)

Steel is an isotropic and homogeneous material, so the same laws apply in all directions and it also behaves similar in tension and compression. The stress-strain diagram of steel is shown in Figure 2.2.

For the sake of simplicity, it is used the diagram depicted in Figure 2.3, which is a good approximation and also makes the modelling easier. In this approach, the yielding plateau is assumed infinite.

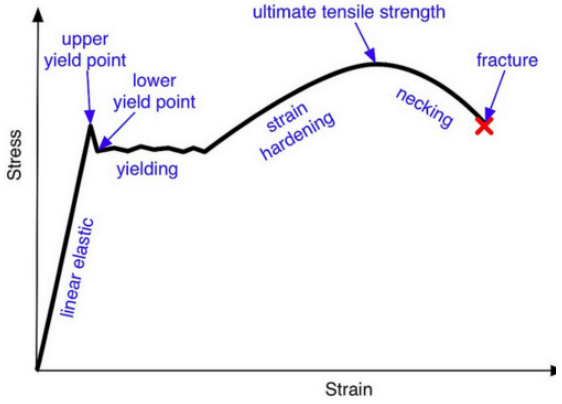

Figure 2.2: Stress-strain curve in tension [http://leancrew.com]

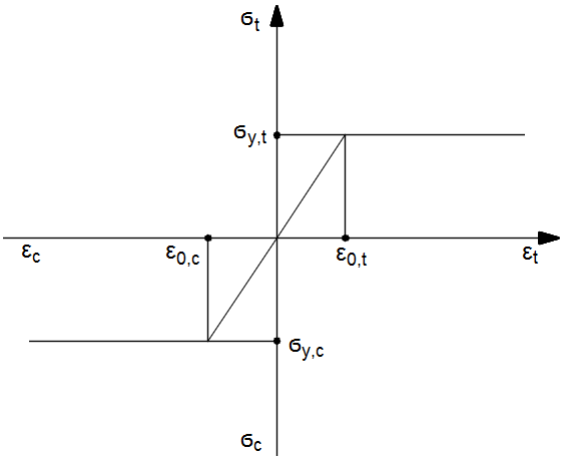

Figure 2.3: Simplified approach for steel stress-strain curve [Autocad]

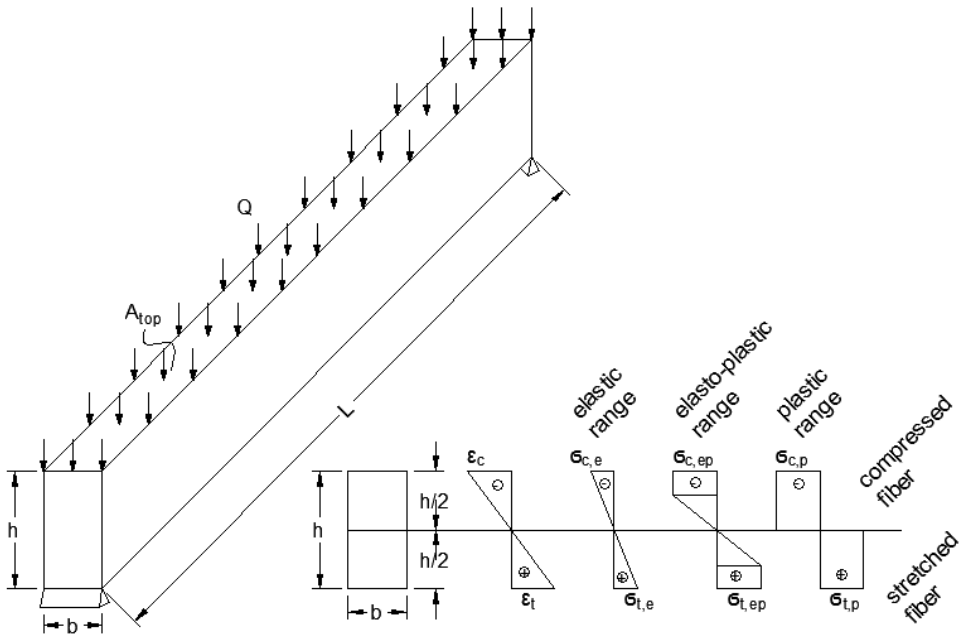

Figure 2.4: Steel beam with rectangular cross-section [Autocad]

The variation of strains and stresses along the cross-section is shown in Figure 2.4. First, the variation is linear. After that, when the load increases s.t. the maximum stress reaches the yielding stress of the steel, plastification occurs. If the load increases even more, at the end, all the cross-section will be yielded.

Yielding is the process where the particles rearrange and any unloading that occurs after that point will give out a residual strain. In the elastic range, i.e. before the occurance of yielding, no residual strain occurs, the unloading taking place back to zero, as shown in Figure 2.5.

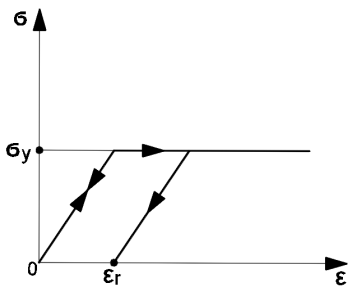

Figure 2.5: Steel unloading [Autocad]

The exercises chosen throughout this report have $[Nmm]$ as units, with the mention:

$$1\ MPa = 1\ \frac{N}{mm^2}$$

Notations:

q	distributed line load $[N/mm]$
L	Length of the beam $[mm]$
M	Bending moment with respect to the axis perpendicular on xoy plan $[Nmm]$
V	Shear force $[N]$
σ_t	Yiealding stress in tension $[MPa]$
σ_c	Yiealding stress in compression $[MPa]$
ε_t	Yiealding strain in tension [ ]
ε_c	Yiealding strain in compression [ ]
Q	distributed surface force $[MPa]$
A_{top}	the top area of the beam $[mm^2]$
b	width of the beam $[mm]$
h	height of the beam $[mm]$
ε_r	residual strain [ ]

2.1.1 Hand calculations of displacements, stresses and strains

Analytically, the displacement is calculated by two different methods:

- *Method 1. Calculation of displacement using the equation of the deflective shape under Bernoulli-Euler beam theory*

  In this method, the displacement is obtained from the second order differential equation:

$$\frac{\partial^2 v}{\partial x^2} = \frac{M(x)}{EI} \tag{2.1}$$

x	beam axis
v	displacement $[mm]$
E	Young's Modulus $[MPa]$
I	Moment of inertia $[mm^4]$
EI	Bending stiffness $[Nmm^2]$

As it can be seen in Figure 2.1, the moment is of parabolic shape. The equation is obtained from the equation of the shear force, which is linear, by integrating, keeping in mind to apply the boundary conditions after losing the integral.

Therefore, the equation of the shear force is

$$V : \frac{x-0}{\frac{L}{2}-0} = \frac{y-\frac{qL}{2}}{0-\frac{qL}{2}} \tag{2.2}$$

$$V : \frac{2x}{L} = \frac{-y+\frac{qL}{2}}{+\frac{qL}{2}} \tag{2.3}$$

$$V : -y+\frac{qL}{2} = \frac{qL}{2}\cdot 2x \cdot \frac{1}{L} \tag{2.4}$$

$$V : -y+\frac{qL}{2} = qx \tag{2.5}$$

$$V : y = -qx + qL/2 \tag{2.6}$$

$$V(x) = -qx+\frac{qL}{2},\ x \in [0, L] \tag{2.7}$$

Now, the moment is given by

$$M(x) = \int V(x)dx \tag{2.8}$$

$$M(x) = -q\frac{x^2}{2}+\frac{qL}{2}x + C \tag{2.9}$$

$$BC : M(0) = 0 \Rightarrow C = 0 \tag{2.10}$$

$$M(x) = -\frac{q}{2}x^2+\frac{qL}{2}x,\ x \in [0, L] \tag{2.11}$$

Now, getting back to Equation 2.1 and replacing with $M(x)$ from Equation 2.11. It is important to take into account the boundary conditions after losing each integral.

$$\frac{\partial^2 v}{\partial x^2} = \frac{-\frac{q}{2}x^2 + \frac{qL}{2}x}{EI} \tag{2.12}$$

$$\frac{\partial v}{\partial x} = \frac{1}{EI}\left(-\frac{q}{2}\frac{x^3}{3} + \frac{qL}{2}\frac{x^2}{2} + C_1\right) \tag{2.13}$$

$$v = \frac{1}{EI}\left(-\frac{q}{6}\frac{x^4}{4} + \frac{qL}{4}\frac{x^3}{3} + C_1 x + C_2\right) \tag{2.14}$$

$$BC : v(0) = 0 \Rightarrow C_2 = 0 \tag{2.15}$$

$$v(L) = 0 \Rightarrow -\frac{qL^4}{24} + \frac{qL^4}{12} + C_1 L = 0 \Rightarrow \frac{qL^4}{24} + C_1 L = 0 \Rightarrow C_1 = -\frac{qL^3}{24} \tag{2.16}$$

Replacing C_1 and C_2

$$v(x) = \frac{1}{EI}\left(-\frac{q}{24}x^4 + \frac{qL}{12}x^3 - \frac{qL^3}{24}x\right) \tag{2.17}$$

$$v(x) = \frac{qx}{24EI}\left(-x^3 + 2Lx^2 - L^3\right) \tag{2.18}$$

In Equation 2.18, the signs mean that displacements will be positive on the positive side of the axis. In reality it is the opposite, so the whole expression has to be multiplied with (-1).

$$v(x) = \frac{qx}{24EI}\left(x^3 - 2Lx^2 + L^3\right),\ x \in [0, L] \tag{2.19}$$

Equation 3.5 represents the equation of the displacement along the beam axis. The maximum displacement occurs at the half of the beam.

$$v(\frac{L}{2}) = \frac{qL}{48EI}\left(\frac{L^3}{8} - 2L\frac{L^2}{4} + L^3\right) \tag{2.20}$$

$$v(\frac{L}{2}) = \frac{qL}{48EI}\left(\frac{L^3 - 4L^3 + 8L^3}{8}\right) \tag{2.21}$$

$$v(\frac{L}{2}) = \frac{5qL^4}{384EI} \tag{2.22}$$

- *Method 2. Calculation of displacement using Maxwell-Mohr formula and Vereschagin integration rules*

  Within this method, both the Bernoulli-Euler and Timoshenko terms that compose the total displacement are considered.

  Equation 2.23, called Maxwell-Mohr Equation, is used.

$$v(x) = \frac{1}{EI}\int Mm_0\ dx + \frac{\beta}{GA}\int Vv_0\ dx \tag{2.23}$$

$$\beta = \frac{I^2}{A\int_A \left(\frac{S}{t}\right)^2 dA} \tag{2.24}$$

$$G = \frac{E}{2(1+\nu)} \tag{2.25}$$

$$A = b \cdot h \tag{2.26}$$

$$I = \frac{b \cdot h^3}{12} \tag{2.27}$$

M	Actual moment $[Nmm]$
m_0	Moment when the structure is loaded with a unit load on the position and direction of the searched displacement $[mm]$
V	Actual shear force $[N]$
v_0	Shear force when the structure is loaded with a unit load on the position and direction of the searched displacement [ ]
β	Active surface reduction coefficient [ ]
G	Shear modulus $[MPa]$
A	cross-section area $[mm^2]$
ν	Poisson's ratio $[N]$

For rectangular cross-sections

$$\beta = \frac{5}{6} \tag{2.28}$$

The moment and the shear term are computed separately. For the Bernoulli-Euler part, i.e. the moment term, only the displacement at the half of the beam will be computed, since it is performed for the purpose of an extra check.

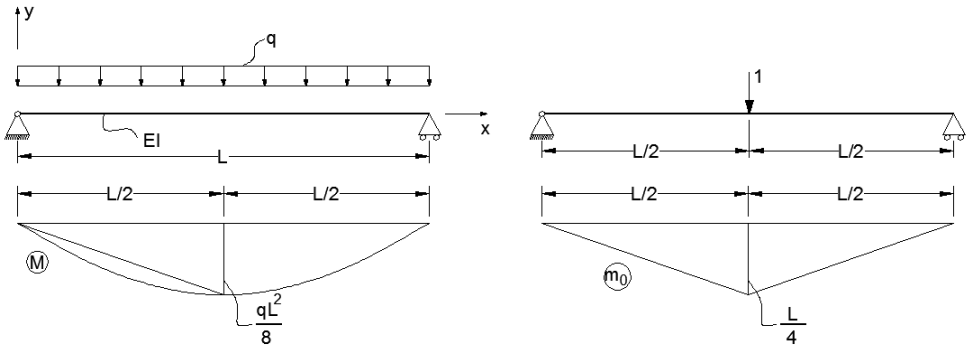

Figure 2.6: Real moment and virtual moment [Autocad]

Vereschagin integration rules are presented in Figure 2.7.

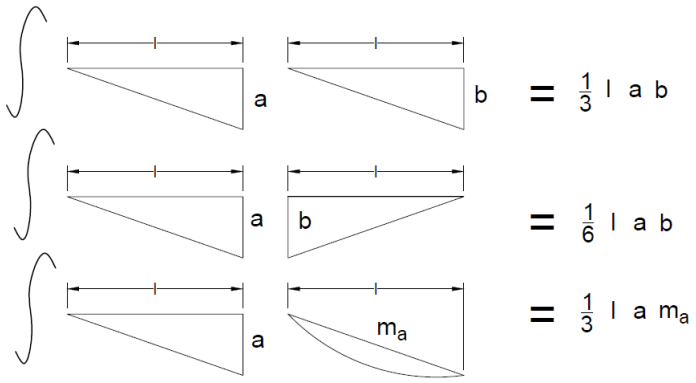

Figure 2.7: Vereschagin integration rules [Autocad]

m_a	Maximum moment created by a uniformly distributed load on a simply supported beam of length l $[Nmm]$

Therefore, the moment term is

$$v_B(\frac{L}{2}) = \frac{1}{EI}\int M(x)\cdot m_0(x)dx \tag{2.29}$$

$$v_B(\frac{L}{2}) = \frac{1}{EI}\cdot 2\left(\frac{1}{3}\cdot\frac{L}{2}\cdot\frac{qL^2}{8}\cdot\frac{L}{4}+\frac{1}{3}\cdot\frac{L}{2}\cdot\frac{L}{4}\cdot\frac{qL^2}{32}\right) \tag{2.30}$$

$$v_B(\frac{L}{2}) = \frac{2}{EI}\left(\frac{qL^4}{192}+\frac{qL^4}{768}\right) \tag{2.31}$$

$$v_B(\frac{L}{2}) = \frac{2}{EI}\cdot\frac{5qL^4}{768} \tag{2.32}$$

$$v_B(\frac{L}{2}) = \frac{5qL^4}{384EI} \tag{2.33}$$

It is observed that the displacement at the half of the beam corresponding to Bernoulli-Euler beam theory is the same in both of the methods.

The shear term is computed with respect to the beam axis, s.t. the total term will be also expressed with respect to the beam axis, for the moment part using Formula 3.5 from Method 1.

As it can be observed in Figure 2.8, there are three different cases.

$$Case(I)\ x \in [0, \frac{L}{2})$$

$$\int Vv_0 \cdot dx = x\left(\frac{L-x}{L}\right)\frac{q(L-2x)}{2} + \frac{1}{2}x \cdot \left(\frac{L-x}{L}\right) \cdot qx - \frac{1}{2} \cdot \left(\frac{L}{2} - x\right) \cdot \frac{x}{L}\frac{q(L-2x)}{2} + \frac{1}{2} \cdot \frac{L}{2} \cdot \frac{x}{L} \cdot \frac{qL}{2} \tag{2.34}$$

$$Case(II)\ x = \frac{L}{2}$$

$$\int Vv_0 \cdot dx = 2 \cdot \frac{1}{2} \cdot \frac{L}{2} \cdot \frac{1}{2} \cdot \frac{qL}{2} \tag{2.35}$$

$$Case(III)\ x \in (\frac{L}{2}, L]$$

$$\int Vv_0 \cdot dx = \frac{1}{2}\frac{L}{2} \cdot \frac{L-x}{L} \cdot \frac{q}{L} - \frac{1}{2}\left(x - \frac{L}{2}\right) \cdot \frac{L-x}{L} \cdot q\left(x - \frac{L}{2}\right) + (L-x)\frac{x}{L} \cdot q\left(x - \frac{L}{2}\right) + \frac{1}{2}(L-x) \cdot \frac{x}{L} \cdot q(L-x) \tag{2.36}$$

Further on, a Matlab code is created to help with the calculations when inserting some specific values for the variables, as shown in Figure 2.9. This is just a fast calculation tool, not to be confused with the Matlab FEA code.

Calculation of the displacements, in both methods, is valid only in the elastic domain but it is a good start for future validation of the Matlab 2D FEA code and of the Abaqus 3D FEA code.

The stresses are calculated by Navier formula, as shown in Equation 2.37. The value of the line load that produces yielding in the extreme fiber is also calculated, as shown in Equation 2.39. The surface plastic load can also be calculated, by dividing the line plastic load to the width of the cross-section, see Equation 2.40.

$$\sigma_{S,d} = \frac{M}{I} \cdot \frac{h}{2} \tag{2.37}$$

$$\sigma_{R,d} = \frac{q_{pl} \cdot L^2}{8I}\frac{h}{2} \tag{2.38}$$

$$q_{pl} = \sigma_{R,d} \cdot \frac{16I}{L^2 h} \tag{2.39}$$

$$Q_{pl} = \frac{q_{pl}}{b} \tag{2.40}$$

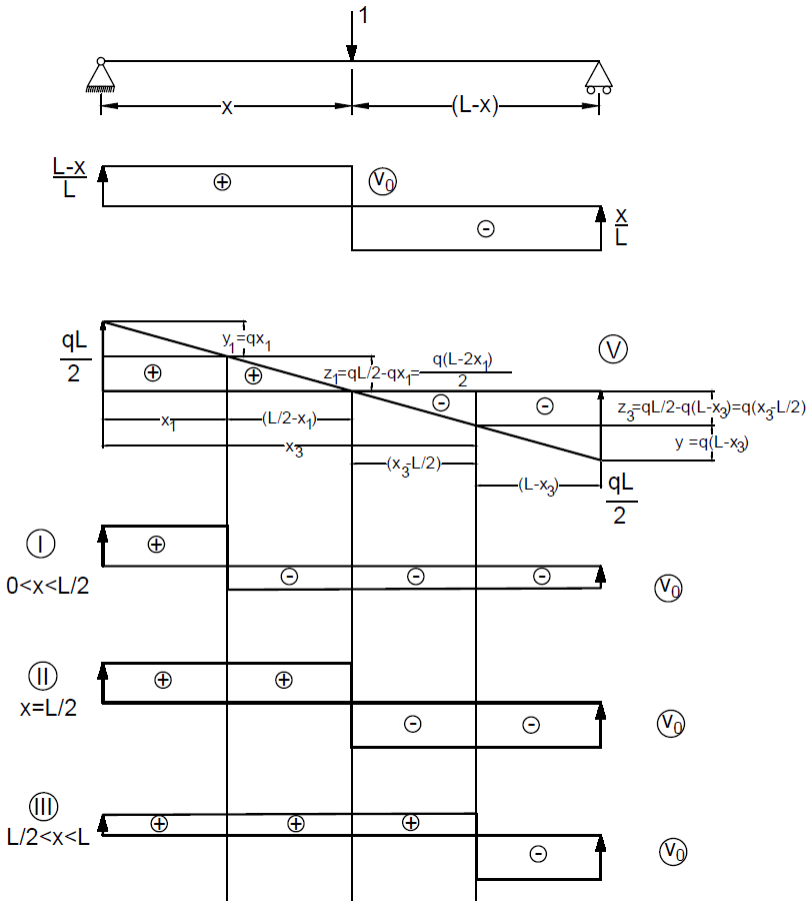

Figure 2.8: Virtual shear force [Autocad]

```
%%% Bending component of displacement(Bernouli-Euler beam theory)
if x_disp_test>=0 && x_disp_test<=L
v_B_test=q_calc_test*x_disp_test/(24*EI_test).*(x_disp_test.^3-2*L*x_disp_t
else disp('Assign x_disp a value between 0 and L!!!')
end

%%% Shear component of displacement (Timoshenko beam theory)
G_S_test=E_S/(2*(1+nu_S)); %shear modullus of concrete
A_test=b_test*h_test; %surface area
Beta_test=5/6; %active surface reduction coefficient for rectangular sectic

if x_disp_test>=0 && x_disp_test<L/2
v_S_test=Beta_test/(G_S_test*A_test)*(x_disp_test*(L-x_disp_test)/L*q_calc_
    else if x_disp_test==L/2
v_S_test=Beta_test/(G_S_test*A_test)*2*1/2*L/2*1/2*q_calc_test*L/2;
        else if x_disp_test>L/2 && x_disp_test<=L
v_S_test=Beta_test/(G_S_test*A_test)*(1/2*L/2*(L-x_disp_test)/L*q_calc_test
            end
        end
end
```

Figure 2.9: Matlab code for total displacement [Matlab]

2.1.2 Matlab 2D FEA

A 2D Matlab Finite Element code is used, with Rod elements, so three degrees of freedom per each node, i.e. two translations and one rotation. Again, this code is only valid in the elastic range but it is a great tool for comparing solution, and also to better understand how do more advanced Finite Element codes, such as Abaqus, function.

- *The input*

  The external loads are applied as boundary conditions, so they can only be applied on nodes. To simulate a uniformly distributed load, the line load was multiplied with the lenth of the beam and the divided to the total number of nodes minus two (-2), since the first and the last nodes (the extremities) are not loaded. This is shown in Figure 2.10.

```
% Material properties and cross sections [N-mm]

L=3000;
b=100;
h=200;

n_nodes=21; %number of nodes
q=200;        %[N/mm] distrubuted load

%For applying the equivalent load to each node, q is multiplied with
%length of the beam and then divided to (n_nodes-2) because it is
%distributed in every node except for the first and the last one.

q_1=q*L;%[N] total load
q_2=q_1/(n_nodes-2); %[N] equivalent nodal load

E = [ 210E3] ; % Young's modulus
A = [ b*h] ; % Cross sectional area
I = [ (b*h^3)/12 ] ; % Second moment of area
rho= [ 7.85E-9 ];  % [T/mm^3]
```

Figure 2.10: Matlab code for modelling a distributed load [Matlab]

Because Finite Element codes are a numerical way of calculation, it is time to introduce some numbers. The same numbers will be used afterwards for the comparison of the results. The geometrical characteristics and material properties are shown, as well, in Figure 2.10.

What can also be observed in Figure 2.10 is that the total number of nodes is encoded, i.e. the nodal coordinates, element topology and boundary conditions are programmed with respect to the number of nodes. That means that the user can easily change the number of nodes for different tests and analyze how do a decrease or increase in number of nodes affect the results. Figure 2.11 shows the contrast between an 11 nodes input and an encoded general one.

- *The main code*

  The main code is capable of calculating the eigenvalues and obtaining results for static loads. I this case, static loads are of interest.

  First, the global stiffness matrix and global mass matrix are constructed, within a loop that goes over all elements and adds all the local components together on the pertinent positions

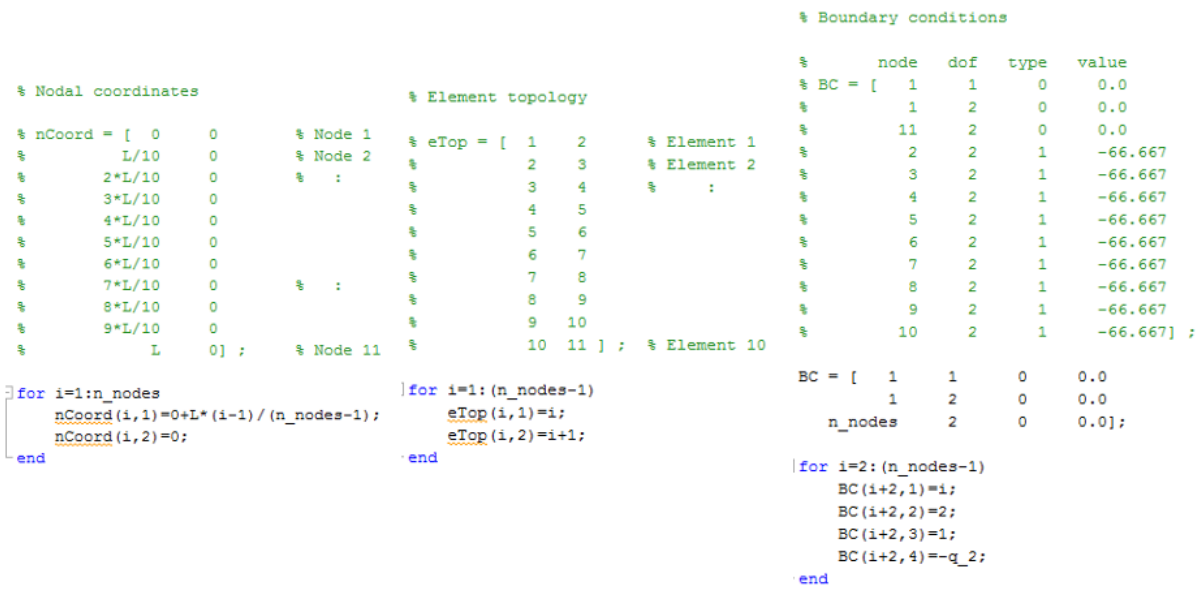

Figure 2.11: Matlab code input [Matlab]

of the global matrices. For optimizing the number of operations, the reduced stiffness matrix and mass matrix are calculated. The difference is that the reduced matrices don't take into account the degrees of freedom that are restricted by the boundary conditions. Therefore, they will be square matrices of a smaller order that the initial ones, fewer operation being conducted in that manner.

```
dRed = Kred\fRed  % to be used for statical analysis
```

Figure 2.12: Solving the reduced system [Matlab]

After solving the reduced system of equations, as shown in Figure 2.12, which is basically the most important equation in Finite Element Analysis, the displacement vector and the force vector are reconstructed so now they include again all the nodes and the results can be better visualized.

- *The output*

  The displacements and stresses can now be plotted.

  Figure 2.13 shows the variation of the displacements for a 21 nodes model, while Figure 2.14 shows the variation of the normal stresses. The results are in $[mm]$ and $[MPa]$, respectively.

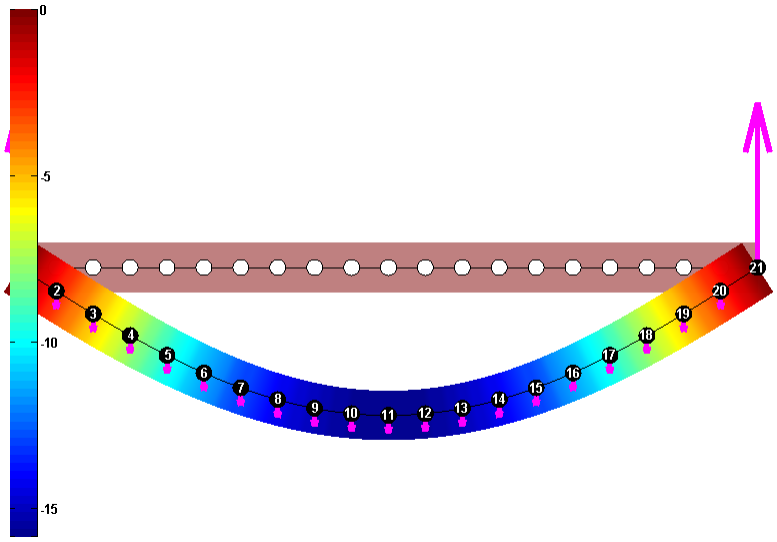

Figure 2.13: Displacement field $[mm]$ [Matlab]

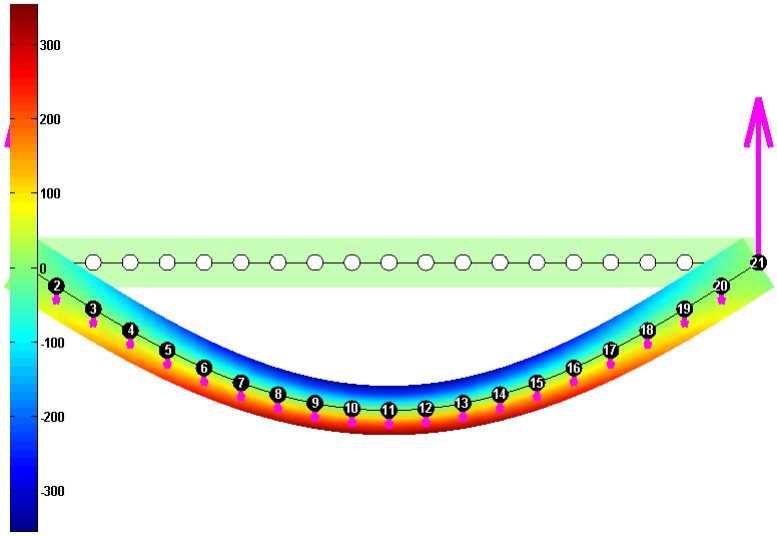

Figure 2.14: Normal stress $[MPa]$ [Matlab]

2.1.3 Abaqus 3D FEA

A 3D model is created in the commercial Finite Element program Abaqus.

First,the geometry of the elements is constructed, the result being shown in Figure 2.15. The beam is supported on two steel plates and not directly on the supports in order to avoid the occurrence of concentrated stresses in the area adjacent to the supports.

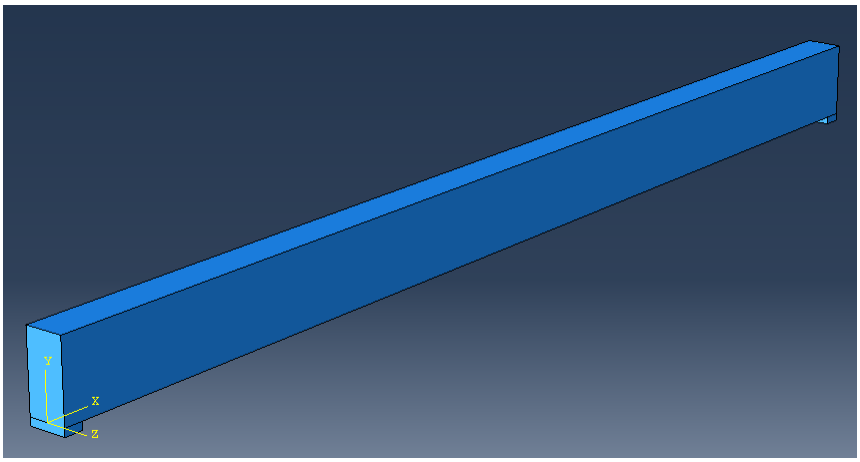

Figure 2.15: Layout of structure [Abaqus]

The material properties are created and then assigned to the elements, as in Figure 2.16. The material is modelled as linear, with an infinitely long yielding plateau set at 350 MPa. The units used are $[Nmm]$.

	Mass Density		Young's Modulus	Poisson's Ratio		Yield Stress	Plastic Strain
1	7.85E-009	1	210000	0.3	1	350	0

Figure 2.16: Material properties $[Nmm]$ [Abaqus]

The boundary conditions, i.e. the supports and the distributed load, are then defined, as shown in Figure 2.17. It can be seen that one of the supports is defined as hinge support and the other as pinned support. The span between the supports is 3000 mm. The load is defined as a surface load. The gravity load is also defined as 9.807 m/s^2, to see how it impacts the output.

After that, the steel plates and the beam are merged. The resulted structure is meshed with Hex type elements, which are 8 nodes elements, see Figure 2.18.

The analysis is then ran. The results for the displacements are shown in Figure 2.19 and the results for normal stresses are shown in Figure 2.20.

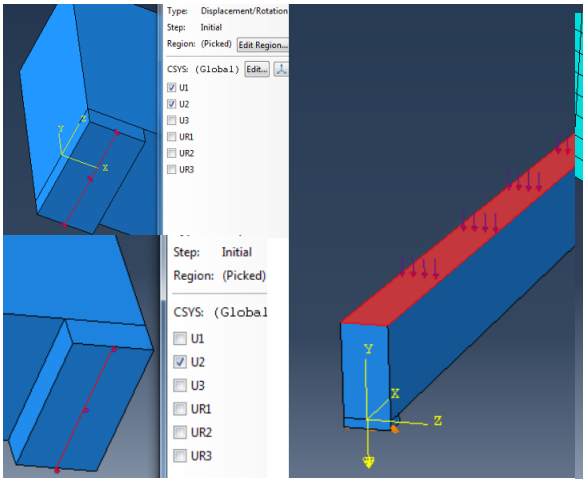

Figure 2.17: Boundary conditions [Abaqus]

Figure 2.18: Mesh with Hex elements [Abaqus]

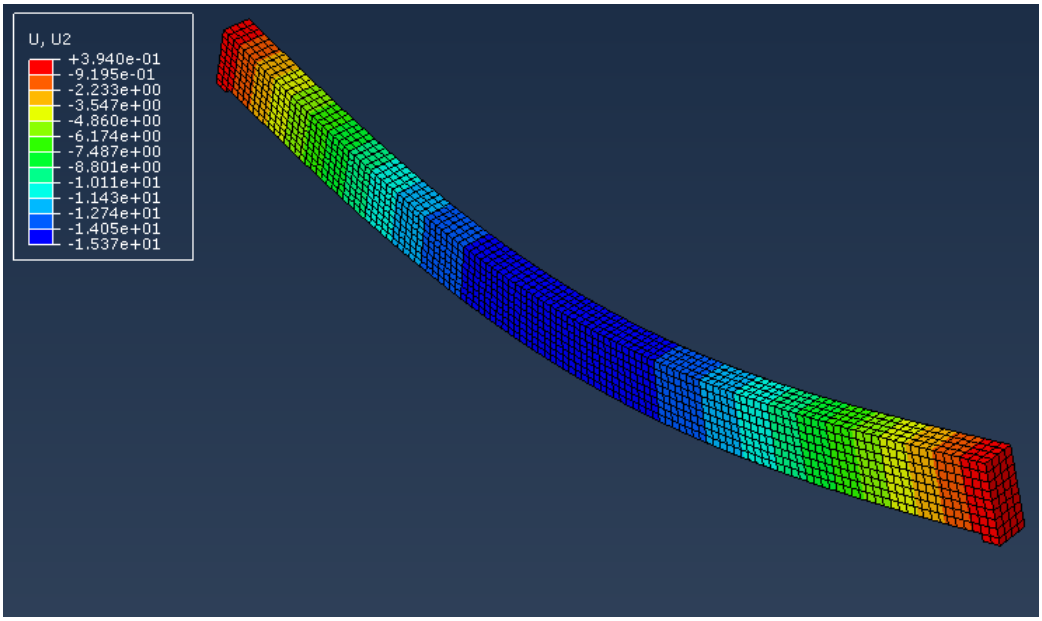

Figure 2.19: Displacement field [Abaqus]

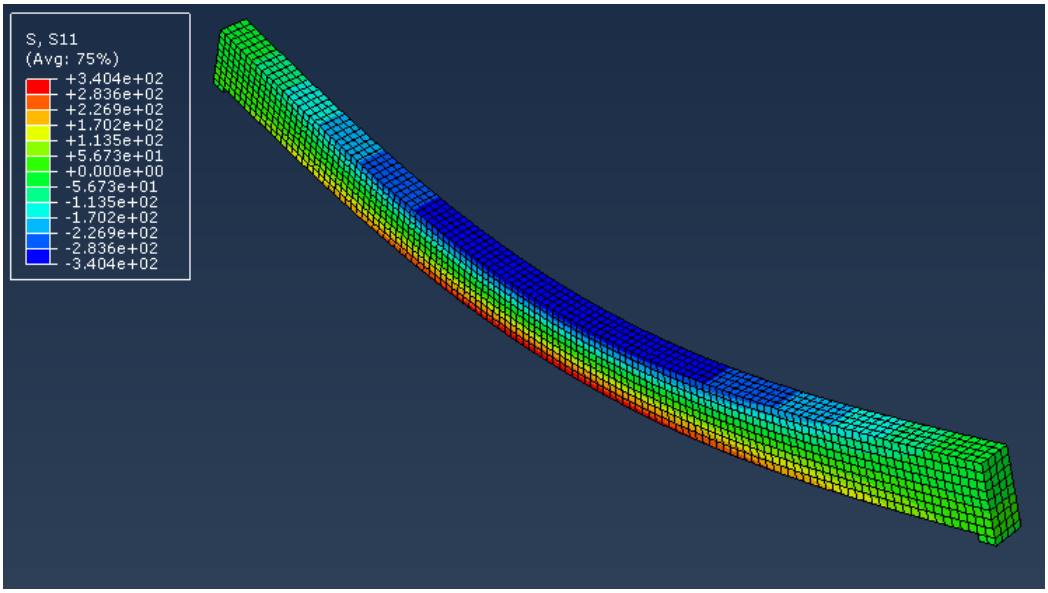

Figure 2.20: Normal stress field - elastic range [Abaqus]

Because the applied load does not induce any plastic response, the stress-strain diagram for the selected element is linear, as in Figure 2.21. The strains are stresses are presented in absolute value.

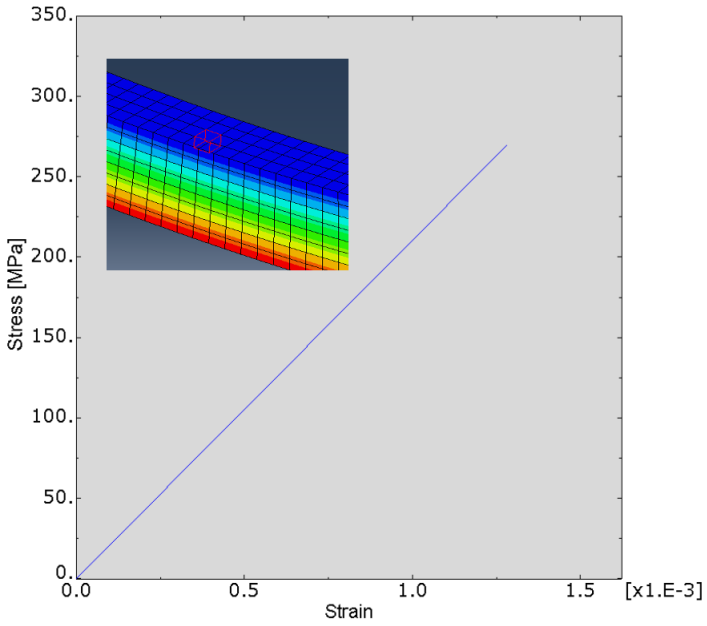

Figure 2.21: Elastic response [Abaqus]

If the chosen load is big enough in magnitude to induce plastic response, the normal stresses are distributed as in Figure 2.22, where it can be observed that, on a large interval at the middle zone, the section is fully plastified.

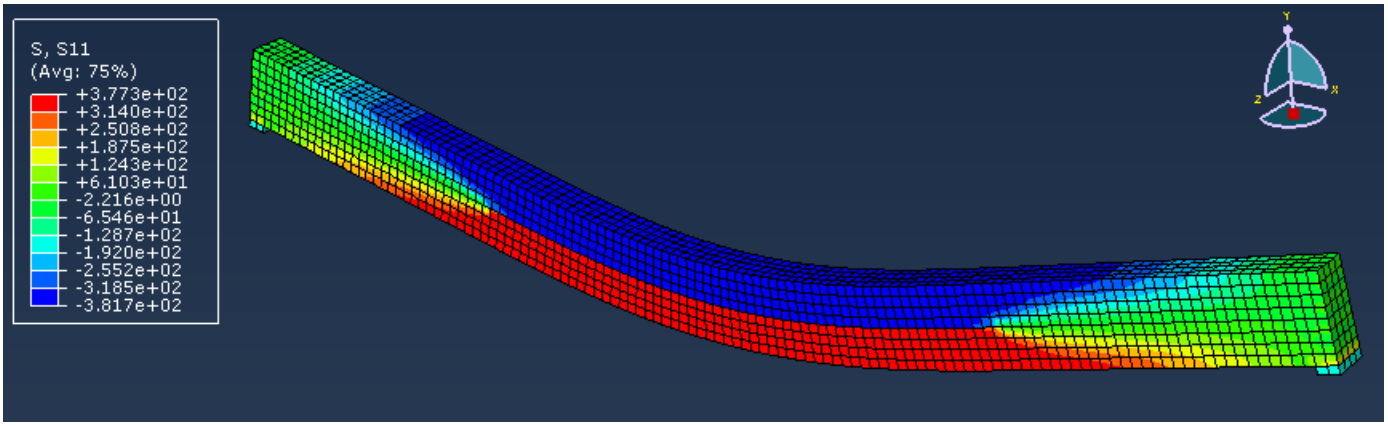

Figure 2.22: Normal stress field - plastic range [Abaqus]

The stress-strain diagram corresponding to the selected element is shown in Figure 2.23. It can be observed that the yielding occurs at as defined, at $350MPa$. The strains are stresses are presented in absolute value.

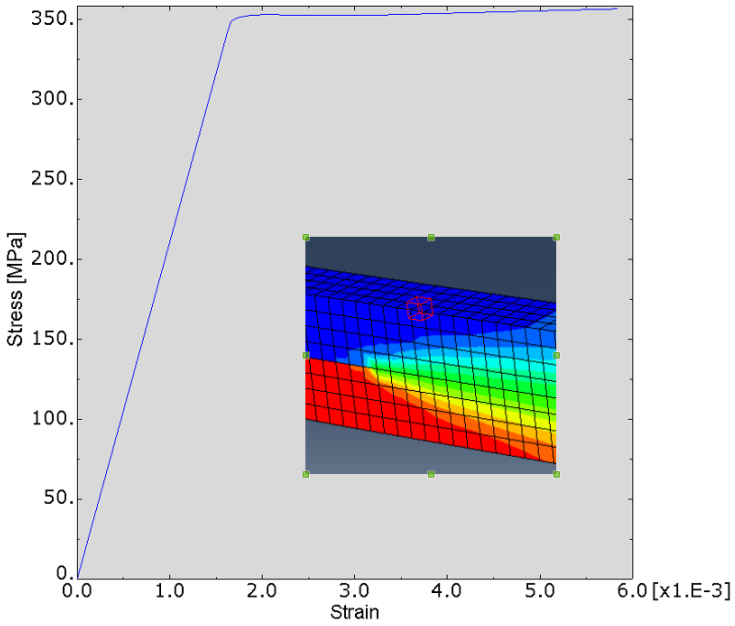

Figure 2.23: Plastic response [Abaqus]

2.1.4 Results, Comparison and Conclusion

The input used in calculations, in all the described methods, is

L	3000 $[Nmm]$ Length of beam
b	100 $[Nmm]$ Width of beam
h	200 $[Nmm]$ Height of beam
E_{steel}	210 $\cdot 10^3[MPa]$ Young's modulus of steel
ν_{steel}	0.3 Poisson's ratio of steel
$\sigma_{R,d\ steel}$	350 $[MPa]$ Strength of steel
q	200 $[\frac{N}{mm}]$ Line load
Q	2 $[\frac{N}{mm^2}]$ Surface load

The results for displacements and stresses obtained at half of the beam by all the described methods, for $q = 200\frac{N}{mm}$ are presented in Table 2.1. At this step, the influence of the gravity is not included. For the numerical approaches. i.e. in Matlab and Abaqus, only the total values for the displacements are given as outcome. The Bernoulli-Euler and Shear components of the displacement, i.e. $v_B(\frac{L}{2})$ and $v_S(\frac{L}{2})$ are pertinent to beam theory and they are associated with the analytical calculations.

	Analytically	Matlab 2D 10E	Matlab 2D 100E	Abaqus
$v_B(\frac{L}{2})$ $[mm]$	15.07	N/A	N/A	N/A
$v_S(\frac{L}{2})$ $[mm]$	0.12	N/A	N/A	N/A
$v_T(\frac{L}{2})$ $[mm]$	15.18	16.61	15.22	15.25
$\sigma_{max}(\frac{L}{2})$ $[MPa]$	337.5	337	355	337.8

Table 2.1: Output, $q = 200\frac{N}{mm}$, no gravity

$v_B(\frac{L}{2})$	Bernoulli-Euler component of displacement
$v_S(\frac{L}{2})$	Shear component of displacement
$v_T(\frac{L}{2})$	Total displacement
$\sigma_{max}(\frac{L}{2})$	maximum normal stress
Matlab 2D 10E	Matlab 2D with a 10 Element beam
Matlab 2D 100E	Matlab 2D with a 100 Element beam

In Table 2.2, the results are presented when the effect of gravity is considered. For the hand calculations and Matlab approach, the gravity is modelled as an extra uniformly distributed load with the value equivalent to the weight of the beam.
Generally, the results are the same regardless the calculation method, which confirms that the work has been done correctly. For this specific geometry and this specific load of $q = 200\frac{N}{mm}$, the gravity doesn't influence the displacement in an important manner because the applied load is much larger with respect to the weight of the beam. When gravity is considered, the weight of the beam represents only 0.8% of the total load. However, it can be observed that the displacements and stresses are slightly increased when gravity is considered, with the same factor of 0.8%.

Even if the shear component of the displacement is only 0.8% from the total displacement (no

	Analytically	Matlab 2D 10E	Matlab 2D 100E	Abaqus
$v_B(\frac{L}{2})$ $[mm]$	15.18	N/A	N/A	N/A
$v_S(\frac{L}{2})$ $[mm]$	0.11	N/A	N/A	N/A
$v_T(\frac{L}{2})$ $[mm]$	15.30	16.74	15.34	15.37
$\sigma_{max}(\frac{L}{2})$ $[MPa]$	340.1	360	340	340.4

Table 2.2: Output, $q = 200\frac{N}{mm}$, gravity included

connection with the 0.8% from the contribution of the gravity), it is clearly seen that when it is added to the Bernoulli-Euler component, the results become closer to the ones obtained by Finite Element analysis.

The plastic response is only studied in Abaqus and the results are the expected ones, see Figure 2.23.

With same results by all the methods, the hand calculations and Matlab 2D approaches are higher time consuming than the Abaqus approach, since Abaqus is a commercial Finite Element program with a user friendly interface.

It can be stated that all the results are roughly the same, the only ones that are slightly inconsistent being the ones obtained by Matab 2D with 10 Elements, where the errors are around 8%, for both displacements and stresses. An increase in elements number in the Matlab 2D approach gives results which are closer to the expected ones, so the fineness of the meshing can have an important impact on the result.

2.2 Reinforced concrete beam

A concrete beam, reinforced with three rebars at the bottom and two rebars at the top is chosen, as shown in Figure 2.24.

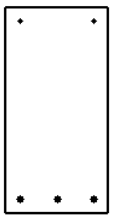

Figure 2.24: Reinforced Concrete - cross section [Matlab]

The supports are kept the same as for the steel beam, i.e. simply supported beam, and the load is also kept uniformly distributed, see Figure 2.1.
The goal is now to obtain results for displacements and stresses for some specific input, by two methods i.e. hand calculations and Abaqus. The Matlab 2D Finite Element code is no longer used,

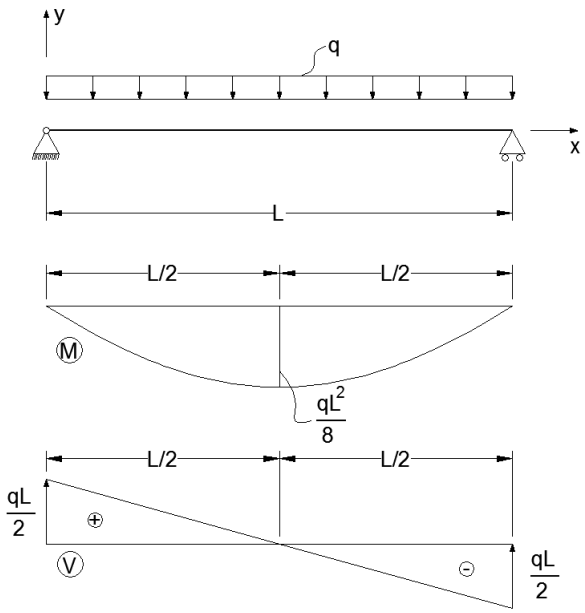

Figure 2.25: Static scheme, moment and shear force diagrams [Autocad]

since that is only valid for linear elastic, isotropic and homogeneous materials, such as steel.

2.2.1 Hand calculation of stresss and displacements

Concrete is a material composed of cement, aggregate and water. It has been known, in its early stages, since the Roman Empire times. The modern concrete appeared with the discovery of the Portland cement, in the 19th century in England, and it is still in use nowadays. It has a relatively good compressive strength but a poor tensile strength, hence the use of reinforcement in the area of the stretched fiber. Sometimes, to further increase the capacity of the element, and also for constructive reasons, e.g. support for the stirrups, reinforcement is also used in the compressed zone. The real stress-strain curve for concrete is shown in Figure 2.26.

For the analytical calculations, a simplified model of the stress-strain curve is used, as shown in Figure 2.27. For this approach, the concrete behaves similar to the steel in compression, i.e. elastic, and has zero tensile strength. It does not describe the real behavior of concrete, but it is an approximation used in hand calculations.

Therefore, at this instance, the concrete is modeled as linear elastic in compression and with zero tensile strength.

The displacements and stresses are computed with the same formulas as for the steel rectangular beam, with two important remarks.

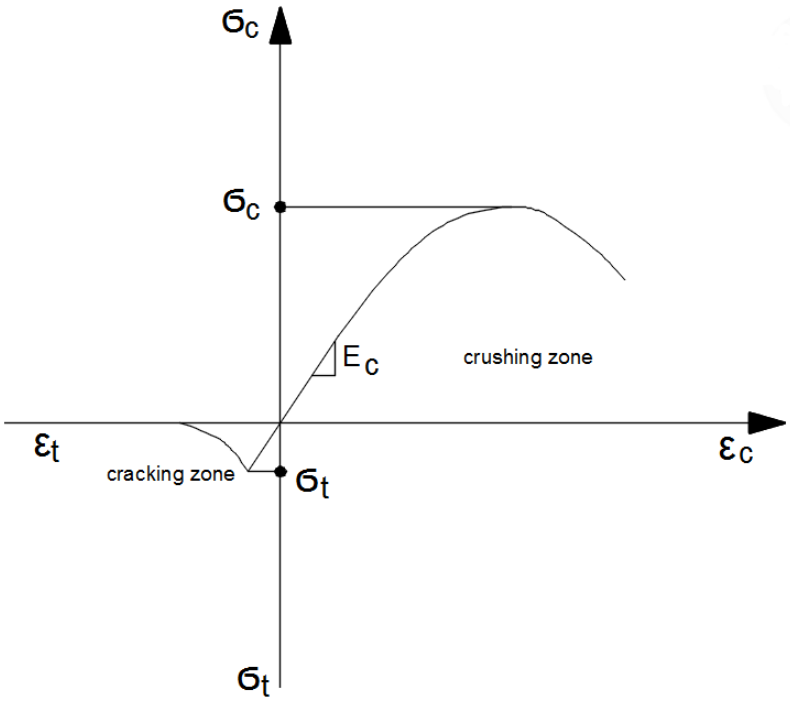

Figure 2.26: Stress-strain curve of concrete [Autocad]

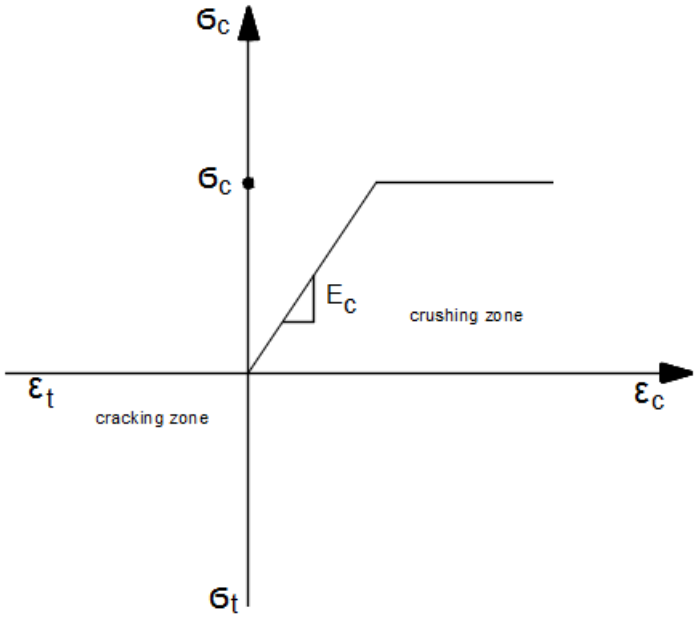

Figure 2.27: Stress-strain curve of concrete, assumption [Autocad]

- *Remark 1*

  The sections is no longer homogeneous, so EI has to be computed in a way that it resembles the equivalent bending stiffness for this cross section composed of different materials.

- *Remark 2*

  Unlike steel, concrete - at least in this model - has zero tensile strength, so not all the section will be active when the beam is loaded. Therefore, when computing the equivalent bending stiffness $'EI'$ and the section area A, this aspect has to be taken into account.

First, the moment capacity of the section shown in Figure 2.28 is calculated.

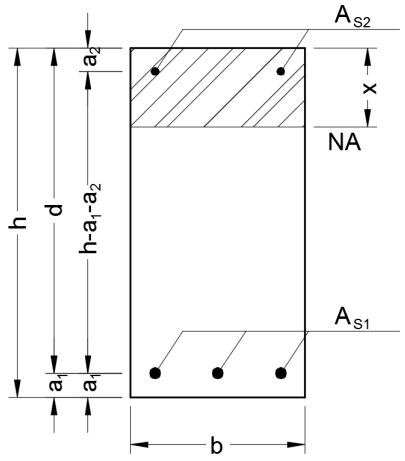

Figure 2.28: Sketch of the cross section [Autocad]

Notations

h	height of the section $[mm]$
b, b_w	width of the section $[mm]$
a_1	concrete covering in the stretched zone $[mm]$
a_2	concrete covering in the compressed zone $[mm]$
A_{S1}	area of the stretched reinforcement $[mm^2]$
A_{S2}	area of the compressed reinforcement $[mm^2]$
A_1	area of one stretched reinforcement $[mm^2]$
A_2	area of one compressed reinforcement $[mm^2]$
ϕ_1	diameter of one stretched reinforcement $[mm]$
ϕ_2	diameter of one compressed reinforcement $[mm]$
x	height of the compressed zone $[mm]$
d	effective height of the cross section, i.e. difference between the section height and the stretched concrete covering $[mm]$
M	bending moment $[Nmm]$

ϵ_C	strain in the extreme compressed concrete fiber [ ]
ϵ_{S1}	strain in the stretched reinforcement [ ]
ϵ_{S2}	strain in the compressed reinforcement [ ]
f_{ck}	characteristic strength of concrete $[MPa]$
f_{yk}	characteristic yielding stress of steel $[MPa]$
σ_C	stress in the extreme compressed concrete fiber $[MPa]$
σ_{S1}	stress in the stretched reinforcement $[MPa]$
σ_{S2}	stress in the compressed reinforcement $[MPa]$
$M_{R,d}$	capable bending moment $[Nmm]$
q_{pl}	line load the creates a moment equal to the capable moment $[N/mm]$
$'EI'$	equivalent bending stiffness $[Nmm^2]$

- *Approach 1, Linear elastic with zero tensile strength*

  The distribution of the strains and stresses is shown in Figure 2.29.

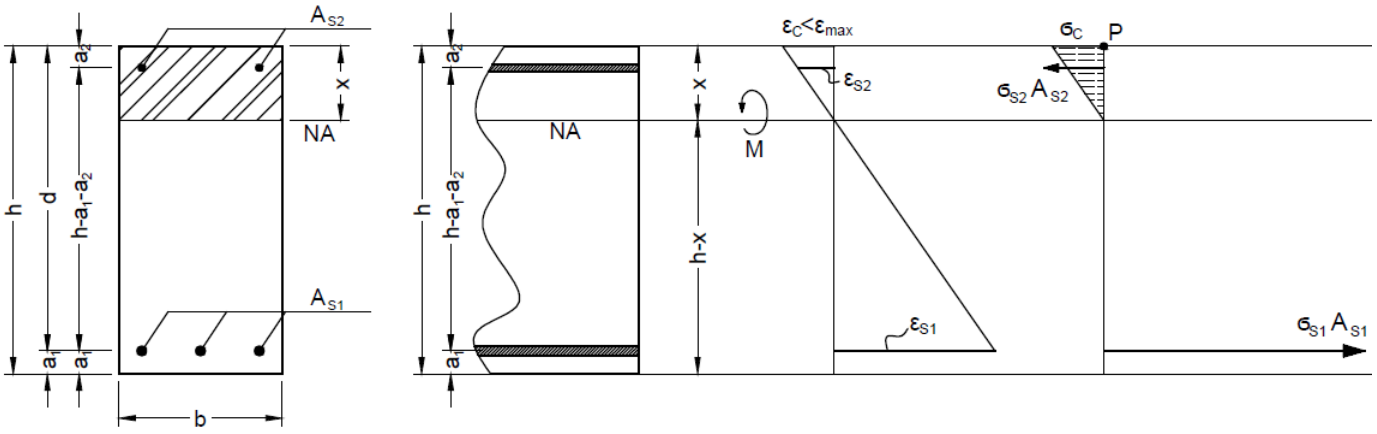

Figure 2.29: Strain and stress distribution, Approach 1 [Autocad]

The moment capacity of the section is computed under the assumption that the stress in the extreme compressed concrete fiber reaches the characteristic strength of concrete.

The stress limitations are

$$\sigma_C = \epsilon_C \cdot E_C = f_{ck} \tag{2.41}$$

$$\sigma_{S1} = \epsilon_{S1} \cdot E_S \leq f_{yk} \tag{2.42}$$

$$\sigma_{S2} = \epsilon_{S2} \cdot E_S \leq f_{yk} \tag{2.43}$$

Sometimes, depending on the type of reinforcement and the reinforcement area, the provision of limiting the maximum compressive stress of the concrete will give stresses in the rebars that exceed the yielding stress. In that case, the maximum yielding stress, which is in this case σ_{S1} is equalized with the yielding stress of the steel. ϵ_{S1}, ϵ_{S1}, ϵ_C, σ_{S1}, σ_{S2} and σ_C are recalculated, having new vales, smaller than the previous ones and proportional to them.

The strains in the reinforcements are

$$\frac{\epsilon_{S1}}{h-x-a_1} = \frac{\epsilon_C}{x} \Rightarrow \epsilon_{S1} = \frac{\epsilon_C(h-x-a_1)}{x} \tag{2.44}$$

$$\frac{\epsilon_{S2}}{x-a_2} = \frac{\epsilon_C}{x} \Rightarrow \epsilon_{S2} = \frac{\epsilon_C(x-a_2)}{x} \tag{2.45}$$

The equilibrium equation on the horizontal direction gives

$$\sigma_{S1} \cdot A_{S1} - \sigma_{S2} \cdot A_{S2} - \sigma_C \cdot x \cdot \frac{1}{2} \cdot b = 0 \tag{2.46}$$

Replacing σ_{S1} and σ_{S2} from Equations 2.41, 2.42 and 2.43 gives

$$\epsilon_{S1} \cdot E_S \cdot A_{S1} - \epsilon_{S2} \cdot E_S \cdot A_{S2} - f_{ck} \cdot x \cdot \frac{1}{2} \cdot b = 0 \tag{2.47}$$

Replacing ϵ_{S1} and ϵ_{S2} from Equations 2.41, 2.42 and 2.43 gives

$$\frac{\epsilon_C(h-x-a_1)}{x} \cdot E_S \cdot A_{S1} - \frac{\epsilon_C(x-a_2)}{x} \cdot E_S \cdot A_{S2} - f_{ck} \cdot x \cdot \frac{1}{2} \cdot b = 0 \tag{2.48}$$

Solving Equation 2.48, which is a second grade equation, gives two solutions, from which one has negative value. The positive solution is the final result for the height of the compressed fiber.

The equilibrium equation around point P gives

$$M = \frac{1}{3} \cdot \sigma_C \cdot x \cdot \frac{1}{2} \cdot b + a_2 \cdot \sigma_{S2} \cdot A_{S2} - (h-a_1) \cdot \sigma_{S1} \cdot A_{S1} \tag{2.49}$$

$$M_{R,d} = \frac{1}{6}\, f_{ck}\, b\, x^2 + \sigma_{S2}\, A_{S2}\, a_2 - \sigma_{S1}\, A_{S1}\, (h-a_1) \tag{2.50}$$

Knowing all the terms in Equation 2.50, the moment capacity of the section is obtained.

From the loading case it is known that

$$M = q \cdot \frac{L^2}{8} \tag{2.51}$$

Therefore the line load q that reaches the beam capacity is

$$q_{pl} = 8\frac{M_{R,d}}{L^2} \tag{2.52}$$

- *Approach 2, Fully plastic with zero tensile strength*

  The moment capacity of the section is computed under the assumption that the concrete develops full plasticity and the stress in the bottom (stretched) reinforcement reaches the yielding stress of the steel.

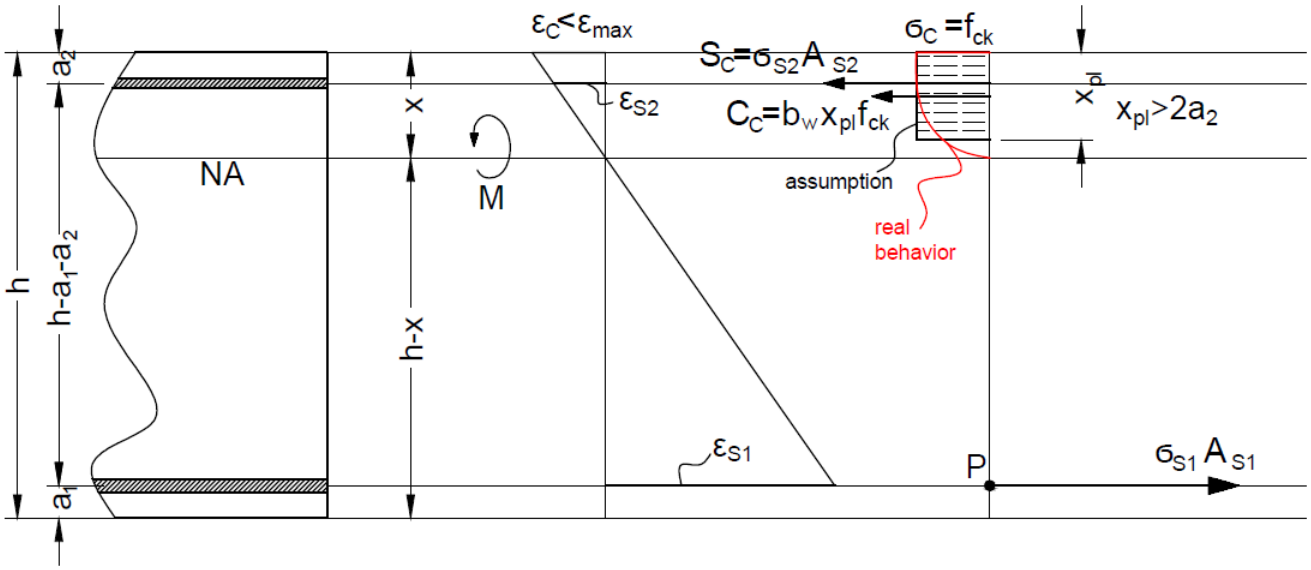

Figure 2.30: Strain and stress distribution, Approach 1, $x \geq 2a_2$ [Autocad]

$$\sigma_{S1} = f_{yk}$$

x_{pl} is the height of the compressed concrete fiber which develops full plasticity, as shown in Figure 2.30.

First, it is assumed that the top (compressed) reinforcement yields as well, see Figure 2.30, which means that

$$\sigma_{S2} = f_{yk} \Rightarrow x_{pl} \geq 2a_2$$

The equilibrium equation on the horizontal direction gives

$$S_T - S_C - C_C = 0 \tag{2.53}$$

$$A_{S1}\ f_{yk} - b_w \cdot x_{pl} \cdot f_{ck} - A_{S2}\ f_{yk} = 0 \tag{2.54}$$

$$x_{pl} \cdot b_w \cdot f_{ck} = A_{S2} \cdot f_{yk} - A_{S1} \cdot f_{yk} \tag{2.55}$$

$$x_{pl} = \frac{(A_{S2} - A_{S1}) \cdot f_{yk}}{b_w \cdot f_{ck}} \tag{2.56}$$

After obtaining x_{pl} from Equation 2.56, it is checked if the imposed condition ($x_{pl} \geq 2a_2$) is satisfied.

If the condition is fulfilled, the moment capacity is computed by applying the equilibrium condition around point P.

$$C_C \left(d - \frac{x_{pl}}{2}\right) + S_C \left(d - a_2\right) + M_{R,d} = 0 \tag{2.57}$$

$$-M_{R,d} = b_w \cdot x_{pl} \cdot f_{ck} \left(d - \frac{x_{pl}}{2}\right) + A_{S2}\ f_{yk}\ \left(d - a_2\right) \tag{2.58}$$

The minus in the expression of the moment means that the moment is acting in the opposite direction than the chosen one.

Replaing x_{pl} from Equation 2.56 and losing the minus sign turns out the final expression of the capable moment, see Equation 2.59.

$$M_{R,d} = \left(A_{S2} - A_{S1}\right) \cdot f_{yk} \left(d - \frac{\left(A_{S2} - A_{S1}\right) \cdot f_{yk}}{b_w \cdot f_{ck}}\right) + A_{S2}\ f_{yk}\ \left(d - a_2\right) \tag{2.59}$$

If the condition is not fulfilled, so ($x_{pl} < a_2$), it means that the assumptions was wrong so the compressed reinforcement does not yield. In this case, x_{pl} cannot be computed and the capable moment is calculated by applying the equilibrium equation around point Q, see Figure 2.31.

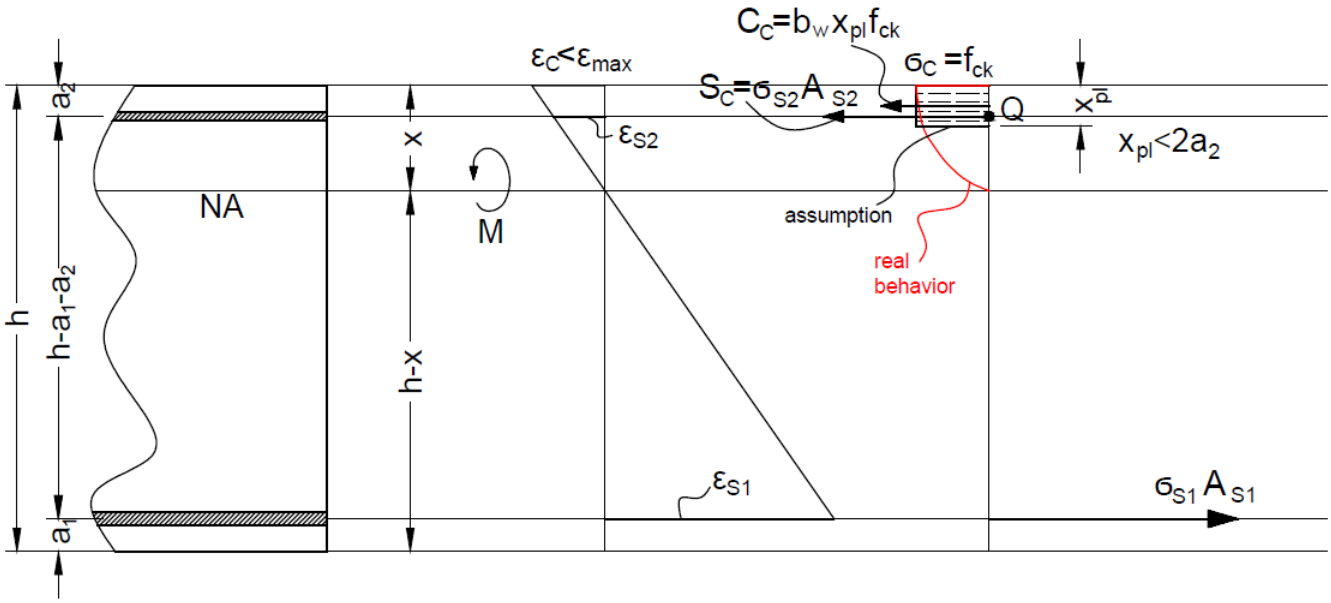

Figure 2.31: Strain and stress distribution, Approach 2, $x < 2a_2$ [Autocad]

$$S_T\ \left(d - a_2\right) + M_{R,d} + C_C\ \left(a_2 - \frac{x_{pl}}{2}\right) = 0 \tag{2.60}$$

$$-M_{R,d} = A_{S1}\ f_{yk}\ \left(d - a_2\right) + b_w \cdot x_{pl} \cdot f_{yk}\ \left(a_2 - \frac{x_{pl}}{2}\right) \tag{2.61}$$

The term $b_w \cdot x_{pl} \cdot f_{yk} \cdot \left(a_2 - \frac{x_{pl}}{2}\right)$ is neglected because $\left(a_2 - \frac{x_{pl}}{2}\right)$ is very small, and nevertheless the capable moment is obtained on the safe side. Therefore, losing the minus sign, that means that the moment acts in opposite direction than the drawn one, the capable moment is given by

$$M_{R,d} = A_{S1}\ f_{yk}\ (d - a_2) \tag{2.62}$$

A limitation of this approach is that the strain in the extreme compressed concrete fiber cannot be checked if x_{pl} is unknown.

The equivalent bending stiffness $'EI'$ of the section is now computed.
First, since the distribution of the reinforcements is not symmetrical on two directions, the centroid of the cross section will fall at $\frac{b}{2}$, but not at $\frac{h}{2}$, see Figure 2.32. It is expected that the centroid will be slightly below the half of the beam, since $A_{S1} > A_{S2}$, so the value of y_C should turnout to be negative.

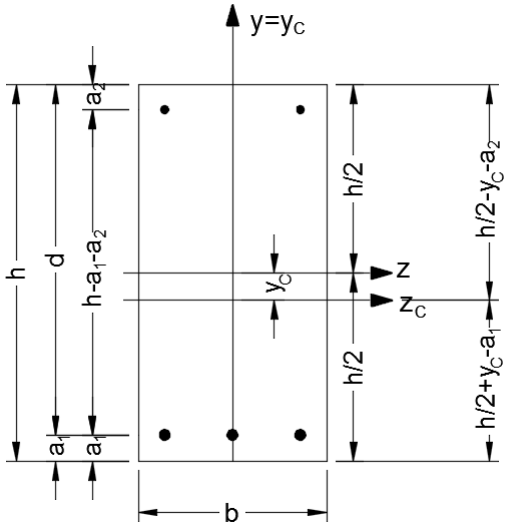

Figure 2.32: Position of the centroid [Autocad]

The static moment S_z is given by

$$S_z = \sum(y_i\ A_i) = y_C * A_T \tag{2.63}$$

In this case, the Young's modulus varies

$$S_z \cdot E_i = \sum(y_i\ A_i\ E_i) = y_C * A_T * \sum(\frac{A_i}{A_T}\ E_i) \tag{2.64}$$

The sums are developed

$$
\begin{aligned}
&- \left(\frac{h}{2} - a_1\right) A_1 \; E_S \cdot 3 + \left(\frac{h}{2} - a_2\right) A_2 \; E_S \cdot 2 - \\
&- \left(- \left(\frac{h}{2} - a_1\right) A_1 \; E_C \cdot 3 + \left(\frac{h}{2} - a_2\right) A_2 \; E_C \cdot 2\right) = \\
&= y_C \cdot b \cdot h \left(\frac{A_{S1} + A_{S2}}{A_T} E_S + \frac{A_T - (A_{S1} + A_{S2})}{A_T} E_C\right)
\end{aligned} \tag{2.65}
$$

y_C is now isolated

$$
y_C = \frac{\left(\frac{h}{2} - a_1\right) A_{S1}(E_C - E_S) + \left(\frac{h}{2} - a_2\right) A_{S2}(E_S - E_C)}{(A_{S1} + A_{S2})E_S + (bh - (A_{S1} + A_{S2}))E_C} \tag{2.66}
$$

The equivalent bending stiffness $'EI'$ can now be computed.

$$
'EI' = \int_A E \; y^2 \; dA \tag{2.67}
$$

$$
\begin{aligned}
'EI' &= \frac{1}{12} b \cdot h^3 \cdot E_C + bh \cdot y_C^2 \cdot E_C - \\
&- \left(3 \cdot \frac{\pi}{4} \left(\frac{\phi_1}{2}\right)^4 + 3A_1 \cdot \left(\frac{h}{2} - a1\right)^2 + 2 \cdot \frac{\pi}{4} \left(\frac{\phi_2}{2}\right)^4 + 3A_2 \cdot \left(\frac{h}{2} - a2\right)^2\right) E_C + \\
&+ \left(3 \cdot \frac{\pi}{4} \left(\frac{\phi_1}{2}\right)^4 + 3A_1 \cdot \left(\frac{h}{2} - a1\right)^2 + 2 \cdot \frac{\pi}{4} \left(\frac{\phi_2}{2}\right)^4 + 3A_2 \cdot \left(\frac{h}{2} - a2\right)^2\right) E_S
\end{aligned} \tag{2.68}
$$

$$
\begin{aligned}
'EI' &= \frac{1}{12} b \cdot h^3 \cdot E_C + bh \cdot y_C^2 \cdot E_C + \\
&+ \left(3 \cdot \frac{\pi}{4} \left(\frac{\phi_1}{2}\right)^4 + 3A_1 \cdot \left(\frac{h}{2} - a1\right)^2 + 2 \cdot \frac{\pi}{4} \left(\frac{\phi_2}{2}\right)^4 + 3A_2 \cdot \left(\frac{h}{2} - a2\right)^2\right) (E_S - E_C)
\end{aligned} \tag{2.69}
$$

Knowing the equivalent bending stiffness, the displacement can now be computed.

$$
v(x) = \frac{1}{'EI'} \int M m_0 \; dx + \frac{\beta}{G_C A^\star} \int V v_0 \; dx \tag{2.70}
$$

G_C is taken as the shear modulus for concrete.

$$
G_C = \frac{E_C}{2(1 + \nu_C)} \tag{2.71}
$$

2.2.2 Abaqus 3D FEA

First, a concrete cube with the side equal to 150 mm is created in Abaqus, see `'Cube150.cae'` in the electronic appendix. The cube is meshed with ten Hex elements of side 15 mm, see Figure 2.33. Hex elements are 8 node 3D elemnts. The purpose is to observe the stress-strain diagram for different load cases and to understand how does Abaqus model concrete.

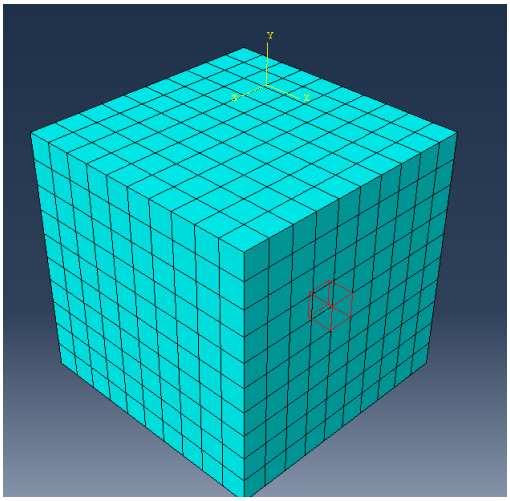

Figure 2.33: Concrete cube 150 mm [Abaqus]

The boundary conditions are imposed such that the red face in Figure 2.34 has restricted motion on x axis, the bottom horizontal red side has restricted motion on y axis and the right vertical red side has restricted motion on the z axis. The arrows show the position of the imposed displacement, which for Figure 2.34 causes compression.

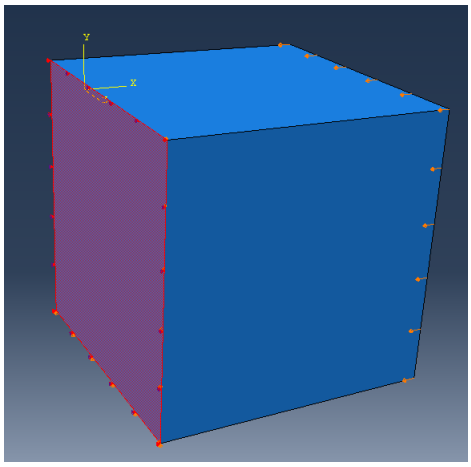

Figure 2.34: Cube 150 mm - Boundary Conditions [Abaqus]

The chosen failure criterion is Concrete Damage Plasticity, with standard default coefficients, see Abaqus User Manual for further details on Concrete Damage Plasticity model. The manual comes along with the installation of the program an it can be easily accessed by the Help function.

Four tests are performed, each of them for different imposed displacements, in compression and tension. The displacements are applied to the face that opposes the one bounded by restricted motion on x axis.

In Test 1 and Test 2, the stress-strain curve of the material is only defined by one compression yield stress and one tensile yield stress, see Figure 2.35. For Test 3 and Test 4, the material is defined with extra fineness, see Figure 2.36.

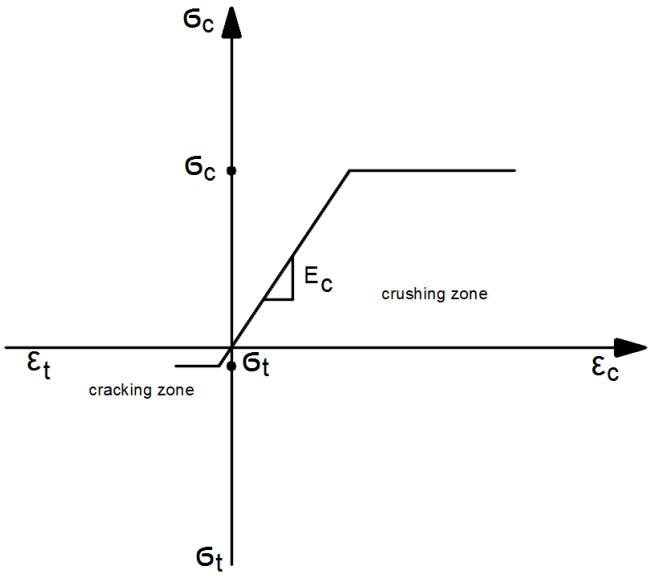

Figure 2.35: Test 1 and 2 approach for material behavior [Autocad]

σ_c	25 MPa
σ_t	2.2 MPa

The compression curve in Figure 2.36 is obtained by third order polynomial Equation 2.72, which is obtained empirically.

$$\frac{f}{f_0} = 2.1\left(\frac{\epsilon}{\epsilon_0}\right) - 1.33\left(\frac{\epsilon}{\epsilon_0}\right)^2 + 0.2\left(\frac{\epsilon}{\epsilon_0}\right)^3 \tag{2.72}$$

The coefficients in Equation 2.72 are

f_0	25 MPa
ϵ_0	0.22 %
ϵ_{min}	0.00 %
ϵ_{max}	0.35 %

The coordinates of the black dots in Figure 2.36 are read for future implementation in Abaqus.

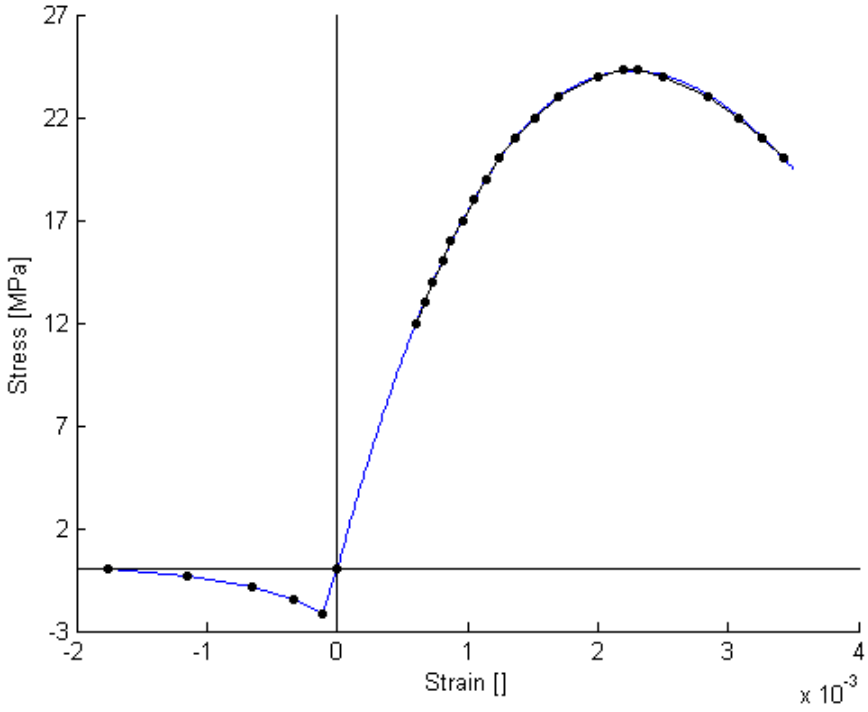

Figure 2.36: Test 3 and 4 approach for material behavior [Matlab]

In Test 1 and Test 3, the imposed displacement is applied statically. In Test 2 and Test 4, the displacement is applied dynamically implicit, in 10 ten steps, each of the steps being equal to 1 second. The imposed displacement increases every step by one tenth until reaching the desired value. These different approaches are performed to see if there is any difference in the response if the load is applied slowly. In all the tests, the element for which the strains and stresses are read is the one marked with red in Figure 2.33.

- *Test 1. Simplified stress-strain curve, Static*

  This test is performed for three different applied compressive displacements.

u_{c1}	0.1 mm red
u_{c2}	0.5 mm blue
u_{c3}	1.0 mm green

  In this approach, it is hard to define a stress-strain curve since Abaqus only shows the stress and strain corresponding to the final state of the element. However, it can be observed in Figure 2.37 that the three points lay on the compression curve pattern from Figure 2.35.

  For the tension test, with imposed displacements u_{t1}, u_{t2} and u_{t3} the results are shown in Figure 2.38. It is observed that the points lay on the tensile pattern described in Figure 2.35.

u_{t1}	0.01 mm red
u_{t2}	0.10 mm blue
u_{t3}	0.50 mm green

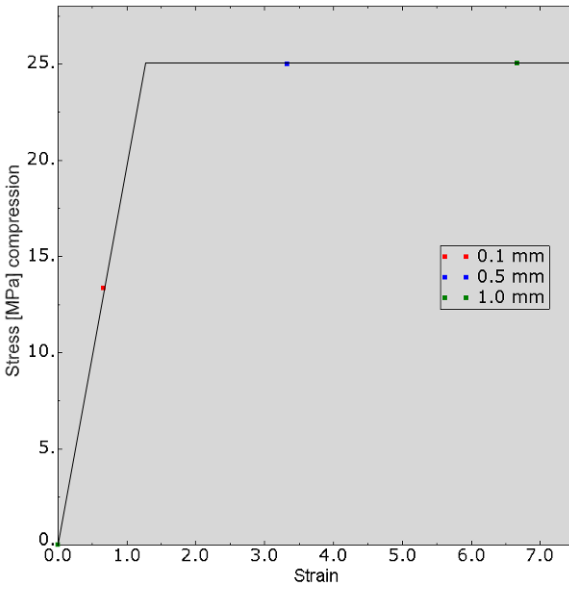

Figure 2.37: Test 1 compression [Abaqus]

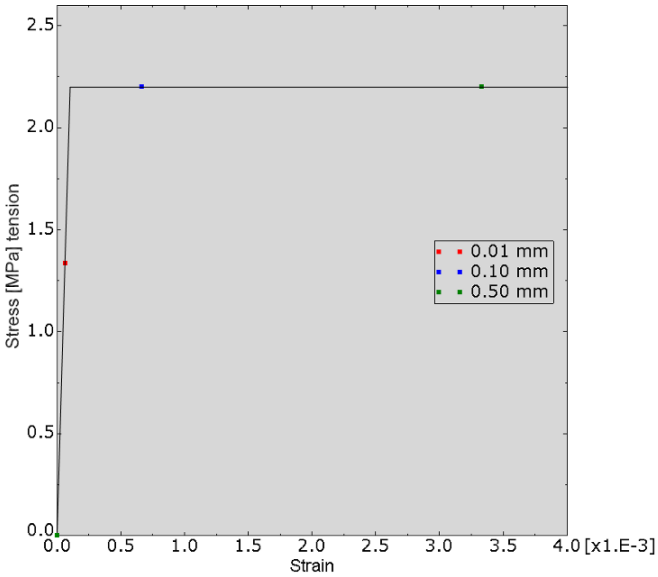

Figure 2.38: Test 1 tension [Abaqus]

- *Test 2. Simplified stress-strain curve, Dynamic implicit*

  As it will be seen, when applying the displacement slowly, the material undertakes less stress, so the internal stresses and strains will be smaller. For this reason, new compressive imposed displacements are used .

u_{t1}	1.00 mm red
u_{t2}	2.00 mm blue
u_{t3}	3.00 mm green

  The results are shown in Figure 2.39.

  It can be observed that, for a displacement of 1.00 mm, the element only undertakes approximately half of the stress that the same displacement induced in Test 1.

  For tension, same displacements as for Test 1 are used. The results are presented in Figure 2.40.

  It can be observed that, for same displacements, the element undertakes less tensile stresses when the load is applied slowly

- *Test 3. Detailed stress-strain curve, Static*

  For the sake of simplicity, only the compressive behavior is studied, since it is the dominant one.

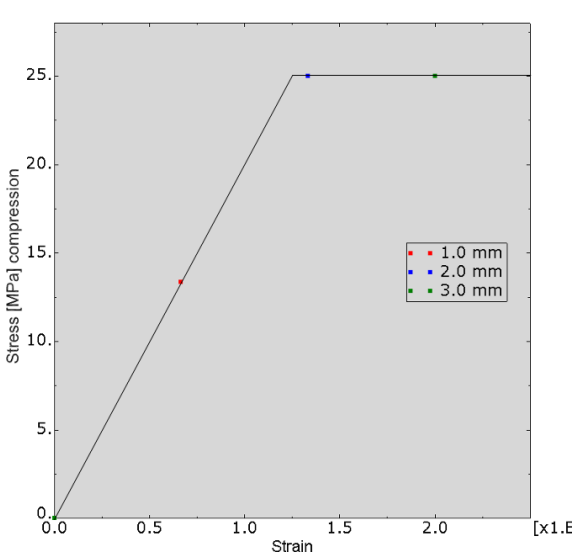

Figure 2.39: Test 2 compression [Abaqus]

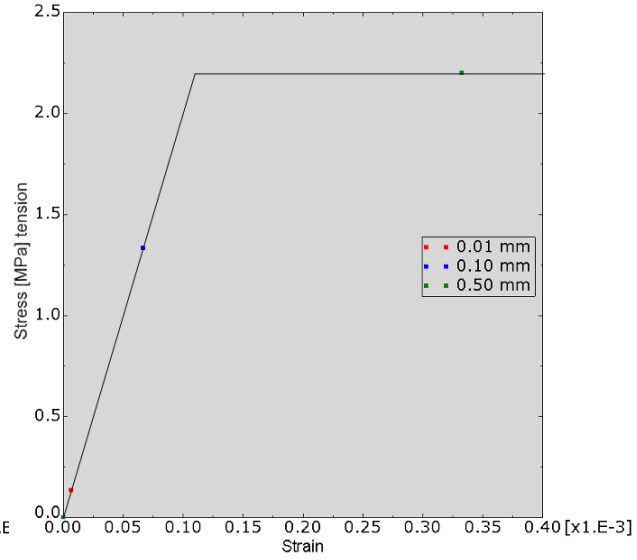

Figure 2.40: Test 2 tension [Abaqus]

The strains are defined by means of inelastic strains, which in other literature can be found by the name of plastic strains. Figure 2.41 describe how plastic strains are defined. The sample first deforms elastic along the Young's modulus and the plastification occurs, i.e. the pattern is no longer linear, reaching point P on the curve. In Figure 2.42 it can be see that for a point P of stress 23 MPa, the plastic strain is equal to 0.0017.

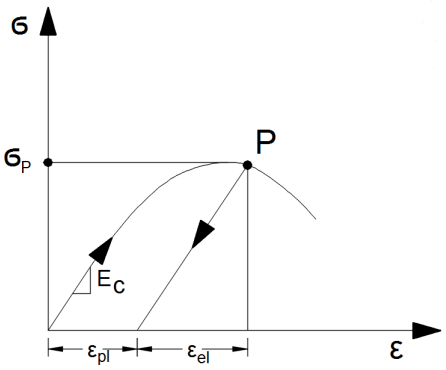

Figure 2.41: Elastic strain, plastic strain [Autocad]

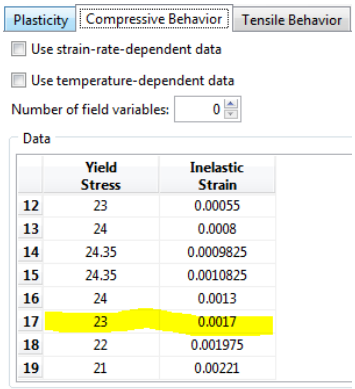

	Yield Stress	Inelastic Strain
12	23	0.00055
13	24	0.0008
14	24.35	0.0009825
15	24.35	0.0010825
16	24	0.0013
17	23	0.0017
18	22	0.001975
19	21	0.00221

Figure 2.42: Defining the plastic strains [Abaqus]

ϵ_{el}	elastic strain
ϵ_{pl}	inelastic strain or plastic strain

The results for different imposed compressive displacements are presented in Figure 2.43.

Just like in Figure 2.36, the maximum stress is almost 25 MPa and then it goes down to about 20 MPa for which it has the strain value of 0.35%. Abaqus considers an infinitely

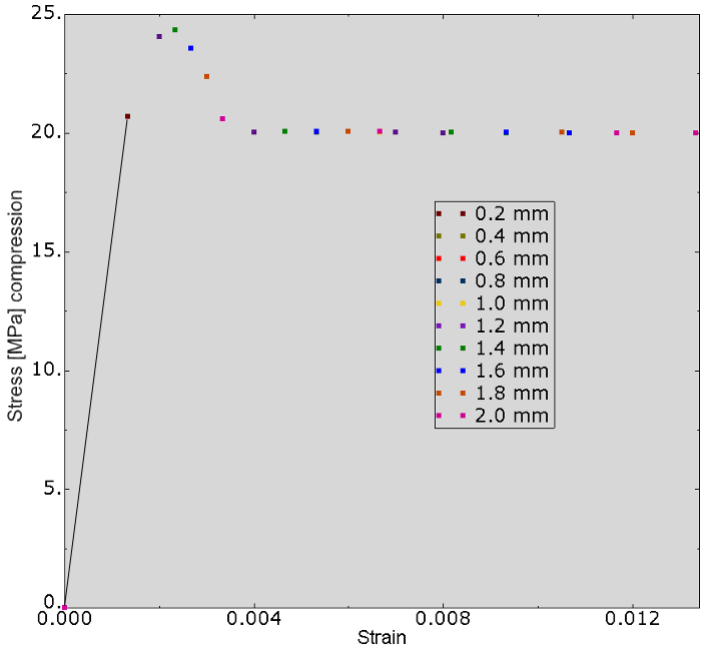

Figure 2.43: Test 3 compression [Abaqus]

long yielding plateau after that point, but strains larger than 0.35% are interpreted as failure. Therefore, in this example the only cases when failure doesn't occur are for 0.2 mm and 0.4 mm.

- *Test 4. Detailed stress-strain curve, Dynamic implicit*

  In this test, it is also the compressive behavior that is of interest.

  The results are shown in Figure 2.44.

  It is observed that the points fit perfectly the behavior defined in Figure 2.36.

Now that several ways of defining concrete in Abaqus, as a material, have been defined, it is time to create a doubly reinforced concrete beam.

The model, that can be found in the electronic appendix in the file `'Thesis2.cae'` has three Parts, each of them defined as Solid Deformable 3D Bodies.

- *The plain concrete beam*

  The plain concrete beam is simply a rectangular parallelepiped with dimensions

b	250 mm
h	500 mm
L	3100 mm

  The element is constructed and the material concrete is assigned to it, first under Test 1 assumptions, see Figure 2.45

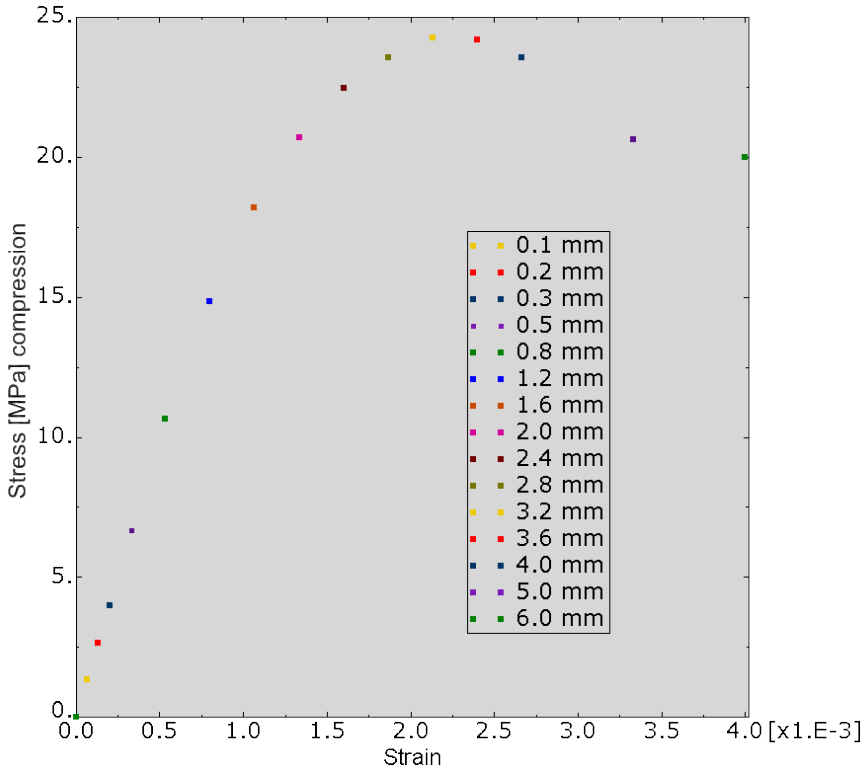

Figure 2.44: Test 4 compression [Abaqus]

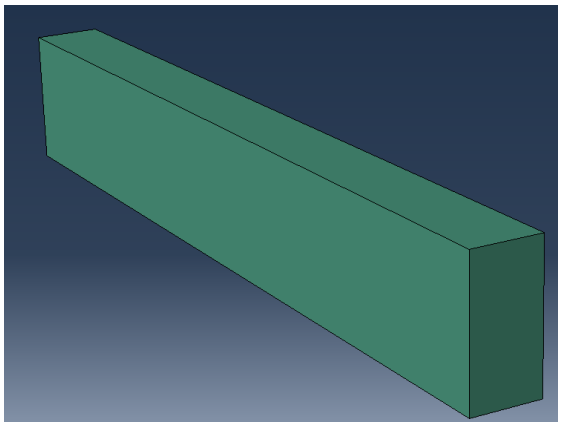

Figure 2.45: Plain concrete beam [Abaqus]

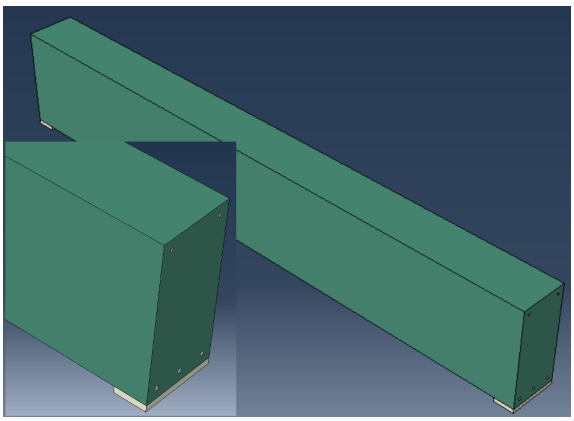

Figure 2.46: The merged beam [Abaqus]

- *The reinforcements*

  The reinforcements, i.e. $3\phi14$ down and $2\phi10$ up of length 3100 mm, are constructed. The concrete cover is, from the extreme fiber to the rebar axis

a_1	35 mm bottom concrete cover
a_2	33 mm top concrete cover

  After the Part is constructed, the material steel is assigned to it, see Figure 2.47.

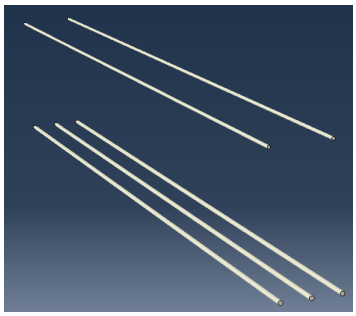

Figure 2.47: Rebars [Abaqus]

Figure 2.48: Steel Plates [Abaqus]

- *The supporting plates*

  The two supporting plates have dimensions of 20 mm x 100 mm x 250 mm and are also made of steel, see Figure 2.48. They are used in order to avoid concentrated stress points in the supports area. The distance between the center of the plates is 3000 mm.

After defining the Parts, an Instance is created by merging the previously defined elements and keeping the boundary contours, see Figure 2.46.

At this step, the meshing has to be performed. To ensure, as much as possible, a uniform and symmetric mesh, which will decrease the computational time of the analysis and also give better results, some cutting planes are defined as shown in Figure 2.49. The meshing is now done, using Hex 8 nodes elements. The meshed beam is shown in Figure 2.50.

The boundary conditions in the support are defined such that the beam is simply supported. One of the supports has restricted motion on y *axis* and x *axis* and the other support has restricted motion on y *axis*, see Figure 2.51.

The uniformly distributed load is now applied on the top of the beam as shown in Figure 2.52. The maximum vertical displacement is computed for different values of the load and the results are shown in Table 2.3.

Gravity is not included in the analysis.

The results are also shown in a graph in Figure 2.54. The pattern of the vertical displacement field can be observed in Figure 2.53.

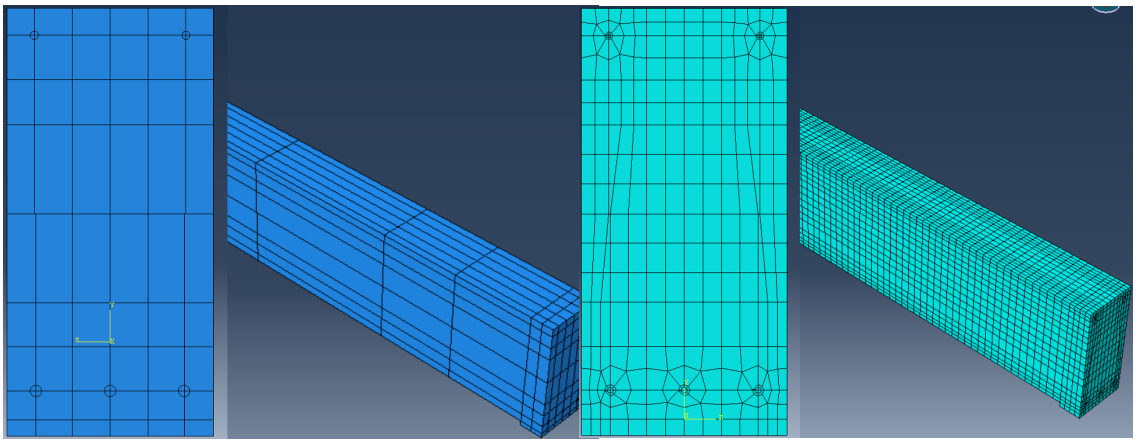

Figure 2.49: The partition planes [Abaqus]

Figure 2.50: Beam mesh [Abaqus]

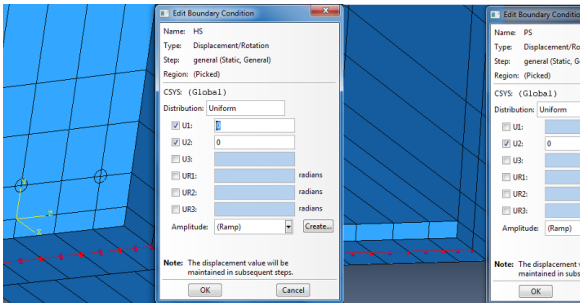

Figure 2.51: Beam boundary conditions [Abaqus]

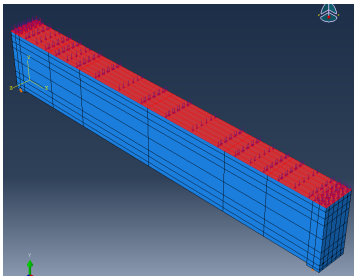

Figure 2.52: Load on beam [Abaqus]

$Q[\frac{N}{mm^2}]$	$q[\frac{N}{mm}]$	$v[mm]$
0.08	20	0.41
0.16	40	0.96
0.24	60	2.03
0.32	80	3.46
0.36	90	4.27
0.40	100	5.12

Table 2.3: Vertical displacement for different loads, solid rebars

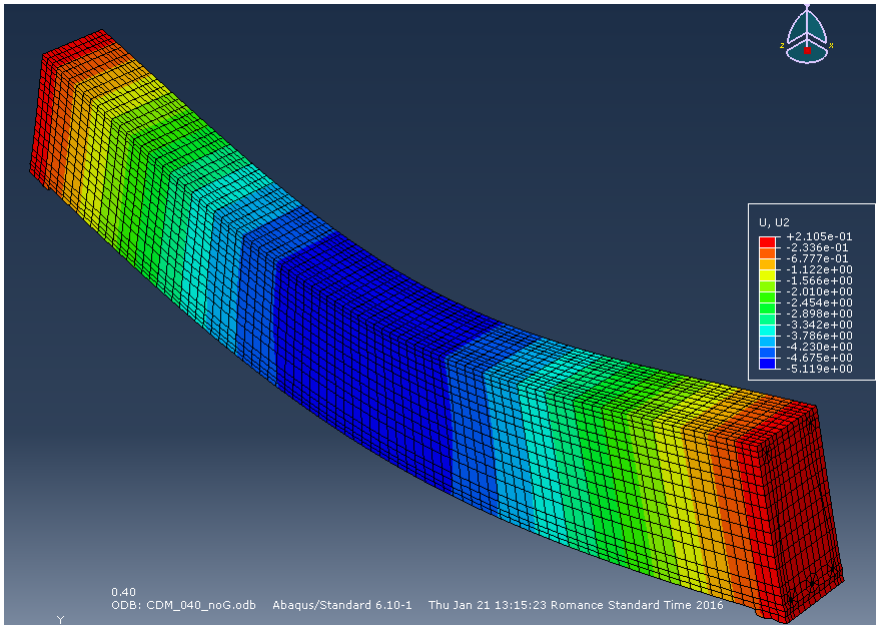

Figure 2.53: Vertical displacement field, solid rebars $Q = 0.4\frac{N}{mm^2}$ [Abaqus]

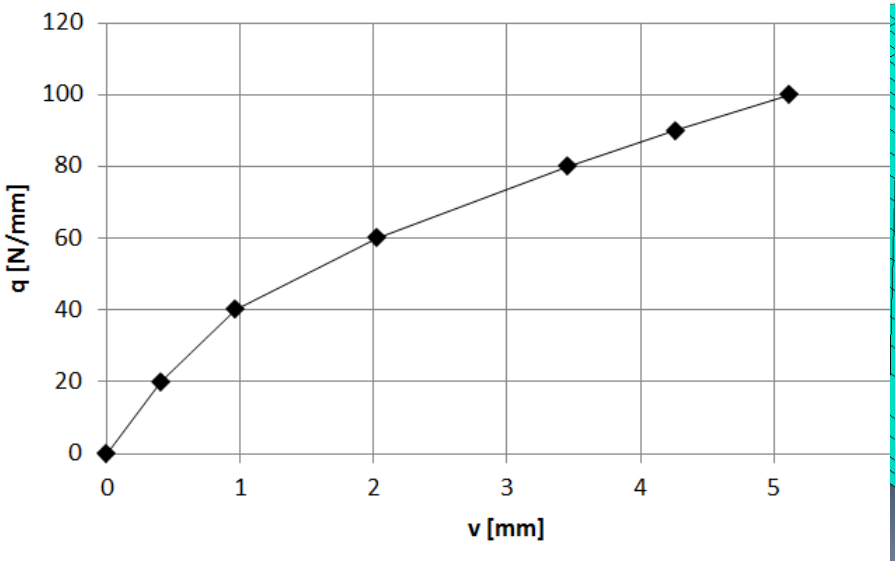

Figure 2.54: Load displacement curve [Microsoft Excel]

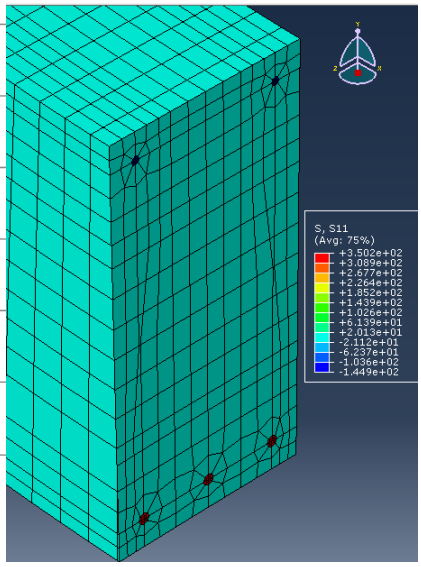

Figure 2.55: Normal stress at half beam, solid rebars, $Q = 0.4\frac{N}{mm^2}$ [Abaqus]

As expected, the normal stresses are compressive in the top reinforcement and tensile in the bottom reinforcement, see Figure 2.55, where it can also be seen that the stretched reinforcement has yielded.

Because the lack of computational power, this beam cannot be analyzed when the material and loads are described by the methods used in Test 2, Test 3 and Test 4. The analysis cannot be completed on a normal computer.

Another way to model reinforced concrete is to model reinforcements as wire. The wire feature is used to describe solid elements that have one of the dimensions much greater than the other two. This approach allows a faster analysis, due to the reduced number of elements, since the mesh is more compact and simple, see Figure 2.57.

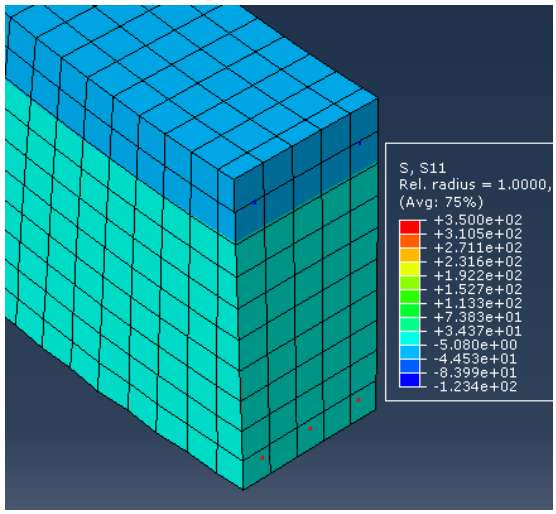

Figure 2.56: Normal stress at half beam, wire rebars, $Q = 0.44\frac{N}{mm^2}$ [Abaqus]

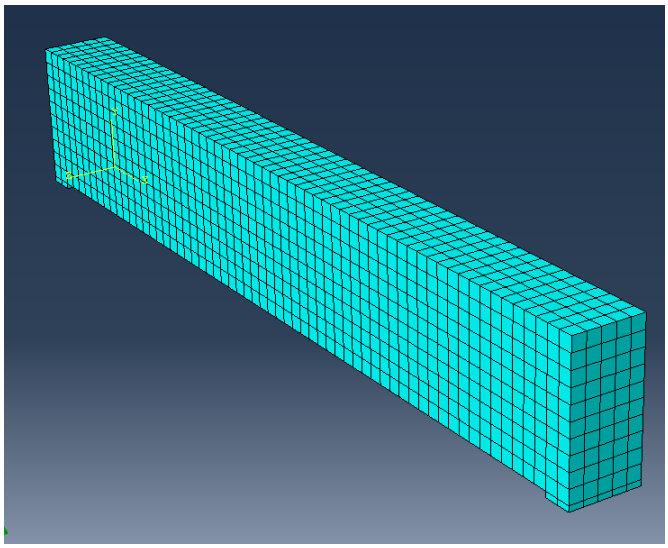

Figure 2.57: Beam mesh, wire rebars [Abaqus]

The maximum vertical displacement for various loads is shown in Table 2.4.

The normal stresses at half beam for an applied load of 0.44 $\frac{N}{mm^2}$ are shown in Figure 2.56. It is observed that the stress in the stretched reinforcement reached yielding, i.e $350MPa$ and the stress in the compressed reinforcement is $123MPa$.

For $Q = 0.5$ $\frac{N}{mm^2}$ it is clear the the beam fails, since the revealed vertical displacement is about 60 cm. The normal stress in all the rebars reached yielding in this loading case.

The advantage of this method of modelling reinforced concrete i.e., wire rebars, is that it allows analyzing the structure when subjected to higher loads then when rebars are modeled as solid. Failure in this case can also be perceived visually. In contrast to Figure 2.53, Figure 2.58 shows

$Q[\frac{N}{mm^2}]$	$q[\frac{N}{mm}]$	$v[mm]$
0.08	20	0.42
0.16	40	0.98
0.24	60	2.02
0.32	80	3.42
0.36	90	4.22
0.40	100	5.03
0.44	110	6.83
0.50	125	585.7

Table 2.4: Vertical displacement for different loads, wire rebars

the vertical displacement field, where it can be observed that the plastification and failure occurred due to the curved shape of the displacement field at half beam.

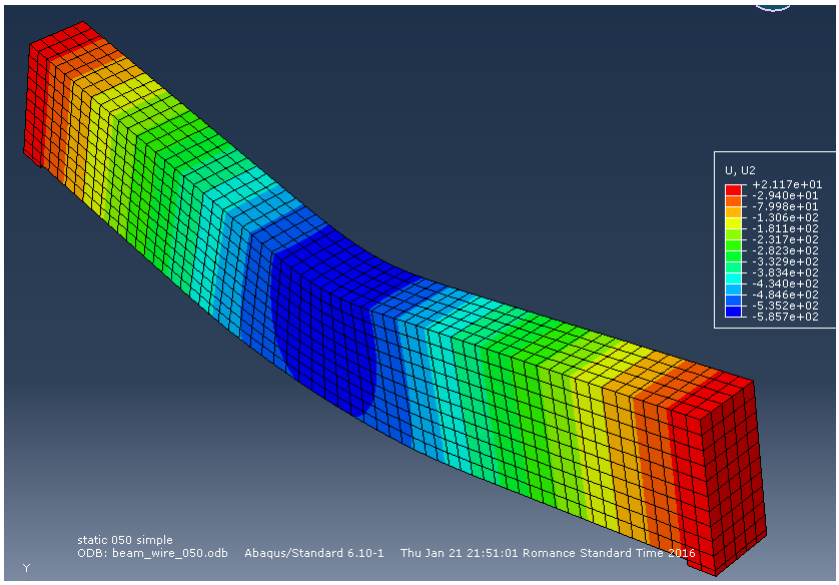

Figure 2.58: Vertical displacement field, wire rebars $Q = 0.5\frac{N}{mm^2}$ [Abaqus]

For the loads the allowed the analysis by both methods of modelling the reinforcement, i.e. with values for Q between $0.08\frac{N}{mm^2}$ and $0.40\frac{N}{mm^2}$, the vertical displacement is the same.

Even though the wire rebar method has some advantages compared do the solid rebar method, the analysis cannot be ran either for assumptions in Test 2, Test 3 and Test 4 on a normal computer, the problem in this case being the computational power.

2.2.3 Results, Comparison and Conclusion

A code is developed in the program Matlab that allows calculation of the moment capacity, centroid position and equivalent bending stiffness for any dimensions of the cross section and any layout

of the reinforcement. Basically, all the previous calculations are encoded s.t. the user can apply them for any example. The code also draws a sketch of the section, so any mistake in the input can be tracked down easily. The file is entitled `'BeamSection.m'` and can be found in the electronic appendix.

Three examples of input used by the code, with the corresponding cross sections sketches given by the code output, are presented in Figure 2.59, Figure 2.60, Figure 2.61.

The characteristic strength of concrete is chosen 25 MPa. Since this thesis has analysis as a purpose and not design, the strength of the concrete is not reduced by any safety factor. The yielding stress of the steel is chosen 355 MPa. The dimensions of the beam cross-section are 250 mm in width and 500 mm in height.

Example 1

```
%% INPUT
b= 250; %width of the be
h= 500; %height of the b

a1= 35; %concrete cover
a2= 33; %concrete cover

%If there will be more t
%two rebars will be plac

diam_1=[14 14 14]; %vect
diam_2=[10 10]; %vector

r1=0; %distance between
r2=0; %distance between

diam_row_1=[0]; %diamete
diam_row_2=[0]; %diamter of the top rebars from the second row on [mm]

fc=25; %compressive strength of concrete [MPa]
fy=355; %yield strength of steel [MPa]
E_S=210*10^3; %Young's modulus for steel [MPa]
E_C=20*10^3;  %Young's modulus for concrete [MPa]
```

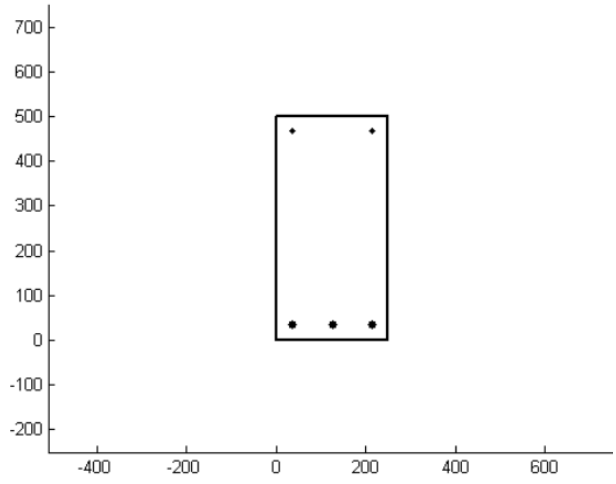

Figure 2.59: 3 ϕ 14 bottom, 2 ϕ 10 top[Matlab]

Example 2

```
%% INPUT
b= 250; %width of the b
h= 500; %height of the

a1= 35; %concrete cover
a2= 33; %concrete cover

%If there will be more
%two rebars will be pla

diam_1=[16 16 16 16]; %
diam_2=[12 12]; %vector

r1=0; %distance between
r2=0; %distance between
```

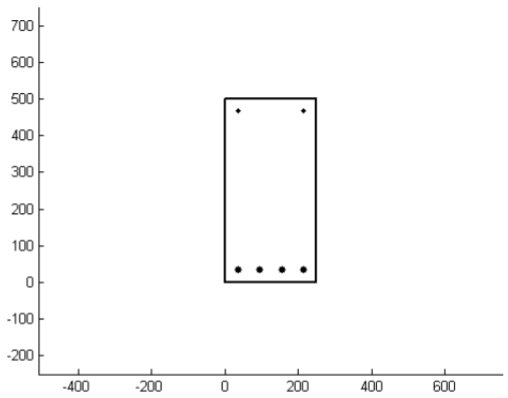


```
diam_row_1=[0]; %diameter of the bottom rebars from the second row on
diam_row_2=[0]; %diamter of the top rebars from the second row on [mm]

fc=25; %compressive strength of concrete [MPa]
fy=355; %yield strength of steel [MPa]
E_S=210*10^3; %Young's modulus for steel [MPa]
E_C=20*10^3;  %Young's modulus for concrete [MPa]
```

Figure 2.60: 4 ϕ 16 bottom, 2 ϕ 12 top [Matlab]

Example 3

```
%% INPUT
b= 250; %width of the
h= 500; %height of th

a1= 35; %concrete cov
a2= 33; %concrete cov

%If there will be mor
%two rebars will be p

diam_1=[16 16 16 16];
diam_2=[12 12 12]; %v

r1=40; %distance betw
r2=0; %distance betwe
```

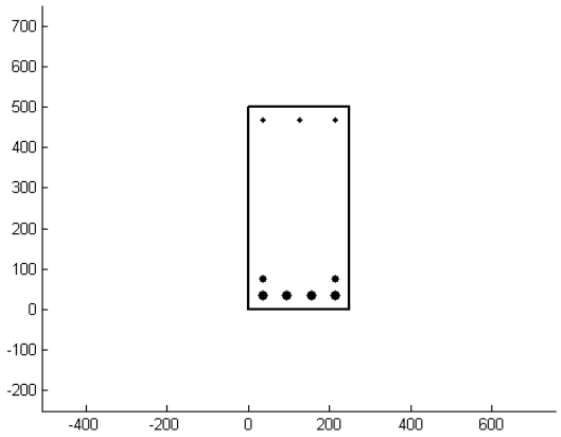


```
diam_row_1=[14]; %dia
diam_row_2=[0]; %diamter of the top rebars from the second row on [mm]

fc=25; %compressive strength of concrete [MPa]
fy=355; %yield strength of steel [MPa]
E_S=210*10^3; %Young's modulus for steel [MPa]
E_C=20*10^3;  %Young's modulus for concrete [MPa]
```

Figure 2.61: 4 ϕ 16 + 2 ϕ 14 bottom, 3 ϕ 12 top [Matlab]

The results for each example are shown in Table 2.5. It is observed that moment capacity computed by Approach 1 is very close to the one computed by Approach 2, almost identical for many of the examples. The with errors vary between 1 % and 3 % for Example 1 and Example 2, as for Example 3, the error is about 6 %. It was expected that Example 3 has the highest error margin because it has the most complicated layout. This fact, that the moment capacity results are similar by both approaches, is encouraging for the future use of the Matlab code, for analysis and also design purposes.

	Approach 1		Approach 2		All section		Active section bottom	
	$M_{R,d}^{bottom}$ $[Nmm]$	$M_{R,d}^{top}$ $[Nmm]$	$M_{R,d}^{bottom}$ $[Nmm]$	$M_{R,d}^{top}$ $[Nmm]$	y_C $[mm]$	$'EI'$ $[Nmm^2]$	$y_C^\star$ $[mm]$	$'EI'^\star$ $[Nmm^2]$
Ex 1	$7.007 \cdot 10^7$	$2.459 \cdot 10^7$	$7.082 \cdot 10^7$	$2.409 \cdot 10^7$	-4.733	$5.749 \cdot 10^{13}$	-51.461	$1.345 \cdot 10^{13}$
Ex 2	$1.196 \cdot 10^8$	$3.513 \cdot 10^7$	$1.233 \cdot 10^8$	$3.469 \cdot 10^7$	-8.728	$6.097 \cdot 10^{13}$	-64.789	$2.119 \cdot 10^{13}$
Ex 3	$1.540 \cdot 10^8$	$5.203 \cdot 10^7$	$1.644 \cdot 10^8$	$5.187 \cdot 10^7$	-10.484	$6.367 \cdot 10^{13}$	-71.942	$2.610 \cdot 10^{13}$

Active section top	
$y_C^\star$ $[mm]$	$'EI'^\star$ $[Nmm^2]$
29.065	$5.358 \cdot 10^{13}$
32.007	$7.535 \cdot 10^{12}$
38.181	$1.082 \cdot 10^{13}$

Table 2.5: Results for various cross sections

The values for the height of the compress zone x, for each example, are shown in Table 2.6.

x	Ex 1	Ex 2	Ex 3
$[mm]$	113.05	119.41	157.16

Table 2.6: Height of the compressed area

$M_{R,d}^{bottom}$ is the moment capacity when the moment diagram is drawn on the bottom part of the beam, i.e. the stretched fiber is down. It is the case for the example used, where the simply supported beam is uniformly loaded with a distributed load. Sometimes, when the beams have embedded supports, the moment diagram is drawn on the top side of the beam, i.e the stretched fiber is up, in the vicinity of the supports, see Figure 2.62.

When subjected to seismic loads, the beam have an envelope moment diagram which is drawn on both bottom and top side, see Figure 2.63.

Therefore, it is useful to know the capacity of the beam section for both bottom and top side. Since the calculations are performed by a computer program, when needed in the future for other examples, the input for that specific case can be introduced and the results will turnout without having to perform other computations. This is the major benefit of computer coding.

y_C represents the distance from the center of the rectangle to the centroid of the cross section, see

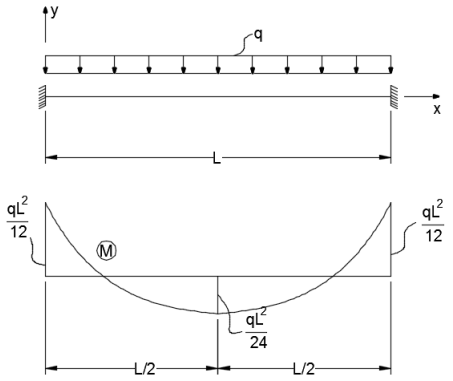

Figure 2.62: Fixed beam at both ends loaded uniformly [Autocad]

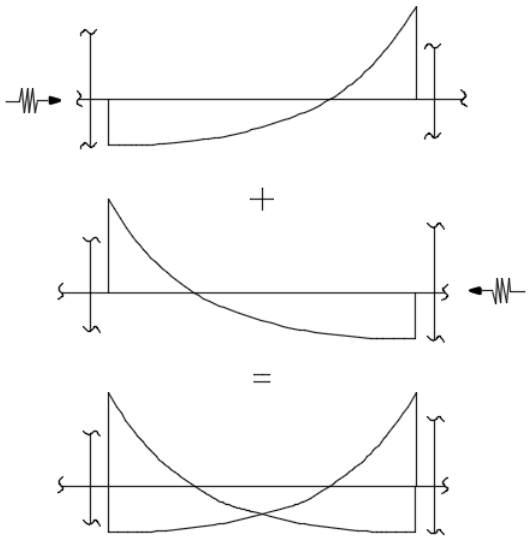

Figure 2.63: Envelope moment diagram [Autocad]

Figure 2.32. The positive sign means that y_C is located above the center of the rectangle, while the negative signs means that y_C is located below the center of the rectangle.

$'EI'$ is the bending stiffness equivalent to the cross section, which in this case is composed of steel and concrete. $'EI'$ is written between the inverted comas because there is not only one E involved, but both Young's modulus of steel and Young's modulus of concrete have a contribution.

$y_C^\star$ and $'EI'^\star$ represent the position of the centroid and the equivalent bending stiffness for a section that comprises the steel and only the compressed area of the concrete, see Figure 2.64. When $y_C^\star$ and $'EI'^\star$ are calculated for 'Active section top', which means the case where the moment diagram is drawn above the beam, i.e. the top fiber is the stretched fiber. The compression area is a different one in that case, so $y_C^\star$ and $'EI'^\star$ will have different values.

`'BeamSection.m'` also calculates the values of the normal stresses in the reinforcements corresponding to the capable bending moment. The results are shown in Table 2.7. The stresses in the rebars are the same in Approach 1 and Approach 2.

	σ_{S11} $[MPa]$	σ_{S12} $[MPa]$	σ_{S2} $[MPa]$
Ex 1	355	N/A	80.7
Ex 2	355	N/A	119.4
Ex 3	355	308.9	143.2

Table 2.7: Normal stress in the reinforcements

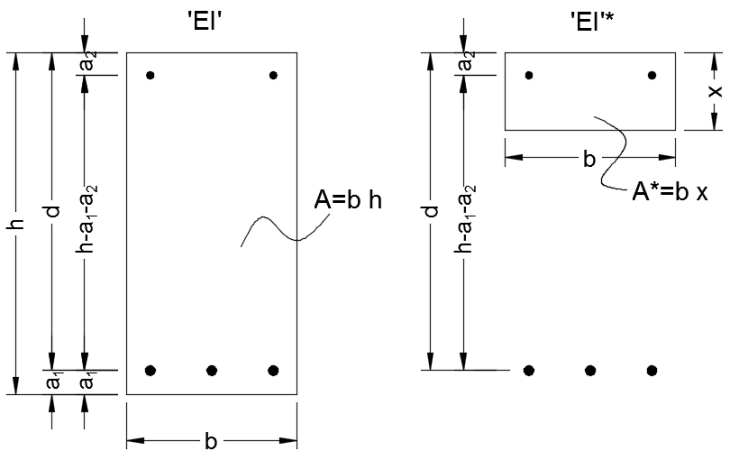

Figure 2.64: Equivalent bending stiffness [Autocad]

For the calculation of the displacements by the analytical method to be valid, the line load q needs to be less or equal than q_{pl}, see Equation 2.51. The minimum capable moment from all the examples is $7.007 \cdot 10^7$, from Example 1, which gives

$$q_{pl} = 62.222 \ [N/mm]$$

The chosen values of loads used for computing the maximum displacement, i.e. the displacement at the half of the beam are shown in Table 2.8.

q_1 $[N/mm]$	q_2 $[N/mm]$	q_3 $[N/mm]$
20	40	60

Table 2.8: Chosen values for line loads

The displacements are calculated by another code, named `'Thesis.m'` that can also be found in the electronic appendix. The results represent the total displacement, i.e. the sum between the Bernoulli-Euler (Moment) component and the Timoshenko (Shear) compoment.

Table 2.9 shows the values of the displacements when all the section is considered and Table 2.10 shows the values of the displacements when the equivalent bending stiffness $'EI'$ and area $A^\star$ are taken for the active area, i.e. compressed concrete area plus reinforcements.
The results, when gravity is included, are 5% higher for q_3, 8% higher for q_2 and 15% higher for q_1. In other words, the higher the load, the less the contribution of gravity, because the load increases, while the self weight remains constant. There is a big difference in results between using all the section and using only the active area, almost 400%. Therefore, using the correct value for the bending stiffness is very important. It is expected that the results for the displacements computed in Abaqus to be between these values, because even though just part of the section, i.e. the com-

v_{max} $[mm]$	q_1	q_2	q_3	q_1	q_2	q_3
Ex 1	0.38	0.77	1.15	0.44	0.83	1.21
Ex 2	0.36	0.73	1.09	0.42	0.78	1.15
Ex 3	0.35	0.70	1.05	0.4	0.75	1.10
	No gravity			Gravity included		

Table 2.9: Displacements for various loads

$v^{\star}_{max}$ $[mm]$	q_1	q_2	q_3	q_1	q_2	q_3
Ex 1	1.65	3.29	4.94	1.89	3.54	5.18
Ex 2	1.07	2.14	3.21	1.23	2.30	3.37
Ex 3	0.86	1.73	2.59	0.99	1.86	2.72
	No gravity			Gravity included		

Table 2.10: Displacements for various loads

pressed part undertakes stresses, the stretched area is still creating extra stiffness.

It is observed that, the displacements computed in Abaqus are indeed in-between the values of the two analytical section considerations and that they are more close to the ones pertinent to the case where the whole section is considered.

$Q[\frac{N}{mm^2}]$	$q[\frac{N}{mm}]$	$v^{solid\ rebars}_{Abaqus}[mm]$
0.08	20 (q_1)	0.41
0.16	40 (q_2)	0.96
0.24	60 (q_3)	2.03
0.32	80	3.46
0.36	90	4.27
0.40	100	5.12

$Q[\frac{N}{mm^2}]$	$q[\frac{N}{mm}]$	$v^{wire\ rebars}_{Abaqus}[mm]$
0.08	20 (q_1)	0.42
0.16	40 (q_2)	0.98
0.24	60 (q_3)	2.02
0.32	80	3.42
0.36	90	4.22
0.40	100	5.03
0.44	110	6.83
0.50	125	585.7

3 Earthquake excitation

In this chapter, the response of certain structures under the action of earthquake is studied by numerical methods. The purpose is to understand the finite element concepts and build up the tools for analyzing more complicated structures.

A finite element code developed in the program Matlab, as well as the commercial finite element program Abaqus are used.

3.1 Rectangular cross-section steel column

First, to ensure that the analysis by both, Matlab FEM and Abaqus FEM, gives valid results, a simple structure such as rectangular section steel column is studied.

The column is fixed at the bottom and has the length L, while the cross section is described by a square of side length b, see Figure 3.1.

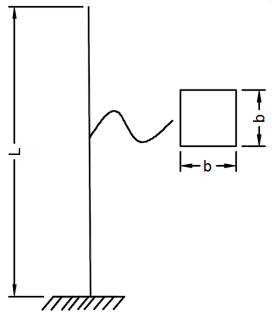

Figure 3.1: Steel column, static scheme [Autocad]

Two different accelerograms are implemented, separately, to the fixed support, i.e. the North-South acceleration component of the El Centro 1940 Earthquake and the North-South component of the Vrancea 1977 Earthquake. The North-South component is the one chosen because it has the highest peak accelerations for both of the earthquakes, as it can be observed in Figure 3.2 and Figure 3.3. The data for the El Centro Earthquake is provided by `http://vibrationdata.com` and the data for Vrancea Earthquake is provided by URBAN INCERC, i.e. Romania's National Institute of Research in Construction.

By applying fft, which is a function that makes the transition from the time domain to the frequency domain, to these accelerograms, the energy release in the frequency domain, for each of the earthquakes can be seen in Figure 3.4 and Figure 3.5. The frequency spectra are also based on the North-South data.

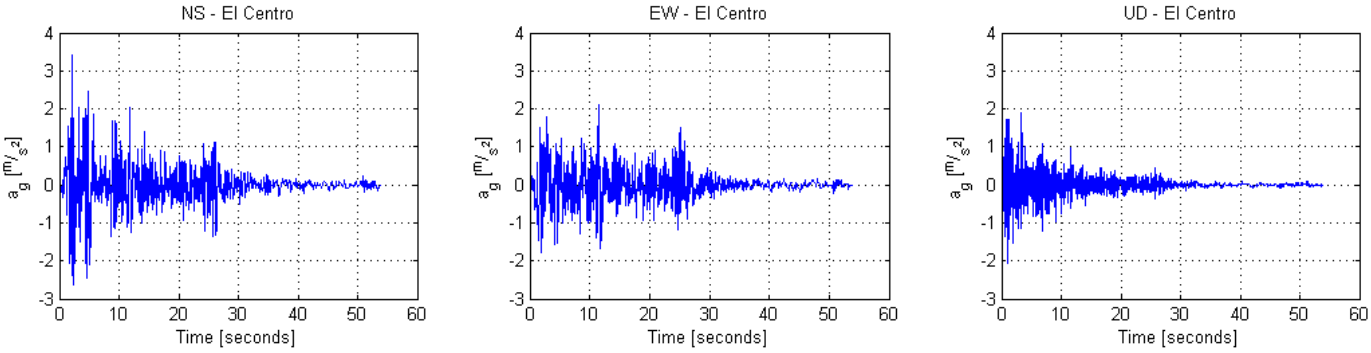

Figure 3.2: California's 1940 El Centro Earthquake accelerograms [Matlab]

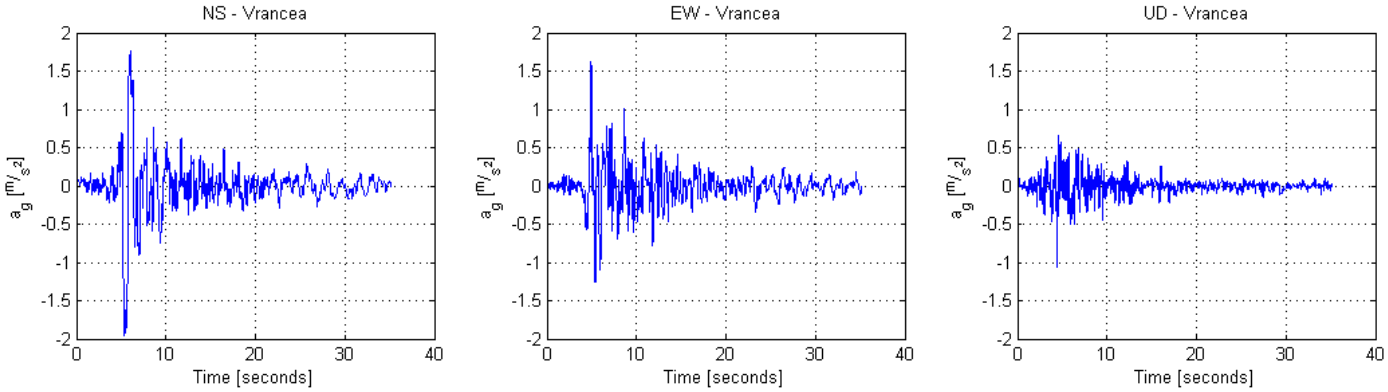

Figure 3.3: Romania's 1977 Vrancea Earthquake accelerograms [Matlab]

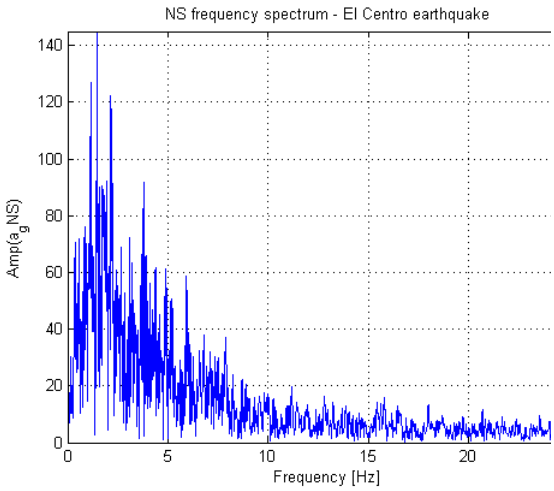

Figure 3.4: Frequency spectrum N-S El Centro [Matlab]

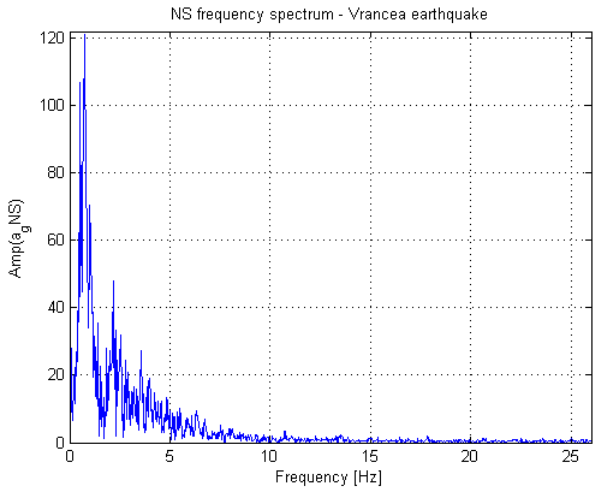

Figure 3.5: Frequency sectrum N-S Vrancea [Matlab]

It is observed that, for both earthquakes, most of the energy is dissipated in the frequency interval $[0-10]Hz$. This means that the modes of vibration with eigen frequencies less than $10Hz$ are highly predominant during the earthquakes.

The objective now is to compute the displacement of the structure's top by the two specified methods and compare the results. At this point, the analysis is performed in the plastic domain, since the Matlab FEA code only functions in that range. After it is checked that the results are trustful, a plastic analysis is performed in Abaqus and stress-strain curves are observed for most loaded elements.
For any future calculation, the time data is squeezed up by a factor of 10 to increase the response of the structure. This means that the accelerograms and the frequency spectra on North-South direction become the ones in Figure 3.6, Figure 3.7, Figure 3.8 and Figure 3.9. It is observed that the frequency range increases from $[0-10Hz]$ to $[0-100Hz]$.

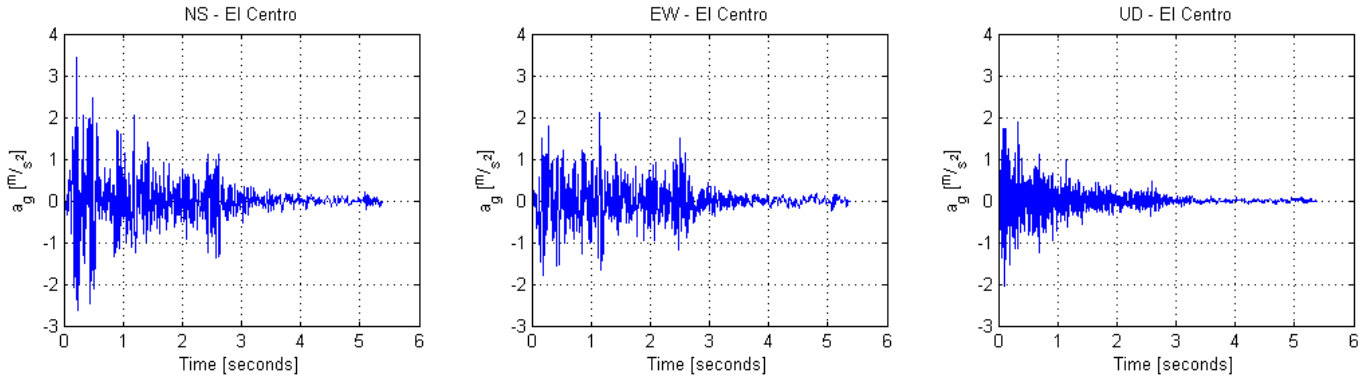

Figure 3.6: California's 1940 El Centro Earthquake accelerograms, squeezed [Matlab]

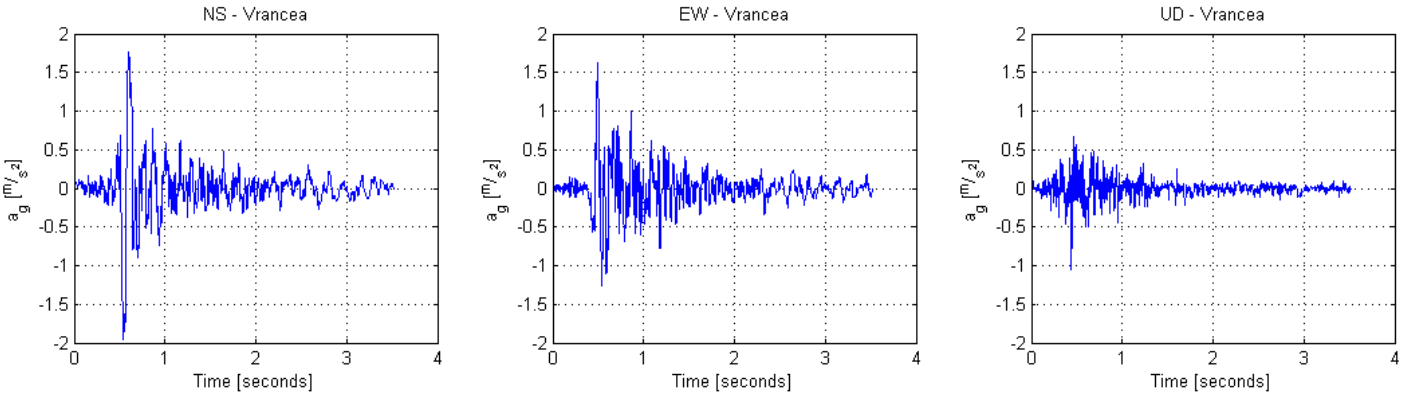

Figure 3.7: Romania's 1977 Vrancea Earthquake accelerograms, squeezed [Matlab]

3.1.1 Matlab 2D FEA

A code is created in Matlab to calculate the displacement in time domain for a structure subjected to the action of an earthquake. The steps are as follows

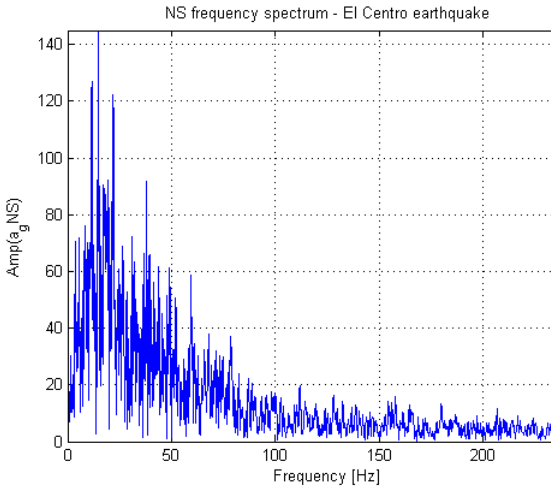

Figure 3.8: Frequency spectrum N-S El Centro, squeezed [Matlab]

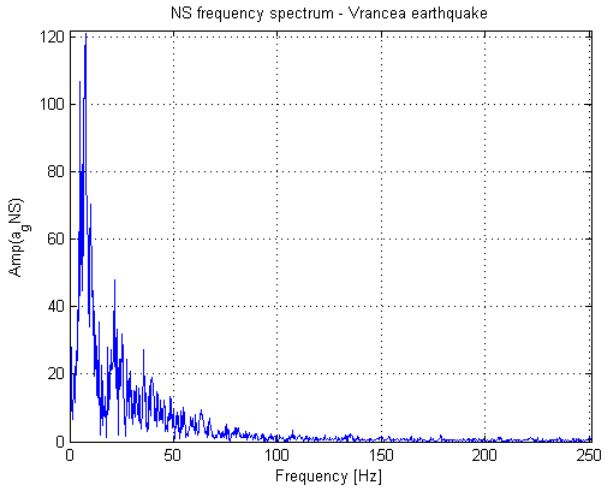

Figure 3.9: Frequency sectrum N-S Vrancea, squeezed [Matlab]

- *Step 1. The input*

  Creating the input file, where the nodal coordinates, materials and boundary conditions are defined.

  The length and cross section specifications are

L	2000 $[mm]$ Length of the column
b	50 $[mm]$ square cross section side

  It is chosen an 11 node and 10 rod elements system, with element length of 200 mm. The rod elements have 3 degrees of freedom, two translations and one rotation, so in total there are 33 degrees of freedom, which means that the mass matrix and the stiffness matrix will be 33x33.

  The material is steel, with

E_{steel}	$210 \cdot 10^3$ $[MPa]$ Young's modulus of steel
ν_s	0.3 [ ] Poisson's ratio of steel
ρ_s	$7.85 \cdot 10^{-9}$ $[\frac{T}{mm^3}]$ density of steel

  The boundary conditions are zero displacements and zero rotation at the column bottom node. This means that three degrees of freedom are blocked. Given that, it can be anticipate that the reduced mass matrix M_{red} and the reduced stiffness matrix K_{red} are 30x30. The reduced matrices are used in calculation to increase computational speed.

  The input file is named `'steel_column_input.m'` and can be found in the electronic appendix.

- *Step 2. Constructing K and M*

  The stiffness matrix K and mass matrix M are constructed, in a loop that goes over all elements. These matrices are 33x33. After that, the reduced stiffnes matrix K_{red} and the reduced mass matrix M_{red} are created. These matrices are 30x30.

  These operation are performed in the file `'Main_code.m'` found in the electronic appendix.

- *Step 3. The eigen value problem*

  The eigen angular frequencies ω are obtained by solving the characteristic equation of the structural system, shown in Equation 3.1.

$$|K - \omega^2 M| = 0 \tag{3.1}$$

  The reduced stiffness and mass matrices are used. Once the eigen angular frequencies are known, the eigen frequencies and eigen periods are obtained as shown in Equation 3.2 and Equation 3.3.

$$f = \frac{\omega}{2\pi} \tag{3.2}$$

$$T = \frac{1}{f} \tag{3.3}$$

  The eigen modes of vibration are proper to the structure and have nothing to do with the earthquake. They are, however, an important tool in the process of structural response under earthquake action, because it can be observed in what frequency range do the ground motion and the eigen frequency superpose. When superposition occurs, the system goes into resonance and the analysis of displacements and stresses in that range is highly required.

  The eigen modes are described by the eigen vectors ϕ and are obtained by Equation 3.4.

$$[K - \omega^2 M]\phi = 0 \tag{3.4}$$

  The first three eigen modes, with their corresponding eigen frequencies are shown in Figure 3.10.

  Mode 1 and Mode 2 are predominant in the vibration compared to Mode 3, because they are in the $[0 - 100Hz]$ range.

  These calculations pertinent to this step can also be found in the file `'Main_code.m'`, located in the electronic appendix.

- *Step 4. Ground motion analysis*

  Knowing the ground acceleration time field, the ground velocity and the ground displacement can be calculated by integration, as in Equation 3.5 and Equation 3.6.

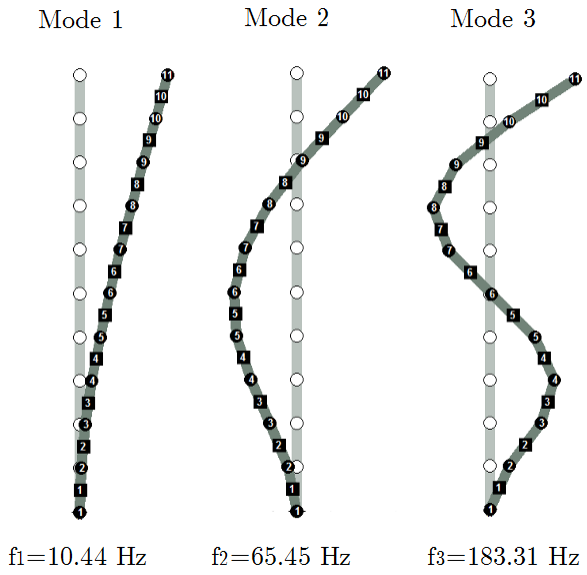

Figure 3.10: Eigen modes, Steel column [Matlab]

$$v_g = \int a_g \, dx \tag{3.5}$$

$$d_g = \int v_g \, dx \tag{3.6}$$

The ground velocity and ground displacement are not correlated to the structure. The North-South component of the ground velocity and ground displacement for the El Centro Earthquake and Vrancea Earthquake are shown in Figure 3.11, Figure 3.13, Figure 3.12 and Figure 3.14

The calculations are performed by numerical trapezoidal integration and the code that generates the above graphs plus the velocity and displacement field graphs pertinent to the other two directions, i.e. East-West and Up-Down, is located in `'ground.m'`.

- *Step 5. Structural motion analysis*

  To include damping in the equation of motion, see Equation 3.7, the damping matrix C needs to be defined.

$$M\ddot{x}(t) + C\dot{x}(t) + Kx(t) = F(t) \tag{3.7}$$

$\ddot{x}$	nodal acceleration vector
$\dot{x}$	nodal velocity vector
x	nodal displacement vector

Mass proportionality is defined. Therefore, the damping matrix C is defined based on the damping ratio the angular frequency in the first mode and the mass matrix, see Equation

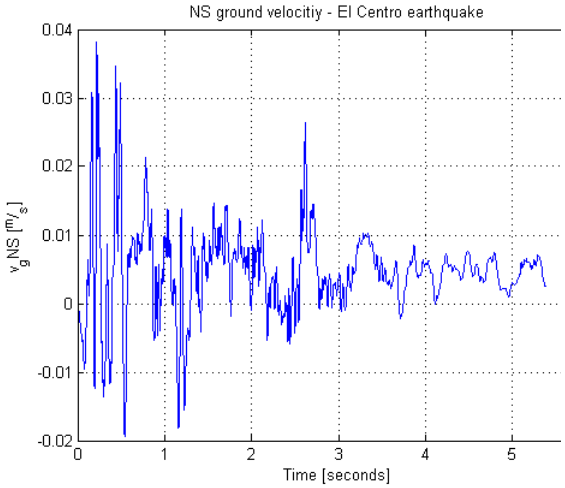

Figure 3.11: Ground velocity N-S El Centro, squeezed [Matlab]

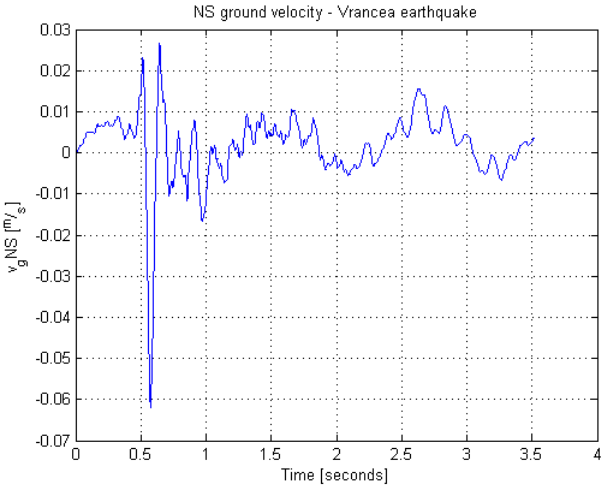

Figure 3.12: Ground velocity N-S Vrancea, squeezed [Matlab]

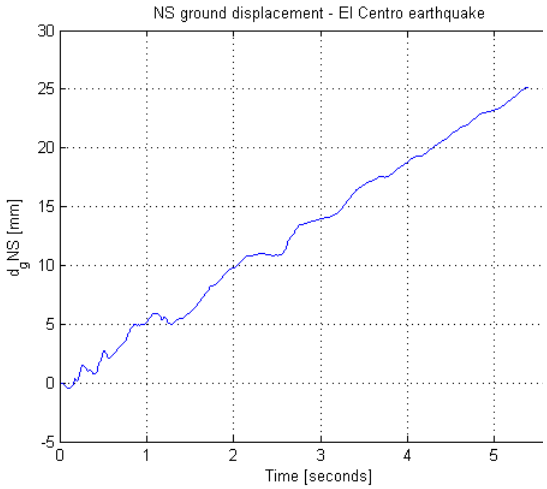

Figure 3.13: Ground displacement N-S El Centro, squeezed [Matlab]

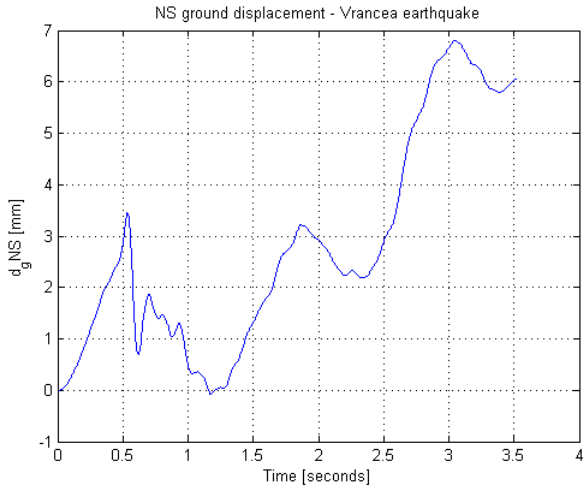

Figure 3.14: Ground displacement N-S Vrancea, squeezed [Matlab]

3.8 The damping ratio is obtained empirically and it is based on the logarithmic decrement, which is a number that describes how fast the magnitude of the oscillations decreases, or how fast the oscillations decay after a disturbance.

ζ	0.0154 [ ] damping ratio
ω_1	65.62 $[Hz]$ damping ratio

$$C = 2 \cdot \zeta \cdot \omega_1 \cdot M \tag{3.8}$$

$F(t)$ is a time varying vector that contains the nodal forces for each node. It is obtained by multiplying the ground accelerations with the mass matrix, as in Equation 3.9. It is very important that only the degrees of freedom that are on the same direction with ground motion should be initiated. The other values remain zero. The minus sign comes from the inertia principle.

$$F = -M \cdot a_g \tag{3.9}$$

Again, the reduced mass and stiffness matrices are the ones used.

Proceeding, there are two options,i.e. performing a regular analysis or a modal analysis.

For the regular analysis, the equation of motion is solved using M, K, C, and F as they are.

For the modal analysis, new parameters have to be computed by Equations 3.10 - 3.13.

$$M_{mod} = \phi_i^T \cdot M \cdot \phi_i \tag{3.10}$$
$$K_{mod} = \phi_i^T \cdot K \cdot \phi_i \tag{3.11}$$
$$C_{mod} = \phi_i^T \cdot C \cdot \phi_i \tag{3.12}$$
$$F_{mod} = \phi_i^T \cdot F \tag{3.13}$$

The letter i represents the number of eigen modes used in the analysis. The modal analysis makes the transition from the real multi degree of freedom structure to a sum of single degree of freedom structures.

Modal analysis is advantageous because it can be applied only for the modes that show resonance to the ground motion frequency spectrum. In this case mode 1 is highly dominant compared to all the others. Performing a modal analysis with one mode will give that M_{mod}, K_{mod}, C_{mod} and F_{mod} are scalars, which makes sense considering that there is only one active degree of freedom. Therefore, instead of using 30x30 matrices (dimensions of reduced mass and stiffness matrices), 1x1 matrices are used. This simplifies the calculations and allows a much faster analysis, which is very important when the structures are more complicated.

For this example, a modal analysis using 30 modes of vibration is the same thing as using the reduced matrices. This is because the system has a number of 30 unrestricted degrees of freedom, so a total number of 30 modes of vibration is computed.

After establishing the type of analysis, the equation of motion is solved by Newmark's algorithm, which gives out the nodal accelerations, nodal displacements and nodal velocities. Newmark's algorithm is a so called implicit dynamic analysis method. The function that encodes Newmark's algorithm is located in `'newmark.m'`

Newmark's algorithm gives out the local nodal displacements. For obtaining the global nodal displacements, the ground displacements need to be added up.

In this case, the regular analysis is performed, since modal analysis in Abaqus is possible for applied loads but not possible for applied (imposed) displacements.

The local horizontal displacement field for node 11 is shown in Figure 3.15. The ground displacement is then added and the results for the global displacement of the same node is shown in Figure 3.16.

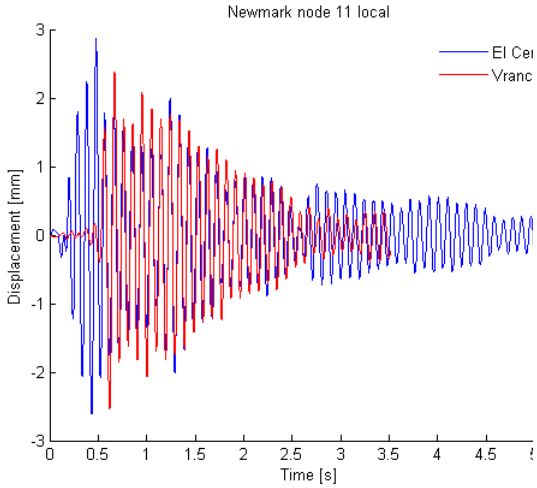

Figure 3.15: Local horizontal displacement, column top [Matlab]

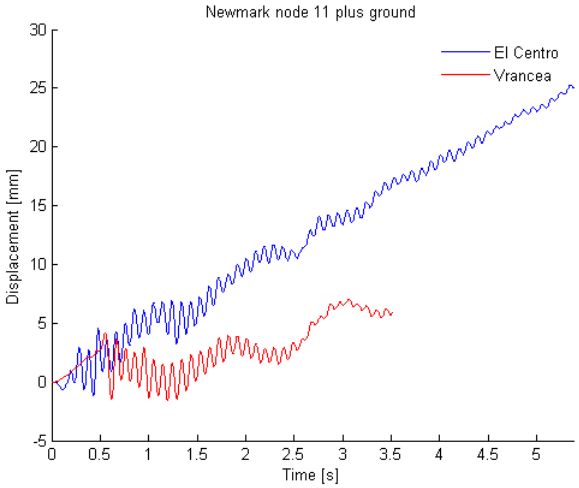

Figure 3.16: Global horizontal displacement, column top [Matlab]

It can be observed that the local displacement have about the same magnitude but the global displacement is higher for the El Centro earthquake. That happens because the El Centro earthquake induces higher ground displacements.

All the calculations in this step are encoded in `'EQ_analysis.m'`.

3.1.2 Abaqus 3D FEA

A column with the same specification is created in Abaqus as a solid 3D deformable body and then meshed with Hex 8 nodes elements, as in Figure 3.17.

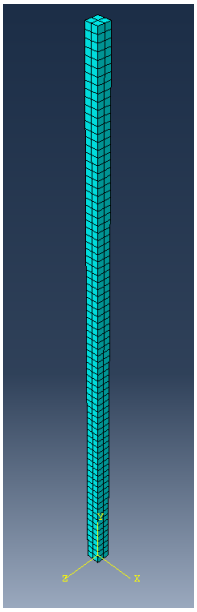

Figure 3.17: Column mesh [Abaqus]

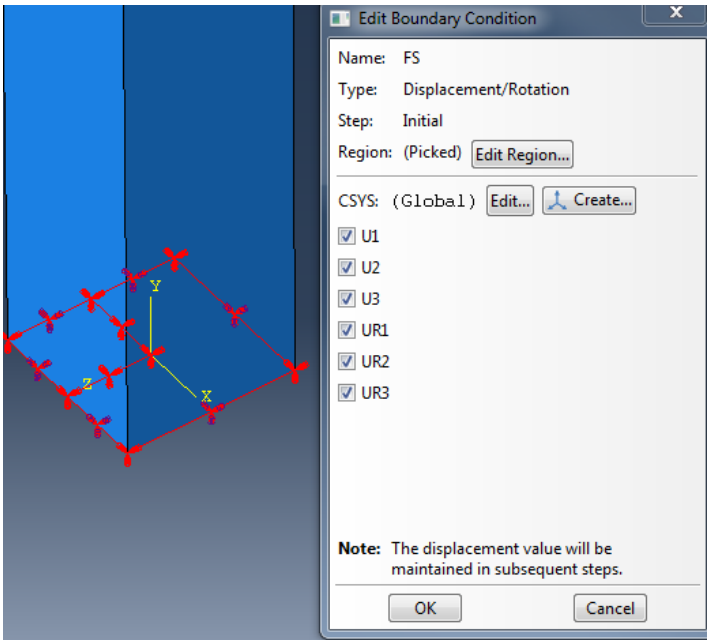

Figure 3.18: Boundary condition - Frequency analysis [Abaqus]

The North-South direction is defined as the z direction in Abaqus.

The boundary conditions are zero displacement of the base on x and y and zero rotation around all the axes. For analysis of structures subjected to earthquakes, it is important that the material density and gravity load are carefully defined, since they play an important role in the equation of motion.

First, the boundary conditions are set as fixed base, so all the displacements and rotations are restricted at the base, see Figure 3.18, and a frequency analysis is performed.

The first three eigen modes of vibration, together with the pertinent eigen frequencies are shown in Figure 3.19. The are named Modes 1, 2 and 3 for a better comparison with the Matlab FEA code, but in Abaqus they are in fact Modes 1, 3 and 5. Mode 2 and 4 have identical eigen frequencies and eigen shapes with Modes 1 and 3 but they occur on perpendicular directions.

The program that performs this calculation is located in `'steel column final modal.cae'`.

Then, the amplitudes of the acceleration are defined for both earthquakes, as shown in Figure 3.21. It can be seen that acceleration amplitudes can be described on any of the direction, so Abaqus

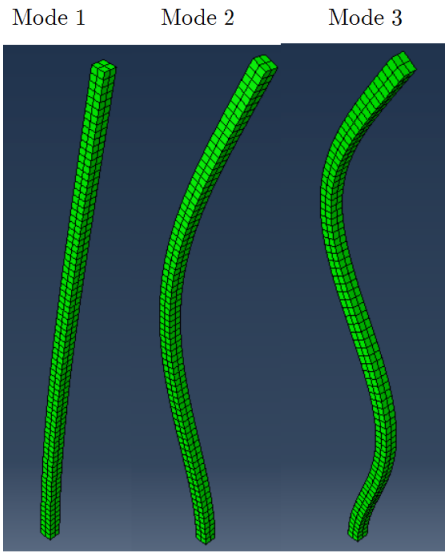

Figure 3.19: Eigen modes, Steel column [Abaqus]

offers the option of analyzing the full 3D response of the structure during earthquake, i.e. with the earthquake disturbance components on all three direction defined. For this report, only the data on z axis (North-South) is considered because the 3D analysis can take very long if the computer doesn't have a very high performance processor and two digit number of RAM gigabytes.

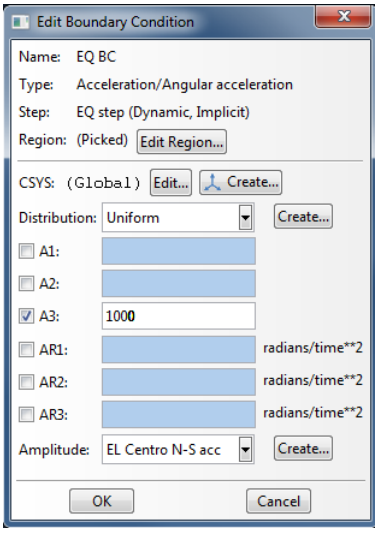

Figure 3.20: Imposed displacement [Abaqus]

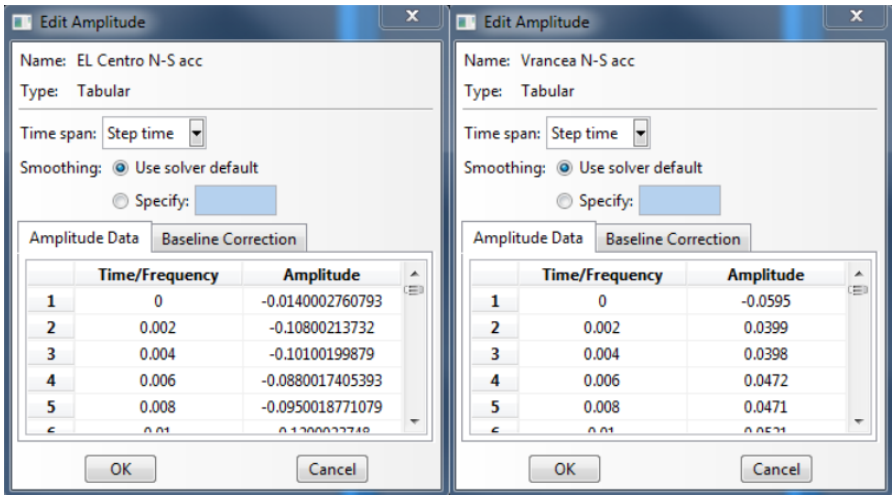

Figure 3.21: Acceleration amplitudes [Abaqus]

The base displacement on z direction is reset to free and another bounday condition, which is set in a 'Dynamic, implicit' step is assigned to the base, as shown in Figure 3.20. At the bottom, the

desired earthquake, i.e. El Centro or Vrancea, can be selected and the amplitudes are multiplied by 1000 because the unit that was chosen for use is Nmm. The amplitudes were initially introduced in $\frac{m}{s^2}$.

The global displacement field for top middle node on z direction is shown in Figure 3.22.

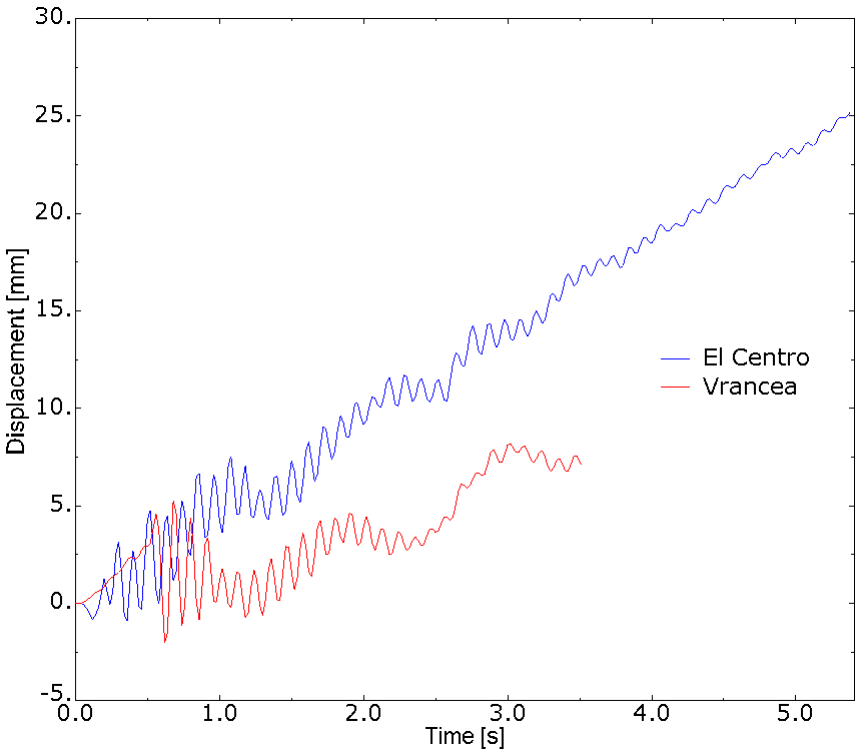

Figure 3.22: Global displacement on z, middle top node [Abaqus]

It is observed that the displacements are very close to the one computed by the Matlab FEA code, which leads to the idea that the calculation were performed correctly.
The normal stresses at the base of the structure vary linear along the Young's modulus of Steel, see Figure 3.24 and Figure 3.25.

Because for both of the earthquakes, the maximum normal stresses at the base of the structure, Figure 3.23, don't exceed 10 MPa, see Figure 3.24 and Figure 3.25, an exaggeration is made in order to study the plastic behavior of the structure. Therefore, the amplitudes of the accelerations are multiplied again with 100 and the yielding stress of the steel is set to 350 MPa. It is good to keep in mind that the calculations are performed in order to understand the working procedure and the concept and not to design real structures.

The stress-strain curves for the first second of each of the earthquakes, pertinent to an element at the bottom of the structures,i.e. highest stresses and strains, is shown in Figure 3.26 and Figure 3.27. It is observed that, for the El Centro earthquake, the strains are mostly tensile, while for

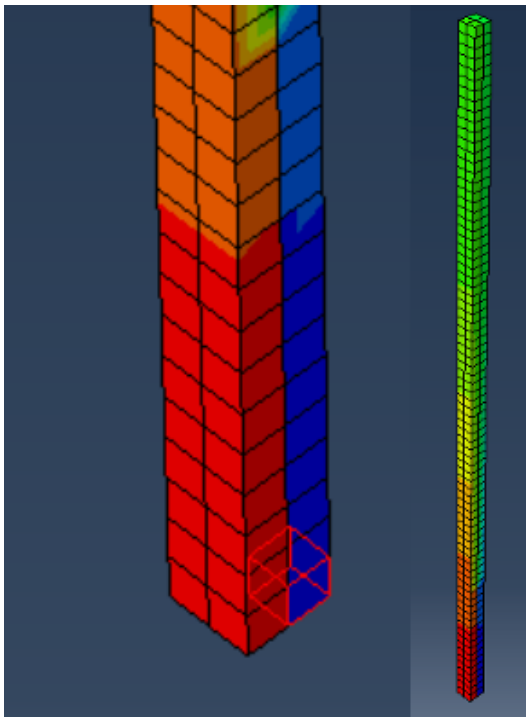

Figure 3.23: Base of structure element [Abaqus]

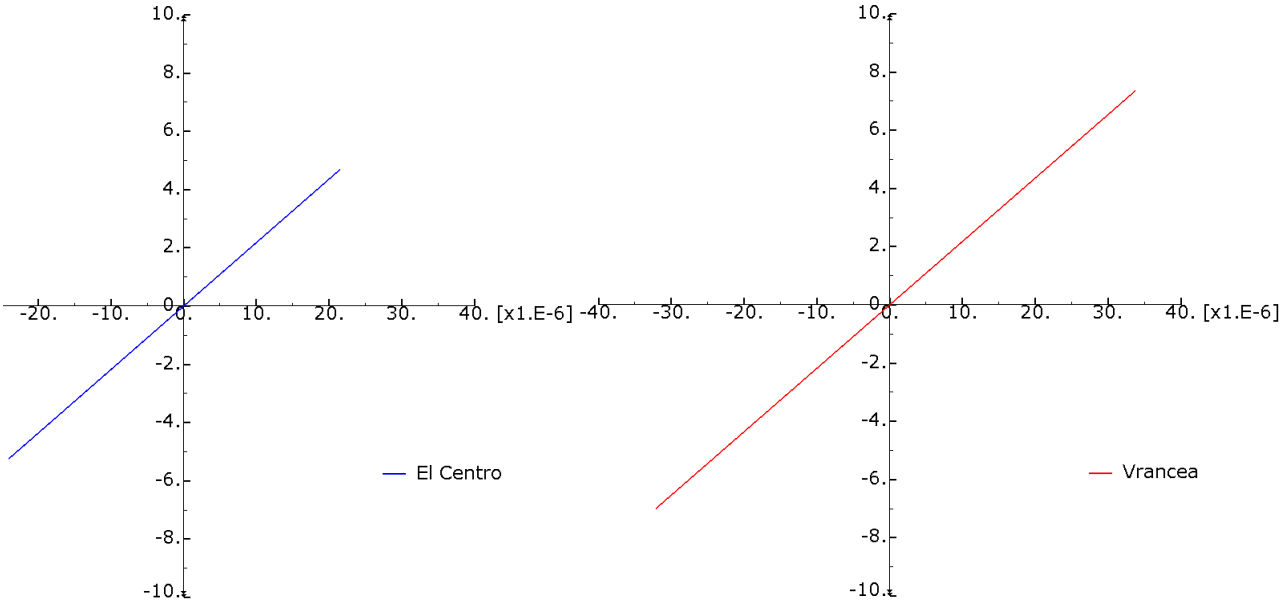

Figure 3.24: Stress (S22)-strain (E22) curve, El Centro [Abaqus]

Figure 3.25: Stress (S22)-strain (E22) curve, Vrancea [Abaqus]

Vrancea earthquake the strains are both compressive and tensile.

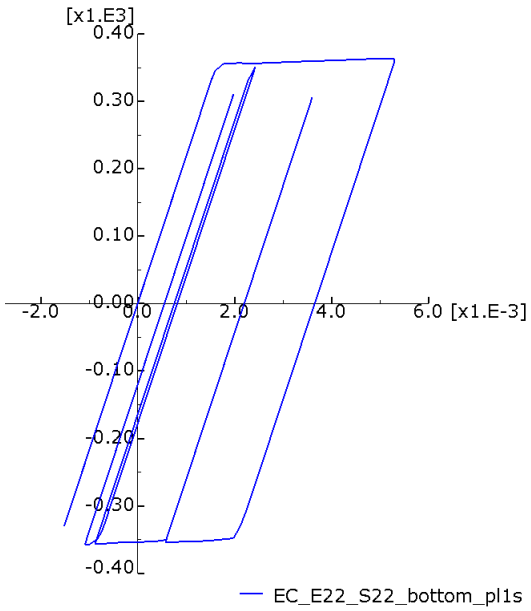

Figure 3.26: Stress (S22)-strain (E22) plastic, El Centro [Abaqus]

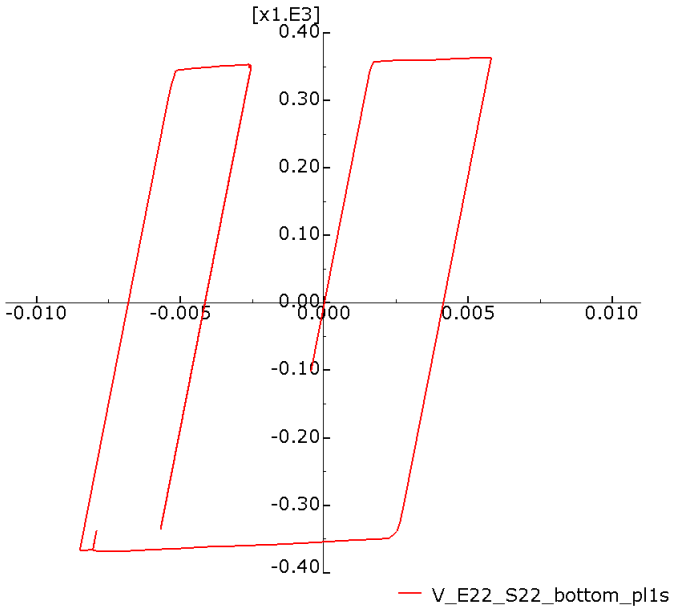

Figure 3.27: Stress (S22)-strain (E22) plastic, Vrancea [Abaqus]

It can be seen that loading and unloading takes place along the chosen Young's modulus of 210 000 MPa and that the yielding plateau obeys the imposed value of 350 MPa. Considering that, the behavior is certainly the expected one and it is considered that the Abaqus Finite Element Analysis program has been used correctly when performing this exercise.
The described calculations are located in the file `'steel column final.cae'`.

3.1.3 Comparison and conclusion

The results from the Matlab FEA code and the Abaqus commercial for eigen modes and displacements are very close, therefore it is considered that the work has been performed correctly, the tools for studying earthquake loading have been assessed and it is now safe to proceed on analyzing a multi-storey structure under seismic action.

3.2 Multi-storey framed steel structure

Since the main problem of steel structures under earthquake action is stability and not undertaking stresses, the analysis of the steel column might be inconclusive.

Generally, a structure subjected to earthquake load needs to fulfill two criteria, namely the strength check and the stability check. For a multi-storey building, the stability check is defined by the assessment of the storey drift. The drift of a storey is a dimensionless parameter and it is given by Equation 3.14.

$$d_s = \frac{u_{up} - u_{down}}{H_s} \tag{3.14}$$

d_s	storey drift
u_{up}	horizontal displacement at the top of the storey
u_{up}	horizontal displacement at the bottom of the storey
H_s	height of the storey

The parameters required to calculate the storey drift are depicted in Figure 3.28.

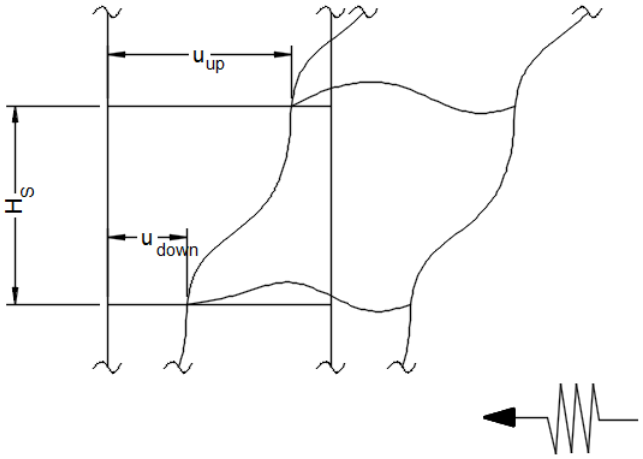

Figure 3.28: Storey drift [Abaqus]

For this reason, a 3 storeys framed steel structure is created in Abaqus, as shown in Figure 3.29. The cross section of both, beams and columns, is of 'H' type, as shown on Figure 3.30. In reality, depending on the number of stories and the structure's functionality, the cross sections of the elements are larger than 45 mm over 45 mm. However, this exercise has as goal the analysis of the plastic response and not the design. Real steel structures are designed such that they do not undergo plastic deformations during earthquakes. The span between the beams is equal on both directions, and it is also equal to the storey height.

The steel used for this structure has the specifications

E_S	210 000 $[MPa]$ Young's modulus
ν_S	0.3 [ ] Poisson's ratio
f_y	255 $[MPa]$ yielding stress

$$L_{beam} = H_{storey} = 2800\ mm$$

The instances are merged together in Abaqus and the resulted instance is then meshed with Hex 3D 8 nodes elements, as shwon in Figure 3.31.

First, the columns are fixed at the bottom on all the degreees of freedom and a frequency analysis is conducted. The first five eigen modes with the corresponding eigen frequencies is shown on Figure 3.32. The file pertinent to the frequency analysis is called `'steel_MS_eigen.cae'` and it is located in the electronic appendix.

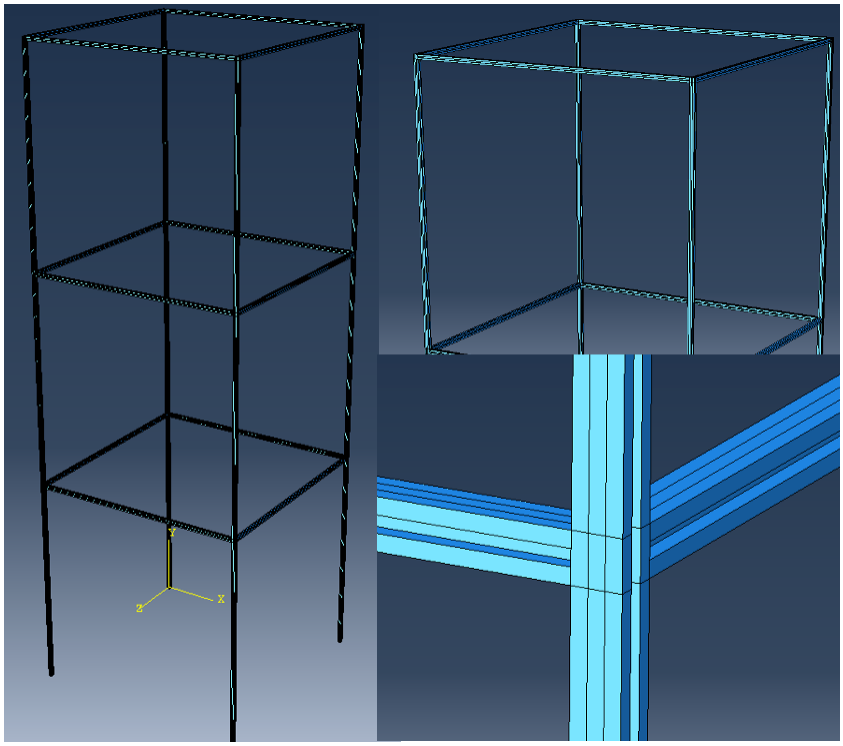

Figure 3.29: Multi-storey framed steel structure [Abaqus]

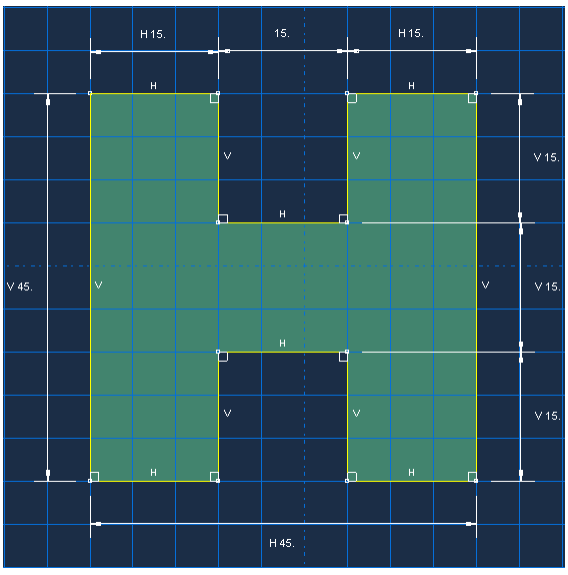

Figure 3.30: Frame cross section [mm] [Abaqus]

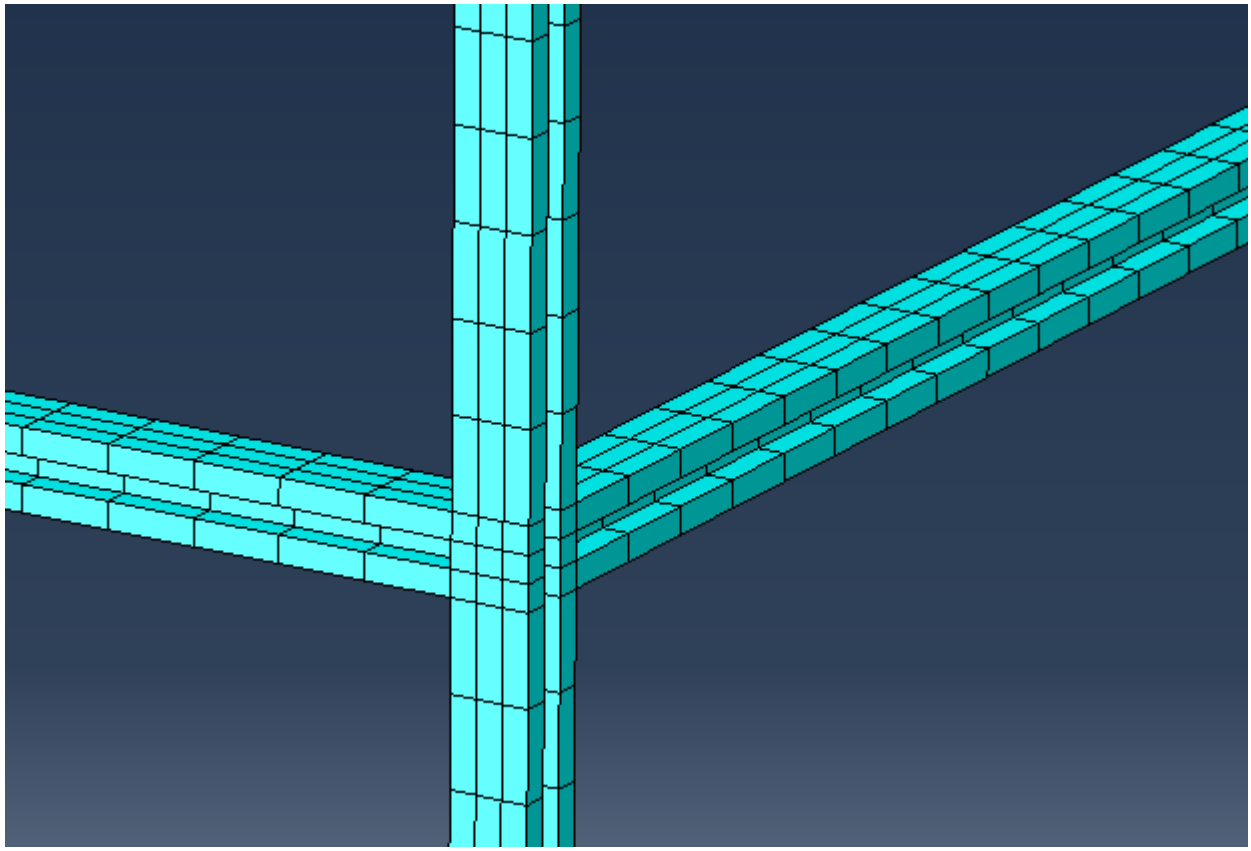

Figure 3.31: Multi-storey structure mesh [Abaqus]

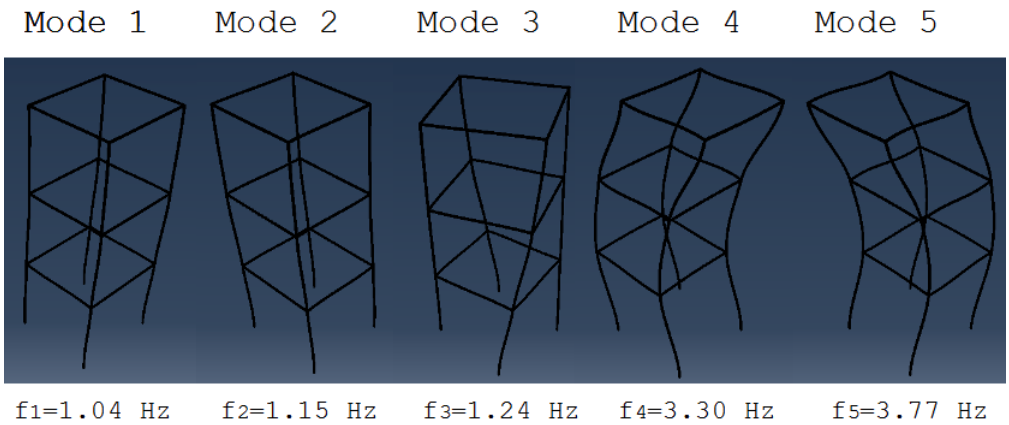

Figure 3.32: Multi-storey eigen modes [Abaqus]

It is observed that all the first five modes are below 5 Hz frequency range, so they will all be active during the earthquake, considering the frequency spectrum of the real earthquakes, i.e. no scaling of time step and amplitudes, in Figure 3.4 and Figure 3.5. It can be observed that Mode 1 and Mode 2 are translation modes in phase, Mode 4 and Mode 5 are translation modes in counter phase, and Mode 3 is a torsional mode.

The purpose now is to analyse the plastic response of the elements around the nodes, i.e. where the stresses and strains are highest, and the storey drift in both elastic and plastic range. For this reason, the seismic data is scaled, i.e. the time series is squeezed up by a factor of ten and the amplitudes are multiplied by 100.

The displacement on the z direction at the base of the structure is reset to free and amplitudes of acceleration are applied in a dynamic implicit step, in the same manner as it has been done for the steel column. The difference is that now the imposed displacements apply to the base of all the four columns.

The duration of El Centro earthquake is 5.378 s and the duration of the Vrancea earthqauke is 3.512 s. This is valid after the time data is squeezed up. The plastic analysis is only performed for the first second of the earthquakes because of the high demands of computational power.

The stress-strain curve in the column at the bottom of Storey 3, see Figure 3.33, are shown in Figure 3.34 and Figure 3.35.

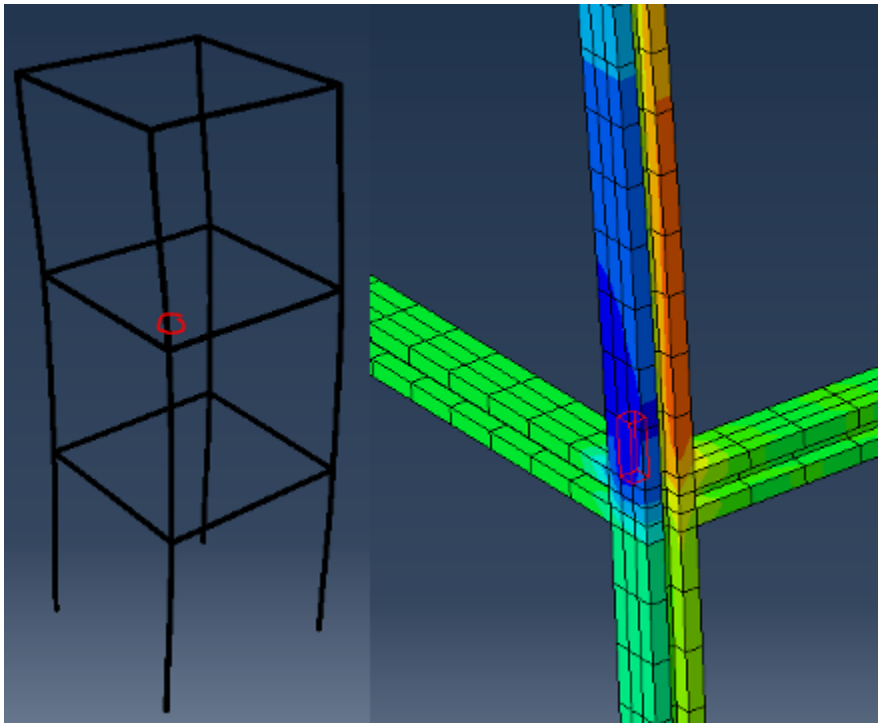

Figure 3.33: Multi-storey steel structure, element [Abaqus]

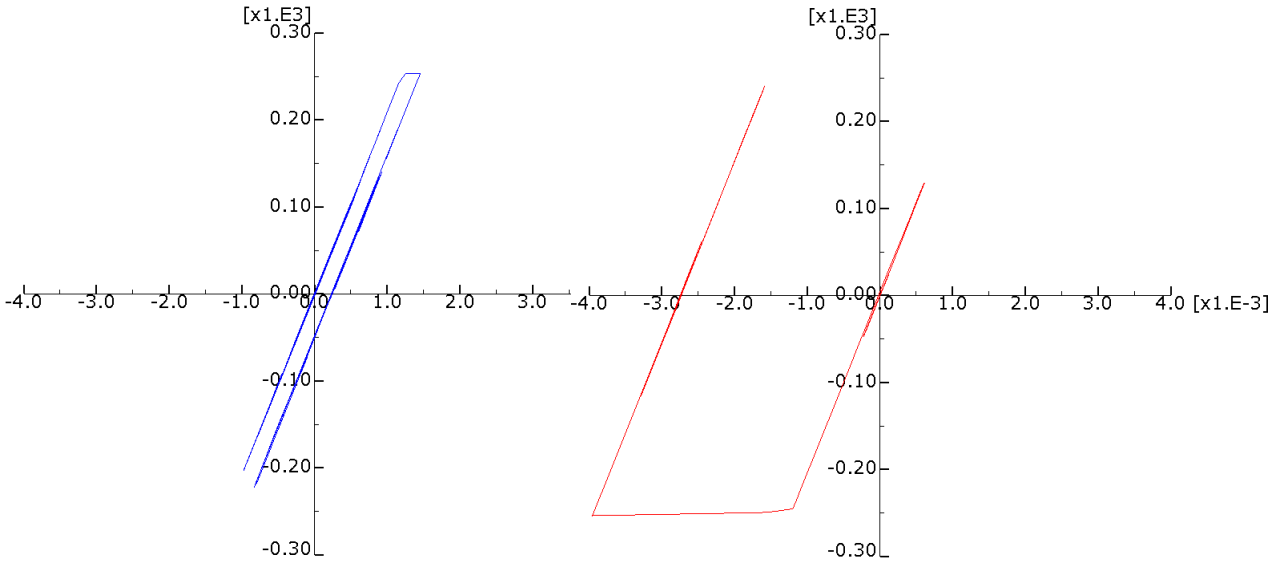

Figure 3.34: Stress (S22)-strain (E22) curve, El Centro [Abaqus]

Figure 3.35: Stress (S22)-strain (E22) curve, Vrancea [Abaqus]

It is observed that Vrancea Earthquake causes higher compressive srains that El Centro Earthquake. Yielding occurs at 255 MPa, as expected.

The storey drift in both, linear and plastic range, are shown in Figures 3.36 - 3.39. Linear range means that no yield stress was defined and the material is linear along the Young's modulus until infinity.

The file pertinent to the elastic and plastic drift analysis is called `'steel_MS.cae'` and it is located in the electronic appendix.

It can be seen in Figures 3.36 - 3.39 that plastification does not cause higher drifts. The problem with the plastic drifts is that they cause permanent displacements, so any load applied on the structure will have an eccentricity that can cause stability loss.

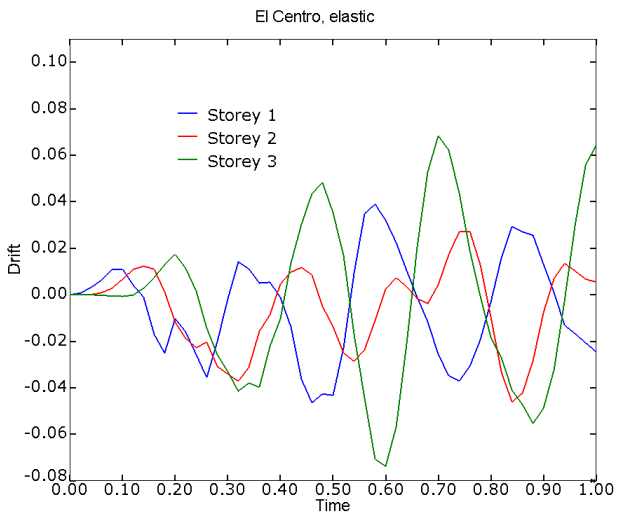

Figure 3.36: Storey drift, elastic, El Centro [Abaqus]

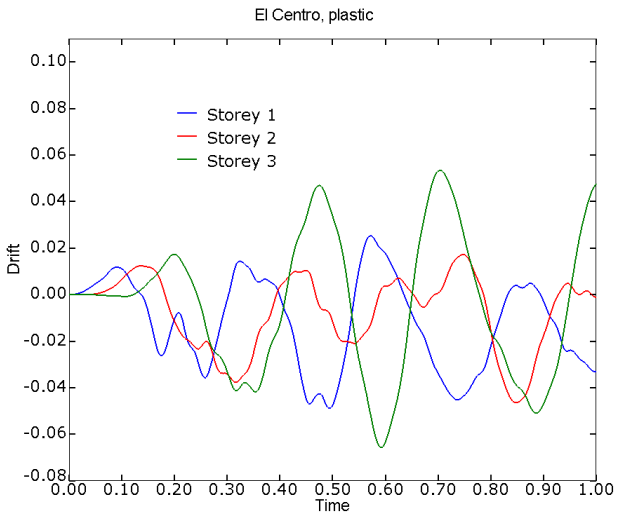

Figure 3.37: Storey drift, plastic, El Centro [Abaqus]

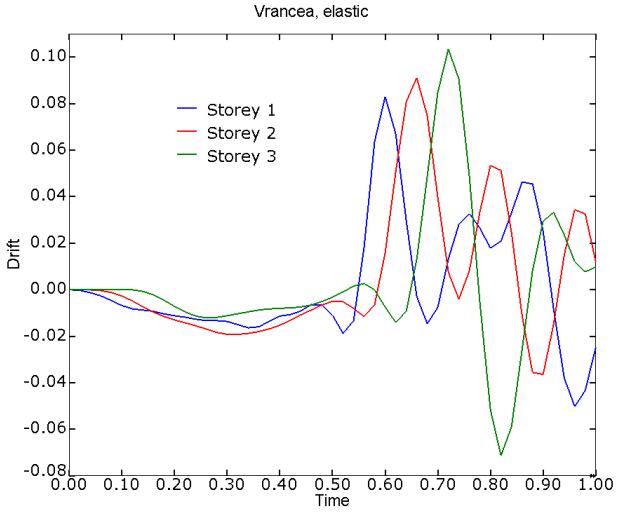

Figure 3.38: Storey drift, elastic, Vrancea [Abaqus]

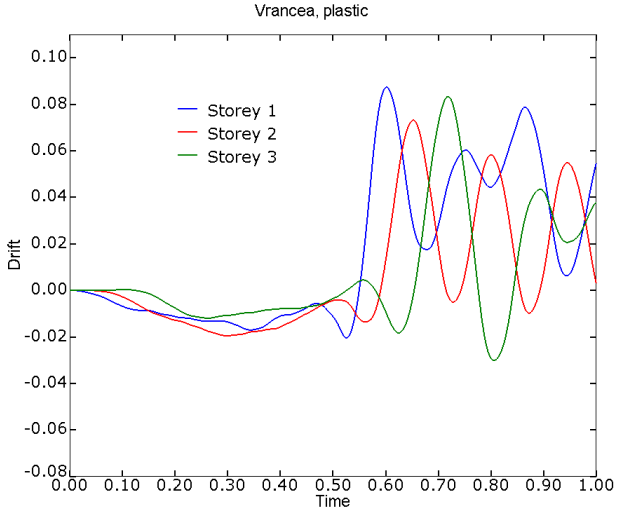

Figure 3.39: Storey drift, plastic, Vrancea [Abaqus]

3.3 Multi-storey framed reinforced concrete structure

3.3.1 Abaqus 3D FEA

A multi-storey framed concrete structure is created in Abaqus. The columns are 300 mm over 300 mm and are 2800 mm in length. Each elements is reinforced with 4 ϕ 14 rebars. The beams have the exact same specifications as the columns.

The seismic analysis is performed in the exact same manner as for the steel multi-storey framed structure. Vrancea (North-South) earthquake is implemented with time series squeezed up by a factor of 10 and acceleration amplitudes multiplied by 100. Because of very high computer performance requirements, only the first 0.55 s out of a total of 3.512 s are implemented.

The concrete plasticity is defined by the yielding stress in compression (25 MPa)and the cracking stress in tension (2.25 MPa), so the stress-strain curve is not defined in detail. For that matter, a very high performance computer would be required.

In Figure 3.40 - 3.46, the most important steps are presented.

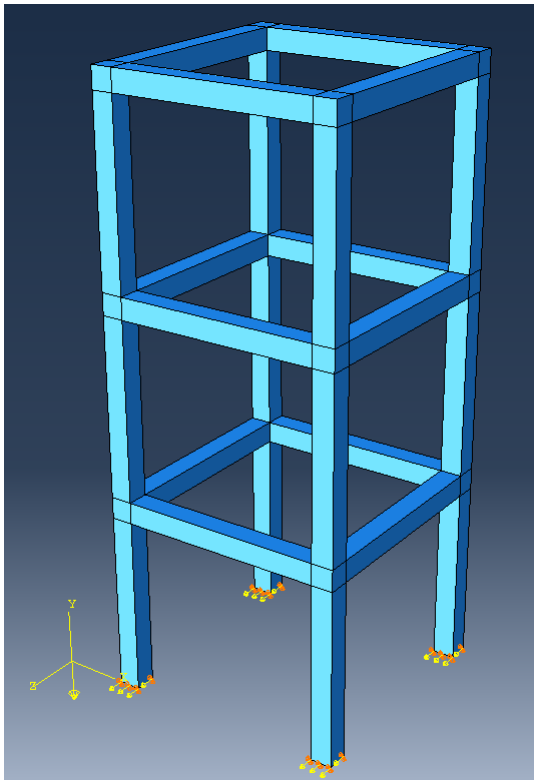

Figure 3.40: Multi-storey reinforced concrete structure [Abaqus]

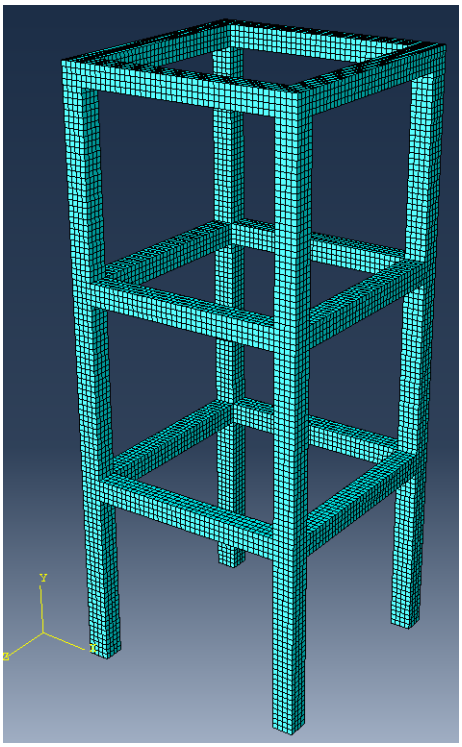

Figure 3.41: Structure mesh [Abaqus]

Figure 3.43 represent the displacement field on the z axis for $t = 0.55$ s. It can be seen that the drift of Storey 1 on is much higher, as shown by the graph in Figure 3.46.

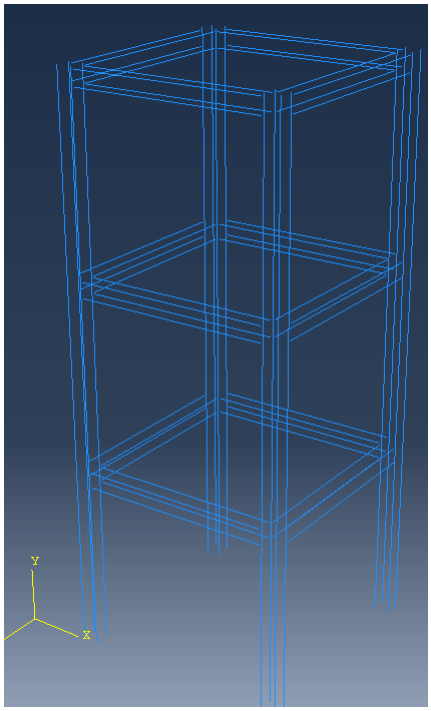

Figure 3.42: Rebars [Abaqus]

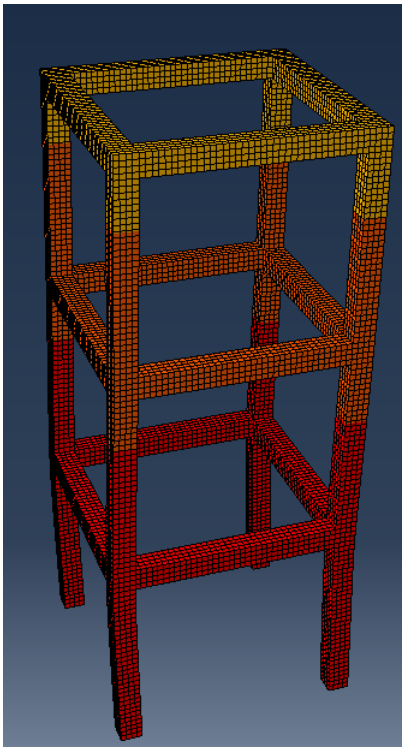

Figure 3.43: Displacement field u3 (z) [Abaqus]

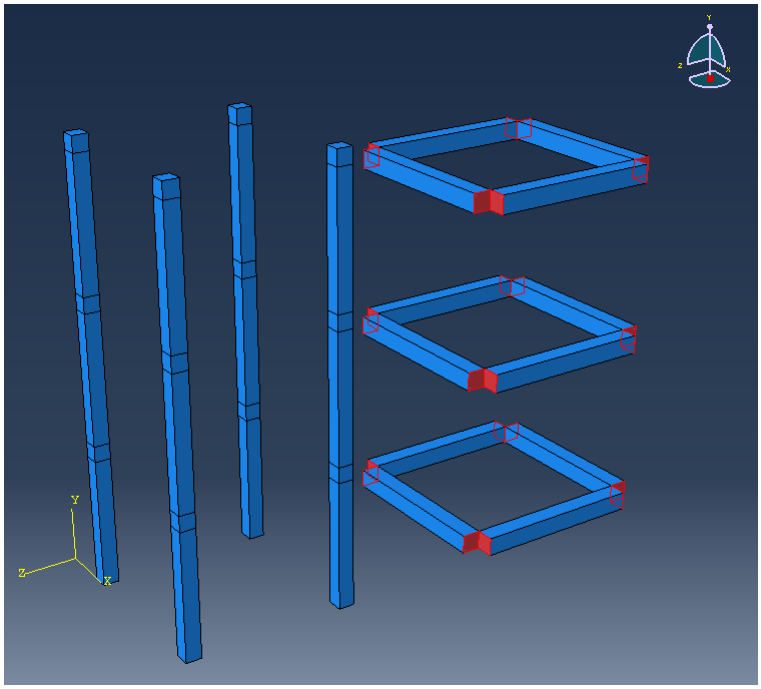

Figure 3.44: Tie connections, beams to columns [Abaqus]

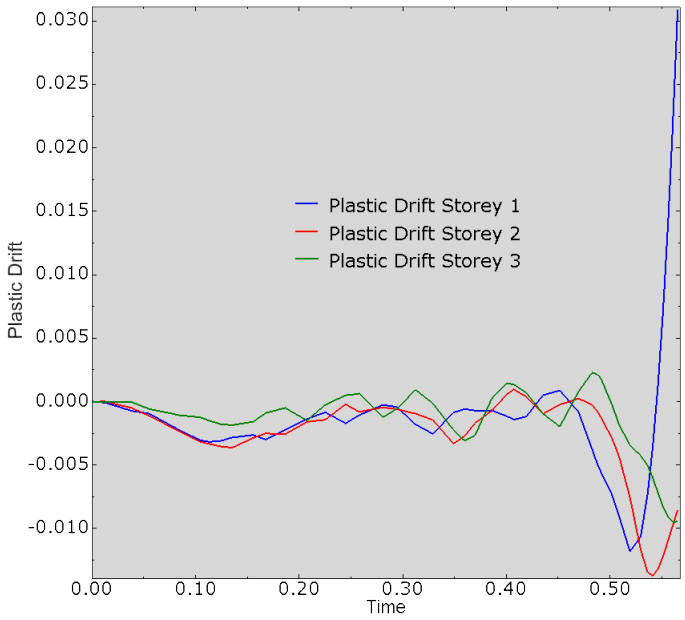

Figure 3.45: Plastic drift [Abaqus]

Figure 3.45 shows the stress-strain curve S22-E22 for an element in a column at the bottom of Storey 3.

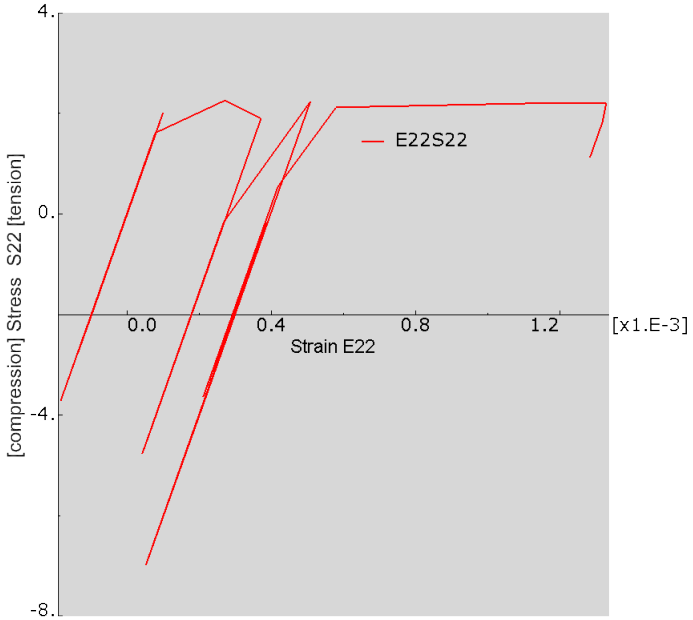

Figure 3.46: Stress-strain, plastic response for $t = 0.55\ s$ [Abaqus]

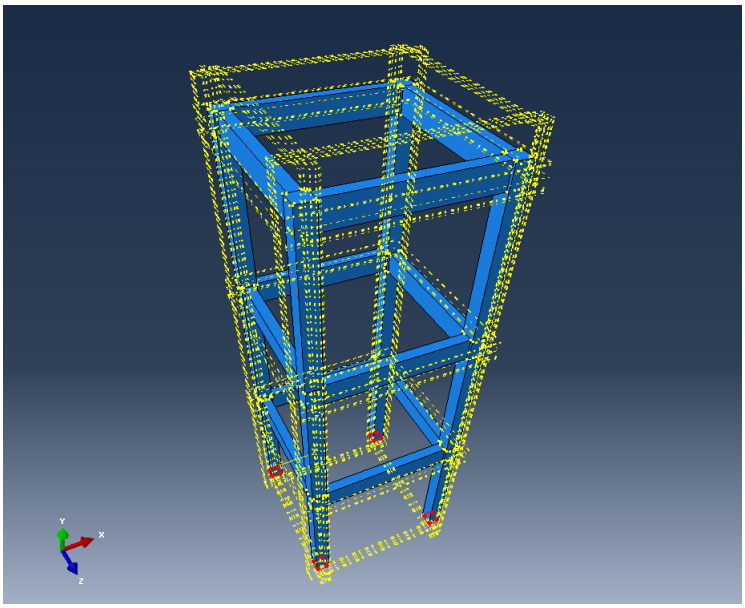

Figure 3.47: Undeformed [Abaqus]

A more complicated and much more detailed structure with solid elements for rebars is modeled and meshed, but again, a normal computer can't even allow its analysis under static loads. The meshing process took six hours to be assessed by the program. See Figures 3.47 - 3.49.

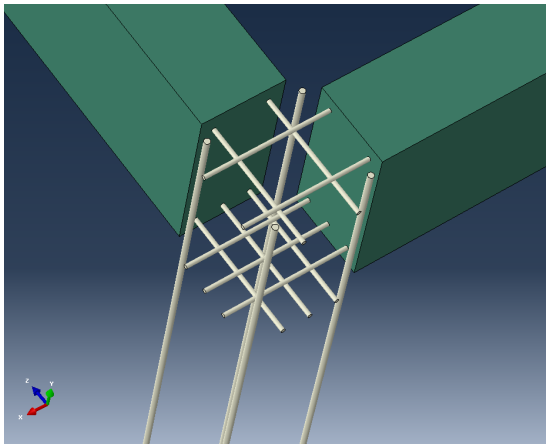

Figure 3.48: Joint detail [Abaqus]

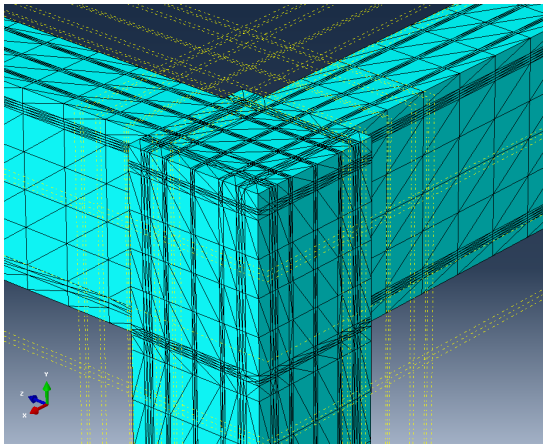

Figure 3.49: Mesh [Abaqus]

4 References

Ion S. Simulescu. *Lectures in Mechanics of Materials Vol. 2.* Conspress, Bucharest, 2010.

Florin Macavei. *Lectures on Dynamics and Earthquake Engineering Introduction.*
Technical University of Civil Engineering Bucharest (TUCEB), 2010

Eugen Lozincă. *Tutorials on Reinforced Concrete Design Part 1.* Technical University of Civil Engineering Bucharest (TUCEB), 2009

Eugen Lozincă. *Tutorials on Reinforced Concrete Design Part 3.* Technical University of Civil Engineering Bucharest (TUCEB), 2010

Mihail Iancovici. *Lectures on Structural Analysis.* Technical University of Civil Engineering Bucharest (TUCEB), 2009

Lars V. Andersen. *Lecture on Structural Mechanics and Dynamics.* Aalborg University (AAU), 2013

Anis Mohamad Ali, Bj. Farid and A.I.M. Al-Janabi. *Stress-Strain Relationship for Concrete in Compression Madel of Local Materials.*
Civil Engineering Department, College of Engineering, University of Basrah, Iraq.

Simulia. *Abaqus CAE 6.10 User Manual.*

Michelle Krummel. *Latex Tutorials Videos.* `https://www.youtube.com`, 2011

Computer programs used

LaTeX

Matlab R2014a

Abaqus CAE 6.10

Autocad 2015

Microsoft Excel 2010

Libre Office 4.4

Windows Snipping Tool

Everything in nature is sensitive to certain frequencies. So are structures. Earthquakes dissipate most of their energy in certain frequency ranges and are less active in other frequency ranges. Earthquake engineers have to ensure that, when a structure is sensitive to the frequency of the earthquake, it behaves properly and the damage is minimum. Earthquakes are unpredictable but catastrophes can be prevented by proper design of new structures and reconditioning of old affected structures. Big European capitals such as Bucharest and Athens are at high seismic risk, due to the large number of affected buildings that have already undergone major earthquakes and still wait to be reconditioned or demolished. Ignorance kills.